AFRL

COMPARATIVE MASS PROPERTIES OF LEGACY AND NEW ANTHROPOMORPHIC TEST DEVICES (ATDS)

Abigail Kerestes [1], Chris Albery[2]

AFRL 711TH HPW, WPAFB, OH

March 2026

Disclaimer Statements

- Unless otherwise noted, imagery in this document are property of the U.S. Air Force
- The views expressed are those of the authors and do not reflect the official guidance or position of the United States Government, the Department of Defense the United States Air Force or the United States Space Force .

Clearances

- This presentation was cleared as Distribution A (Distribution Unlimited)

Introduction

❖ **New LOIS and LARD ATD Production: First Time in 25 Years**

❖ **Collaborated with AFLCMC/ROU**

→ Provided new LOIS and LARD ATDs

❖ **Comparison Testing Conducted**

→
- Mass Properties
- Horizontal Impulse Accelerator (HIA)
- Vertical Deceleration Tower (VDT)

Objectives

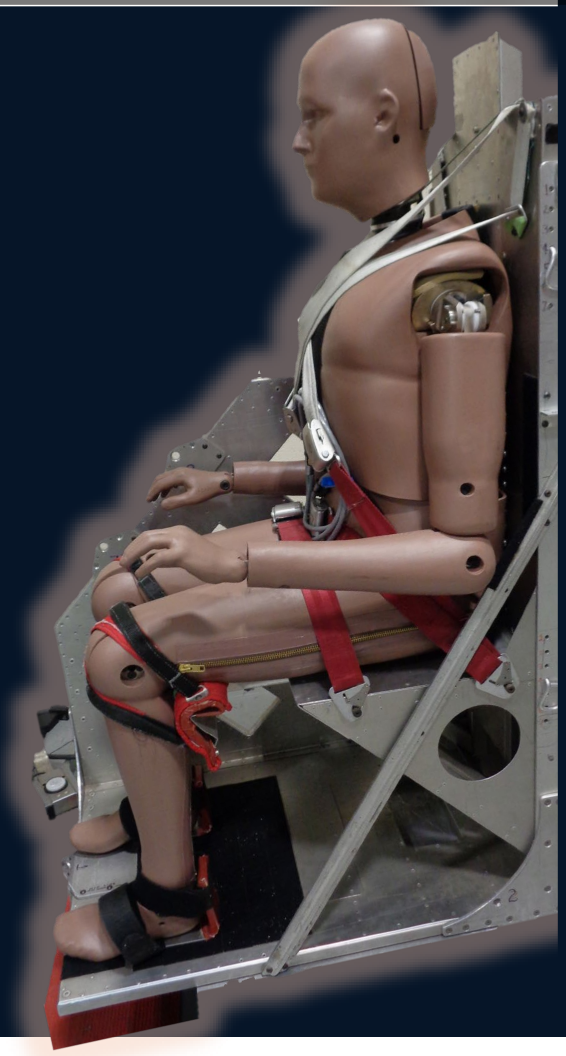

1. Evaluate ATD Segment Weight, Center of Gravity, and Moment of Inertia to determine if differences exist between Legacy vs New Segments.

2. Evaluate Seated, Full Body ATD Weight, Center of Gravity, and Moment of Inertia (with instrumentation and data acquisition system) to determine if differences exist between Legacy vs New in a fully built configuration.

Methods: Weight Calculation

- Test articles secured in support box (12 different sizes)
- Weight: Electronic Scale
- Support Box data subtracted later
- Repeated for each segment

ATD	Weight
Legacy LOIS	101 lb
New LOIS	102 lb

ATD	Weight
Legacy LARD	241 lb
New LARD	242 lb

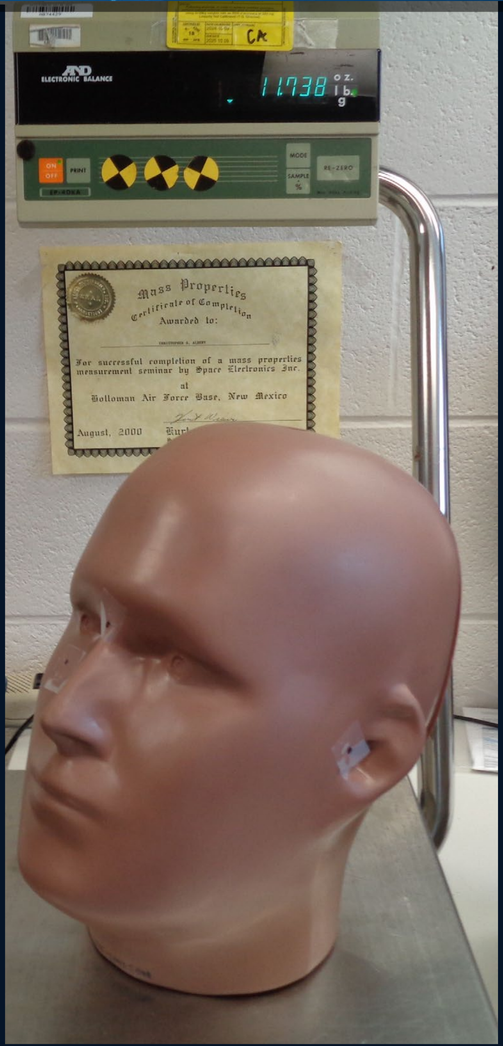

Methods: Center of Gravity Calculation

- ❖ Electronic Scale
- ❖ Reaction Moment Table
- ❖ Box initially included in measurement

Configurations

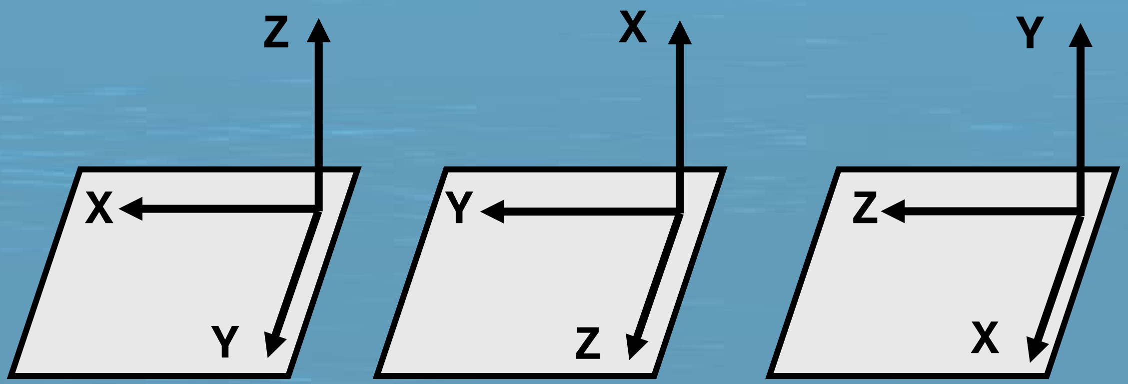

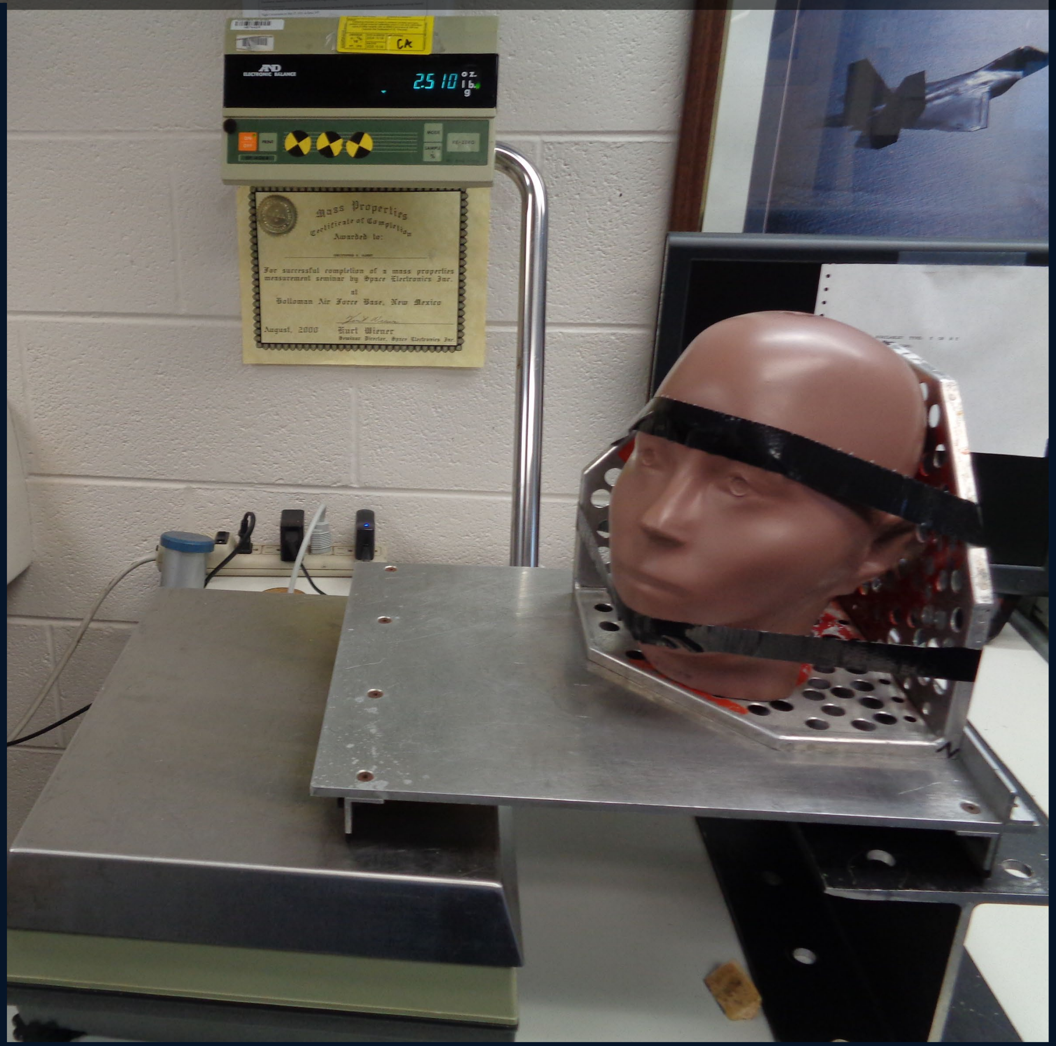

Methods: Center of Gravity Calculation

❖ Removal of box:

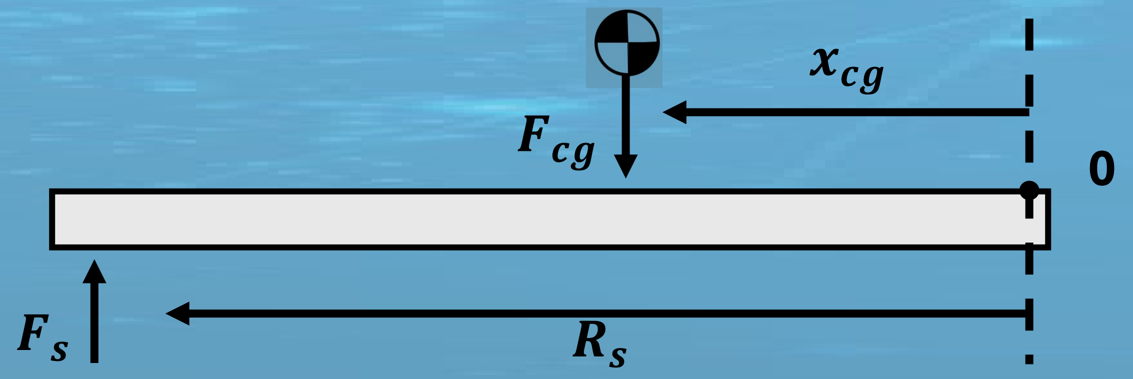

$$x_T = \frac{F_{cg}x_{cg} - F_B x_B}{F_T}$$

Repeat for X, Y, and Z

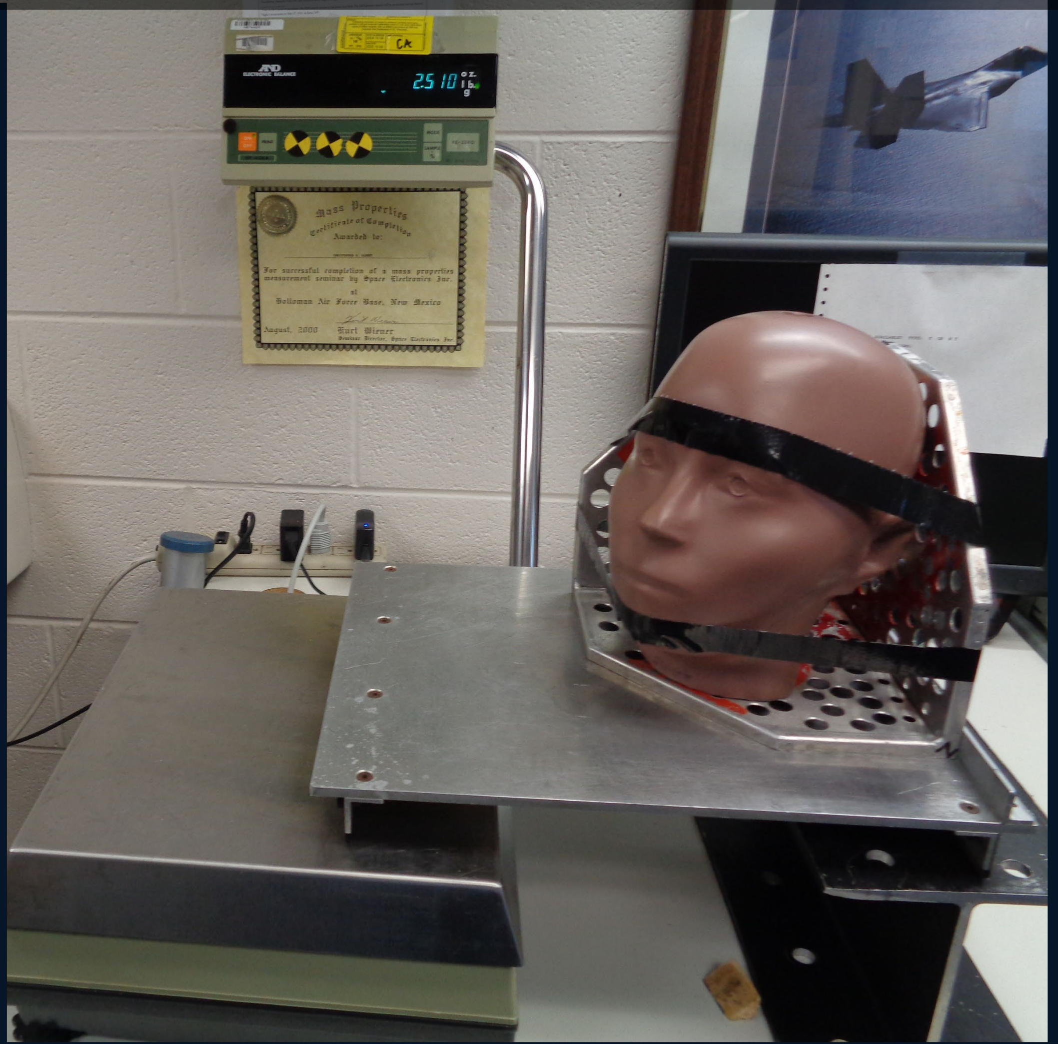

Methods: Principal Moments of Inertia

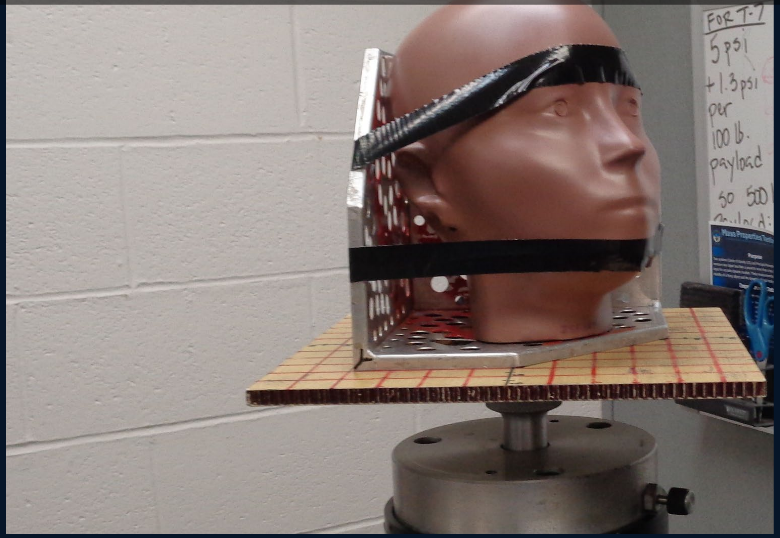

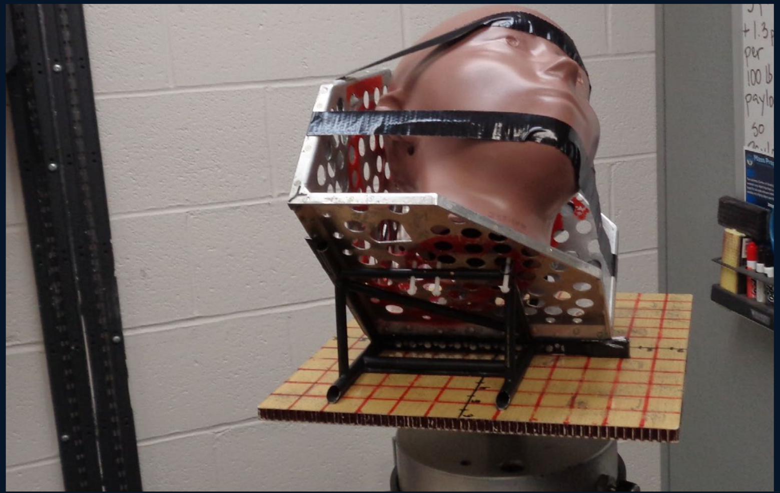

- Instruments used: Space Electronics XR-50 (all segments <50 lb.) & Space Electronics GB3300AX
- Composite placed about test article's CG
- 3 Cardinal Axes MOIs
  - Ix, Iy, Iz
- 3 Non-Cardinal Axes MOIs
  - Ixy, Iyz, Ixz

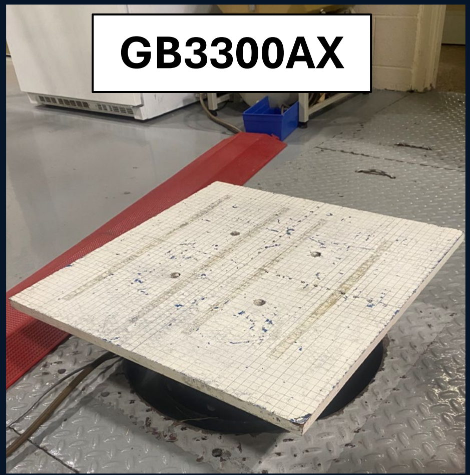

Methods: Center of Gravity Calculation

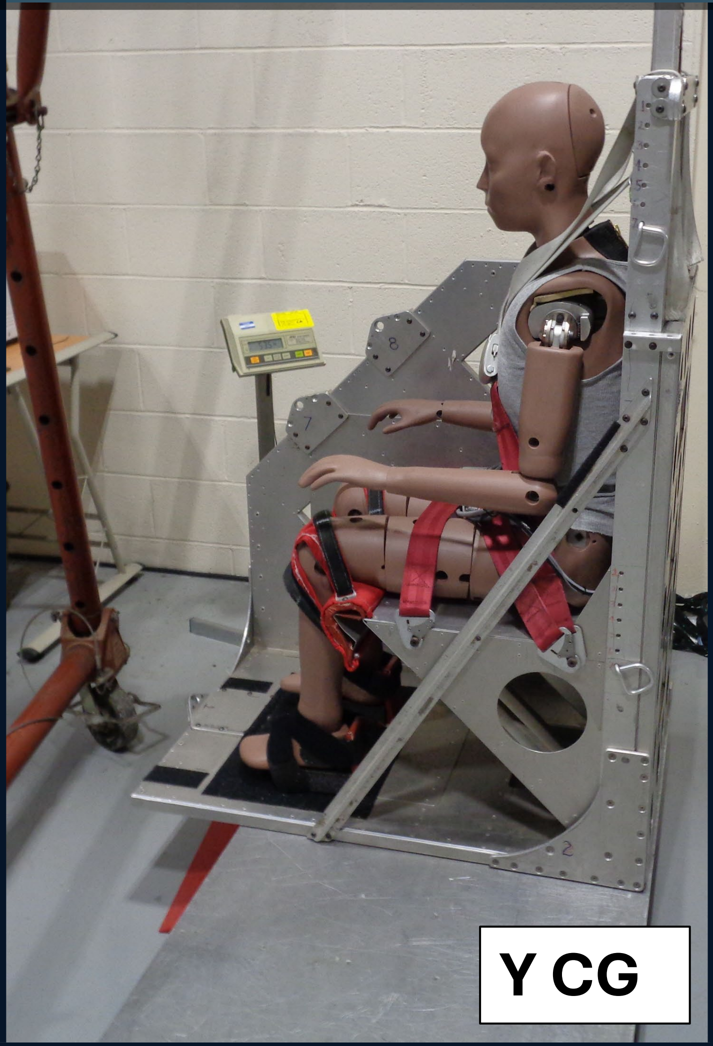

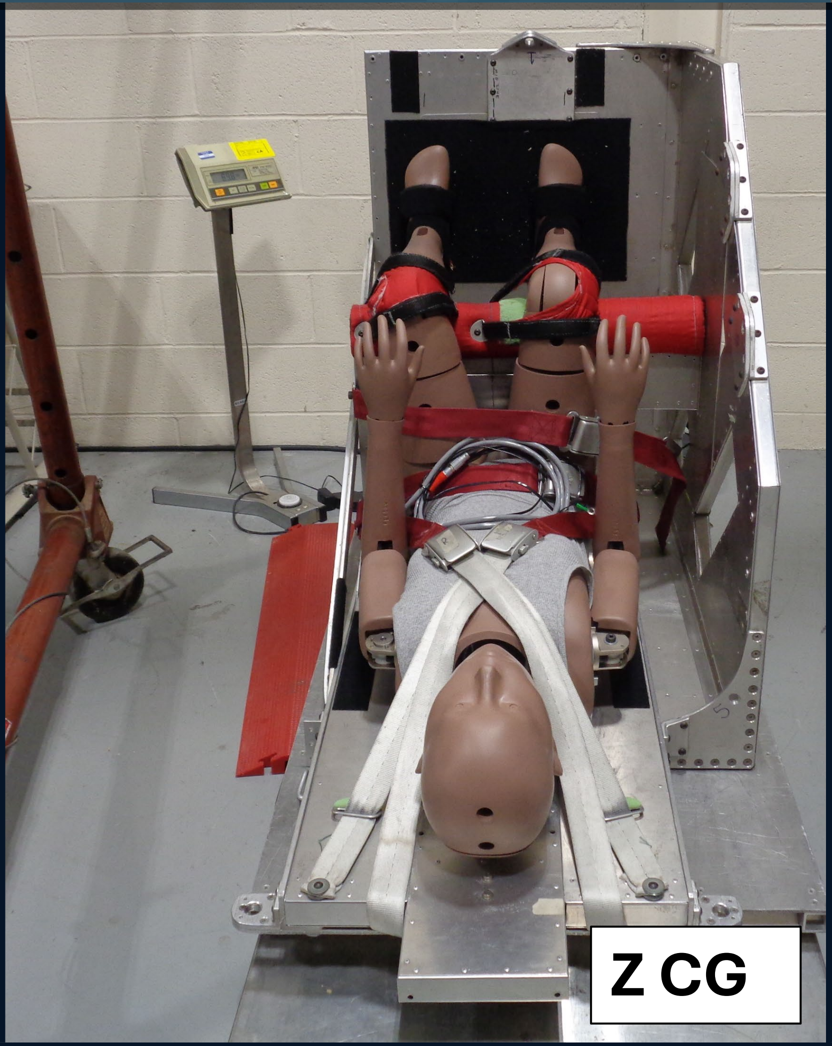

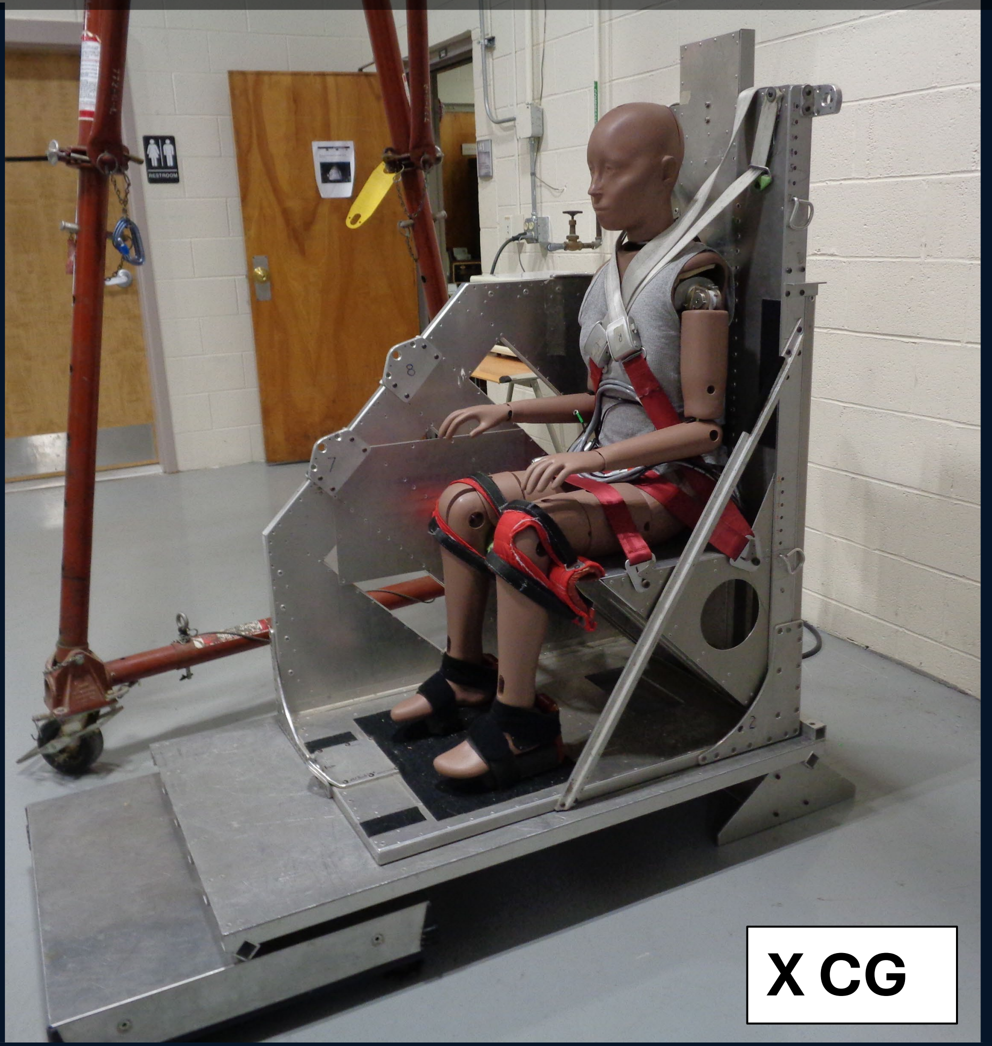

Methods: Principal Moments of Inertia

- ❖ Process repeated for full body LOIS and LARD

Methods: Transformation of Data

- ❖Instrument Used: Faro Arm
- ❖ Digitized points taken: box edges, test article
- ❖Landmarks digitized to set-up segment origin and coordinate system
- ❖Transform data from box coordinate system to segment-based coordinate system w/ predetermined origin

Results: Segment Weight & CG

Legacy LOIS

Segment	Weight (lb)	CG X(in)	CG Y(in)	CG Z(in)
Head	8.70	0.58	-0.11	1.95
Lower Leg	5.91	-0.03	0.1	-5.91
Thigh	8.19	6.35	-0.14	-0.33
Upper Arm	1.53	0.05	-0.1	-4.65
Forearm	1.42	-0.09	0.1	-3.44
Pelvis	19.00	1.31	0.00	-0.4
Thorax	31.01	1.21	-0.05	5.81

New LOIS

Segment	Weight (lb)	CG X(in)	CG Y(in)	CG Z(in)
Head	8.91	0.55	-0.10	1.88
Lower Leg	5.62	0.07	0.00	-5.66
Thigh	8.70	7.36	-0.06	-0.21
Upper Arm	1.50	0.01	0.1	-4.66
Forearm	1.39	-0.11	0.1	-3.34
Pelvis	18.34	1.38	-0.03	-0.42
Thorax	31.80	0.8	0.2	5.55

Results: Segment Weight & CG

New vs Legacy LOIS

- Percent Difference:

Segment	Weight	X CG % Diff	Z CG % Diff
Head	2.42 %	-5.17%	-3.59%
Lower Leg	-4.91%	-333.33%	-4.23%
Thigh	6.22%	15.91%	-36.36%
Upper Arm	-1.96%	-80.00%	0.22%
Forearm	-2.11%	22.22%	-2.91%
Pelvis	-3.47%	5.34%	5.00%
Thorax	2.55%	-33.88%	-4.48%

Results: Segment Weight & CG

Legacy LARD

Segment	Weight (lb)	CG X(in)	CG Y(in)	CG Z(in)
Head	11.62	0.56	-0.07	2.03
Lower Leg	12.74	-0.11	-0.01	-8.05
Thigh	28.33	8.95	0.30	-0.10
Upper Arm	7.43	-0.09	-0.07	-7.04
Forearm	5.06	-0.16	-0.02	-4.73
Pelvis	32.92	1.32	0.11	-0.53
Thorax	72.89	1.45	-0.02	7.46

New LARD

Segment	Weight (lb)	CG X(in)	CG Y(in)	CG Z(in)
Head	11.74	0.61	-0.10	2.04
Lower Leg	13.07	-0.06	-0.03	-8.08
Thigh	29.08	9.29	0.24	-0.12
Upper Arm	7.21	-0.10	-0.06	-6.96
Forearm	5.00	-0.14	0.14	-4.7
Pelvis	35.67	1.22	0.10	-0.39
Thorax	66.91	1.18	0.00	7.58

Results: Segment Weight & CG

New vs Legacy LARD

❖ **Percent Difference:**

Segment	Weight	X CG % Diff	Z CG % Diff
Head	1.03%	8.92%	0.49%
Lower Leg	2.59%	-45.45%	0.37%
Thigh	2.64%	3.79%	20.00%
Upper Arm	-2.96%	11.11%	-1.14%
Forearm	-1.18%	-12.5%	-0.63%
Pelvis	8.35%	-7.58%	-26.42%
Thorax	-8.20%	-12.62%	1.61%

Results: Full Body Weight & CG

Seated Full Body Legacy vs New LOIS

ATD	Weight (lb)	CG X(in)	CG Y(in)	CG Z(in)
Legacy LOIS	101.00	7.79	0.18	8.90
New LOIS	102.00	7.87	-0.04	8.89

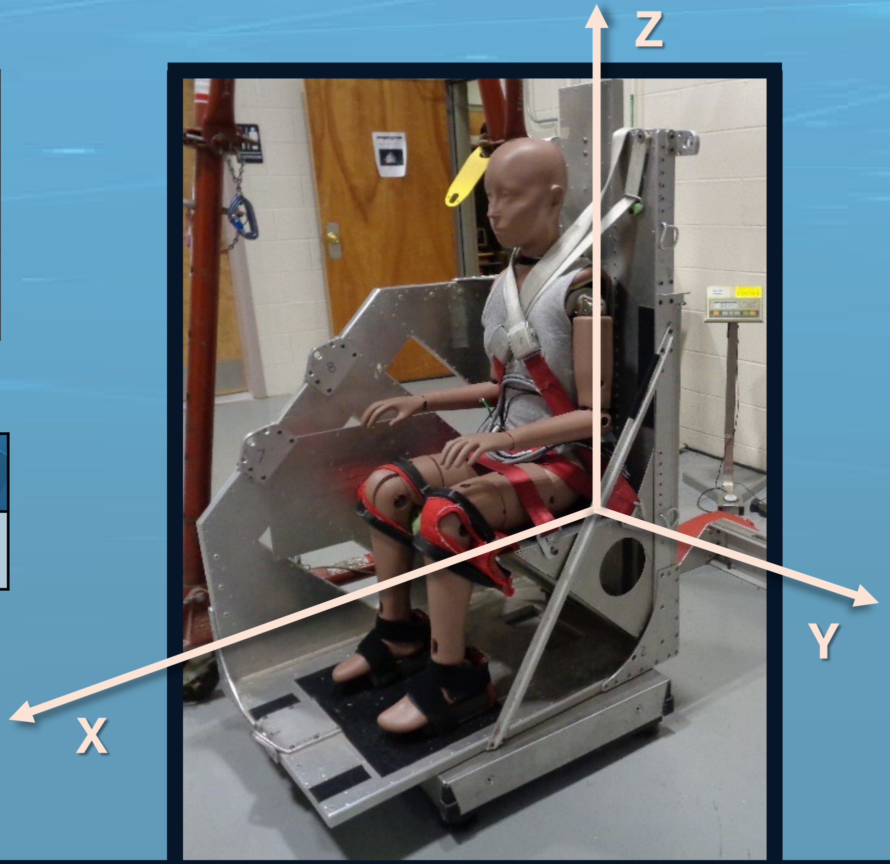

❖ Percent Difference:

X CG % Diff	Z CG % Diff
1.03%	-0.11%

❖ The 2 LOIS ATDs weighed within a pound of each other and the CGs were within 0.15 in. of each other in the forward (CGx) and upward (CGz) axes

Results: Full Body Weight & CG

Seated Full Body Legacy vs New LARD

ATD	Weight (lb)	CG X(in)	CG Y(in)	CG Z(in)
Legacy LARD	241.00	10.19	-0.10	9.90
New LARD	240.00	10.33	-0.02	9.75

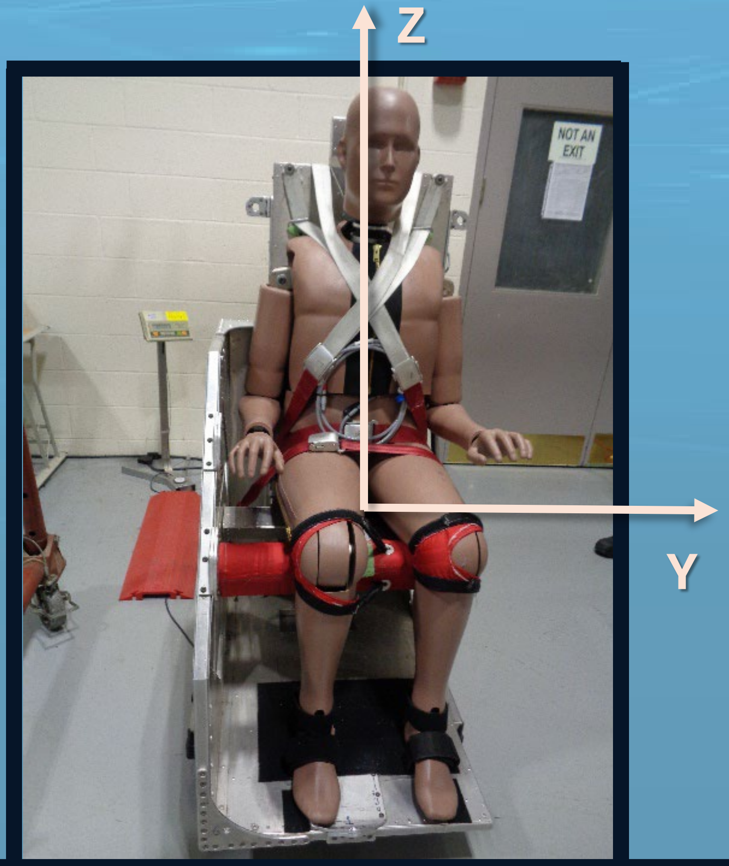

❖ Percent Difference:

X CG % Diff	Z CG % Diff
-1.35%	-1.51%

❖ The 2 LARD ATDs weighed within a pound of each other and the CGs were within 0.15 in. of each other in the forward (CGx) and upward (CGz)

Results: Full Body MOI

Seated Full Body Legacy vs New LARD

ATD	Legacy vs New	X (lb-in^2)	Y (lb-in^2)	Z (lb-in^2)
LOIS	Legacy	12699.53	14660.42	3521.60
	New	13259.17	14451.43	3729.18
LARD	Legacy	48441.99	47864.89	12662.33
	New	47505.81	48533.98	13004.64

❖ Principal moments within 1% of each other

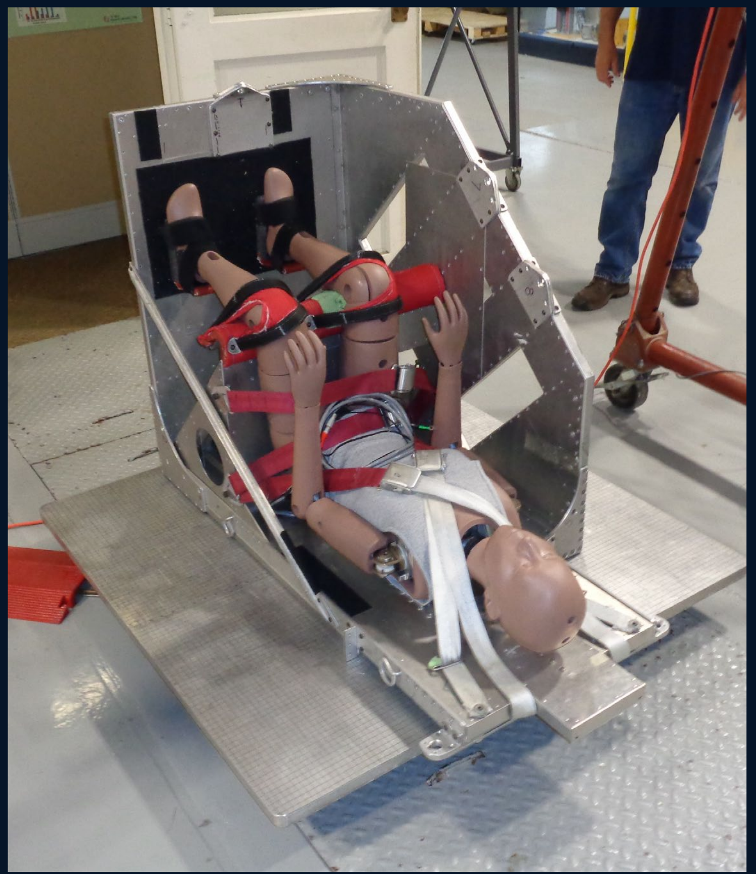

Limitations

- ❖Density of foam in lower leg in question (too squishy) → sent back after testing ended
- ❖Time constraint (few weeks to complete)
- ❖Only comparison of one Legacy and New ATD for LOIS and LARD

Conclusion

- Comparison of segmental CG: within 1 inch of each other

- Comparison of full body seated CG: with 0.15 inch of each other

- Comparison of full body seated MOI: within 1% of each other

BIODYNAMICS OV1 OVERVIEW

IDENTIFY — PREPARE — TEST — MODEL — EVALUATE

CONTACT US:

AFRLBiodynamicsLab@us.af.mil

BIODYNAMICS WEBSITE

Collins Aerospace

SPACEX

GENTEX CORPORATION

MB

NASA

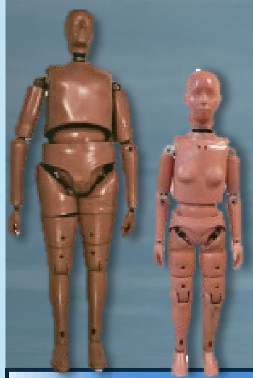

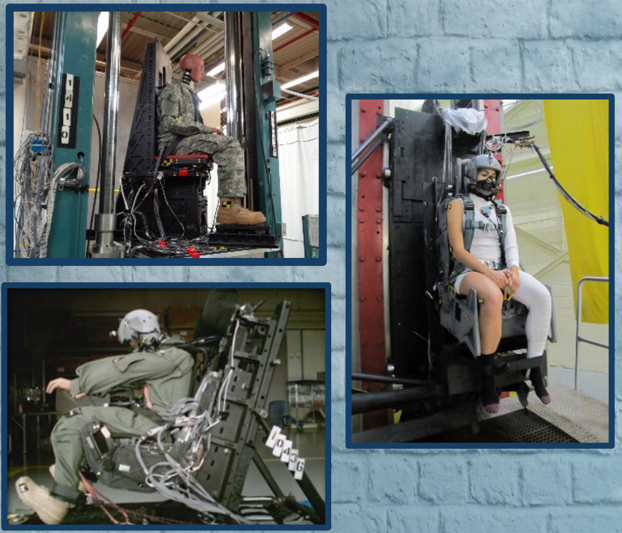

Available Facilities:

- Vertical Deceleration Tower
- Horizontal Impulse Accelerator
- Vertical Impact Device
- Vertical Impulse Accelerator
- Six Degree of Freedom Vibration System

- 3D Scanning/ Model Development
- ATD/ Scalable Occupant FE Models
- Risk Mitigation Modeling
- Digital Modeling

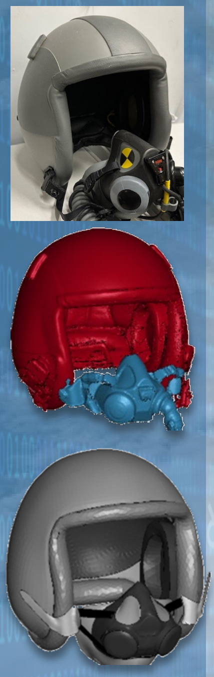

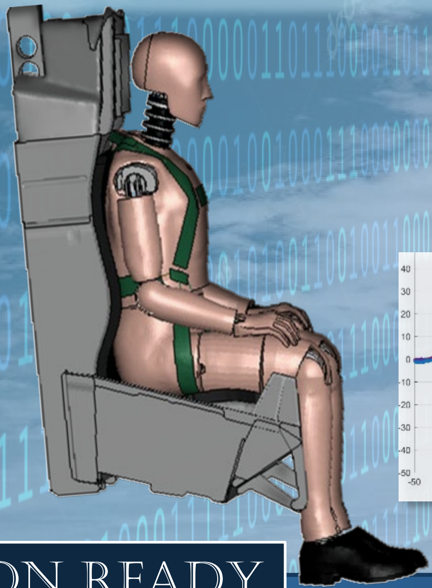

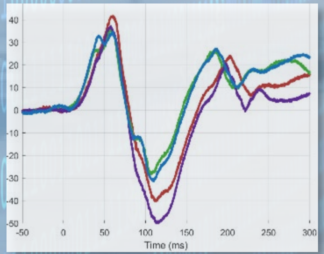

MISSION READY

QUESTIONS?

Quantifying Equivalent Muscle Reactions of a CG Adjusted Helmet

Gabriel N. Payne[1], Emily C. Deschamps[1], Alaina J. Schroeder[1], Timothy L Norman[1] & Jennifer Whitestone[2]

Cedarville University, Cedarville, OH
SENTIR Laboratories, Fairborn, OH

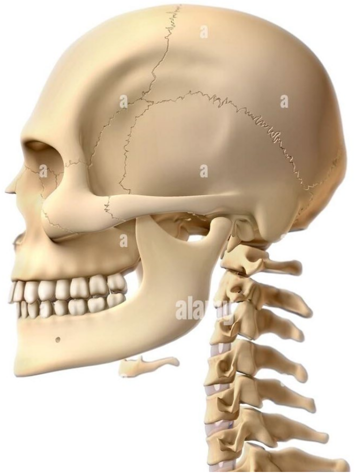

Background

Increasing Commonality of Front-Mounted Airman's Helmet Attachments

Background

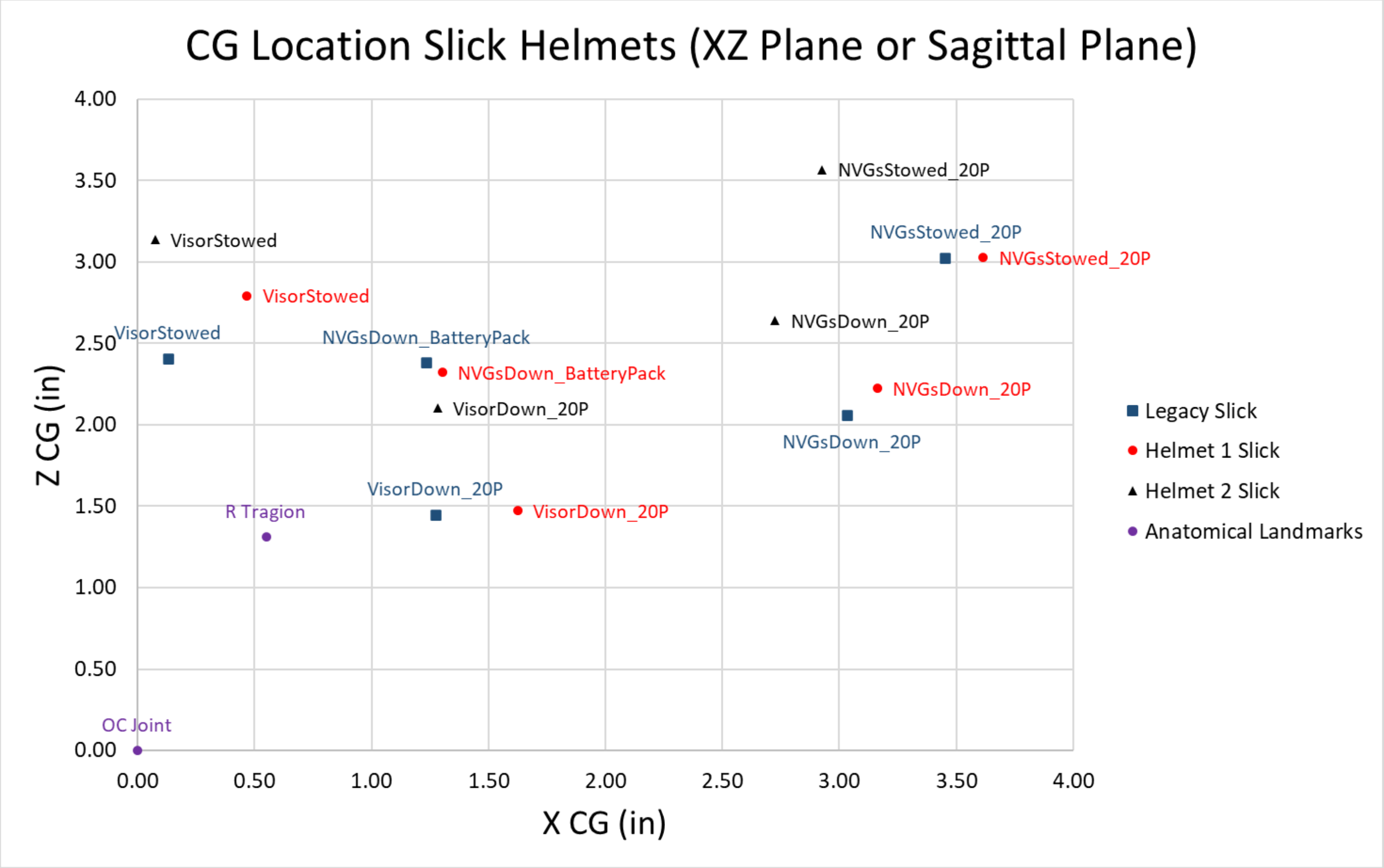

Forward CG Shifts due to Front Mounted Attachments

Figure 1 From Hicks et al., Customization of Airman's Helmet using Anthropometric Models

Background

Nominal CG Helmet **Forward CG Helmet**

Figure 1 From Callagher, Caldwell and Albery, "Neck Muscle Fatigue Resulting from prolonged wear of weighted Helmets," 2008

Background

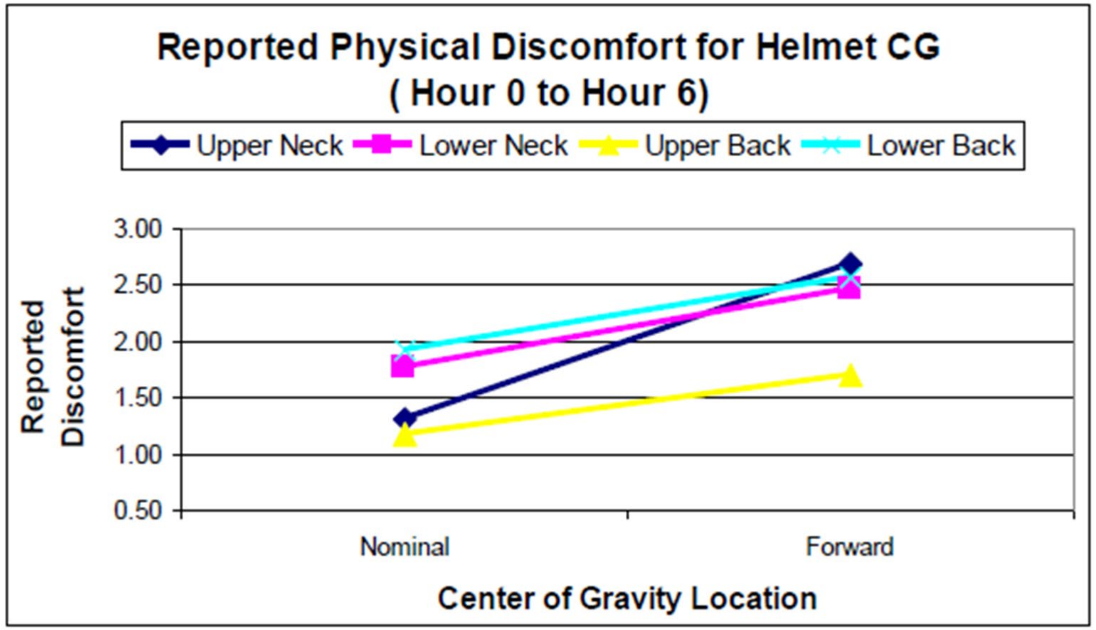

Forward CG Helmets vs Nominal CG Helmet

Figure 19 From Callagher, Caldwell and Albery, "Neck Muscle Fatigue Resulting from prolonged wear of weighted Helmets," 2008

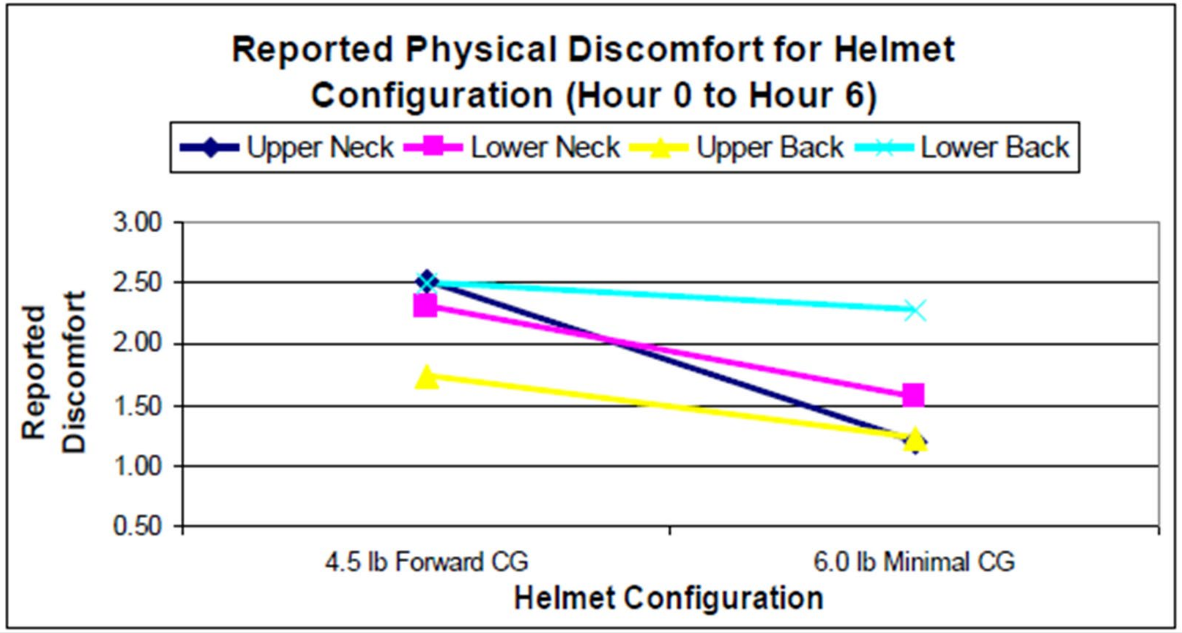

Forward CG Helmets vs Nominal CG Helmet

Figure 20 From Callagher, Caldwell and Albery, "Neck Muscle Fatigue Resulting from prolonged wear of weighted Helmets," 2008

Background

Reduced Neck Load Using Counterbalance

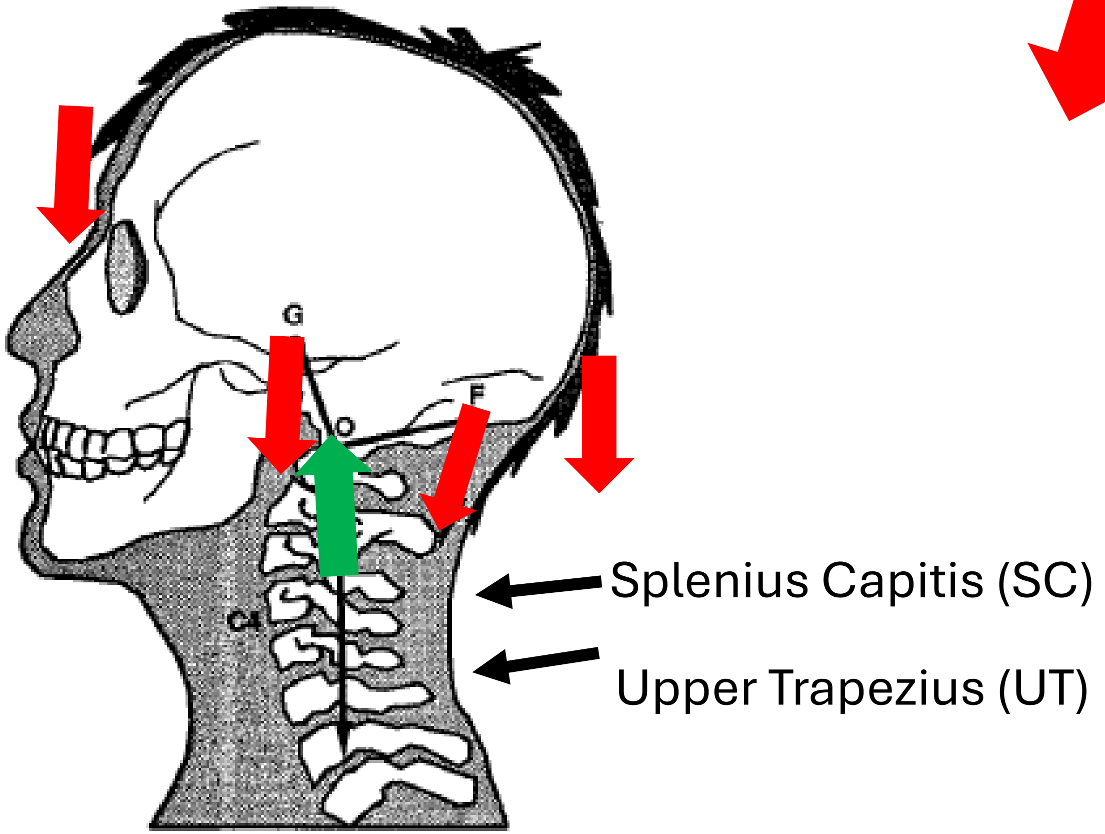

Figure 1 From Perry, Buhrman and Knox, "Biodynamic Testing of Helmet Mounted Systems," 1993 (taken from Anton, 1987)

Background

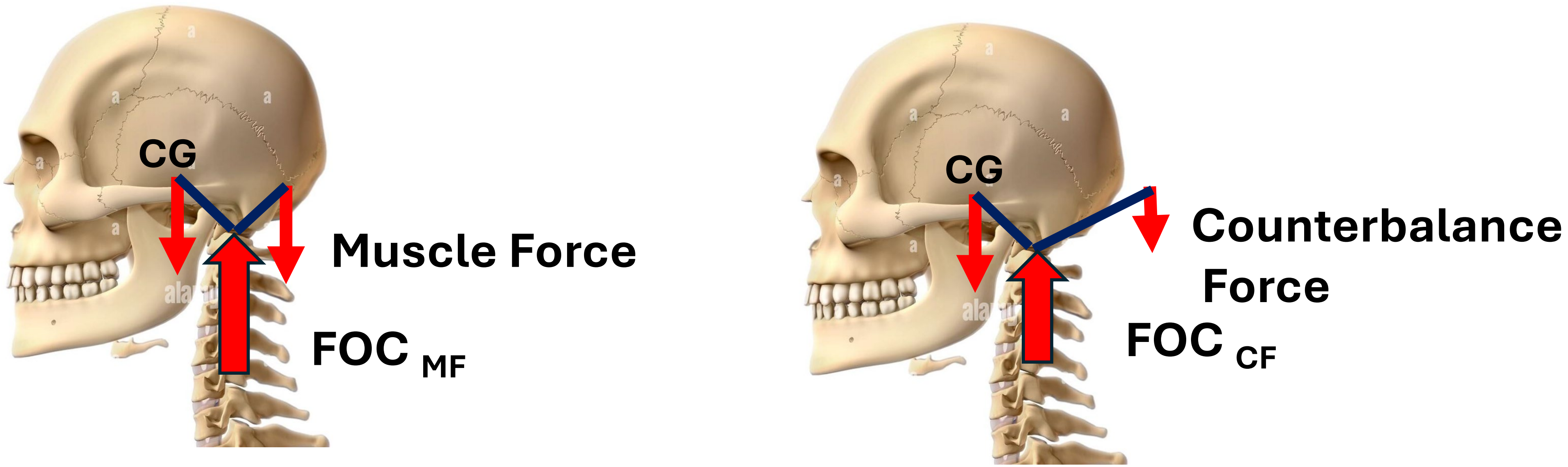

Muscle Force > Counterbalance Force

$FOC_{CF} < FOC_{MF}$

Background

Proposed Solution: Rear Mounted Helmet Weights

Based on 2D Mechanics,

- A counterbalanced Helmet significantly reduces neck muscle force
- A counterbalanced Helmet reduces force applied to the OC joint

Therefore, if true, a counterbalanced helmet should,

- Reduce Injury risk
- Reduce neck pain and neck fatigue

Key Questions

1. How much rear weight is required to mitigate the forward CG shift?
2. What is the relationship between the counterbalance weight and the neck muscle force it removes?

Main Objective

Objective:
To determine the rear attachment mass necessary to offset anterior center of gravity shift and quantify the equivalent reduction in cervical muscle forces due to rear attachment

Experimental Method:

1. Physical Model Testing
2. Data Analysis and Curve Fitting
3. Development of Numerical Model
4. Anatomical Data Research
5. Application of Numerical Model

Physical Model Testing

Fulcrum-Scale Method

- Determines location of the helmet's center of gravity
- Requires only one scale for measurement

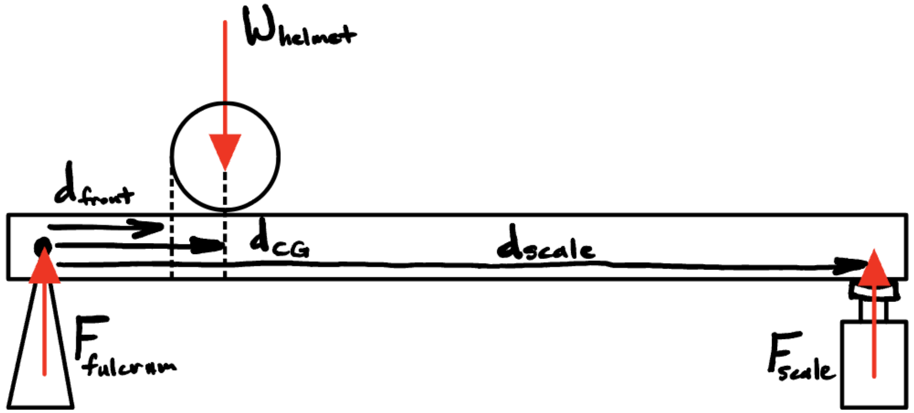

$$\Sigma M_{fulcrum} = 0 = F_{scale} d_{scale} - W_{helmet} d_{CG}$$

$$\boldsymbol{d_{CG} = \frac{F_{scale} d_{scale}}{W_{helmet}}}$$

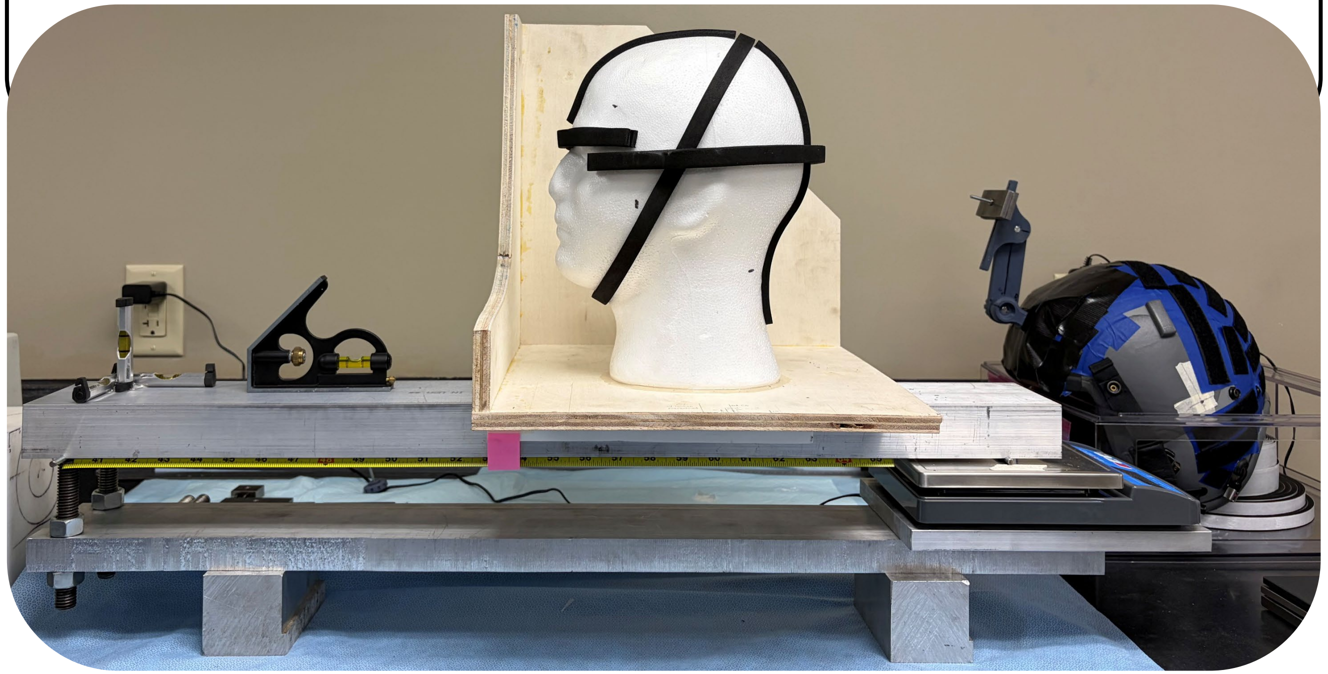

Physical Model Testing

True Equipment Configuration

Variable CG Helmet Configuration

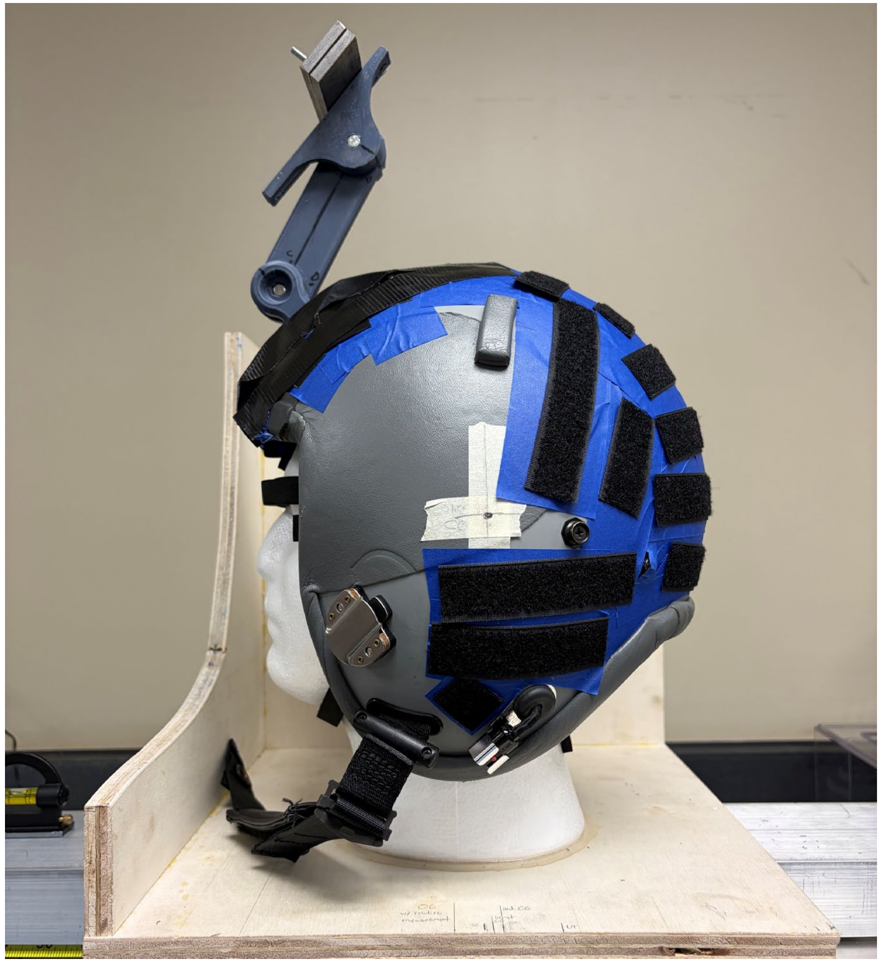

Physical Model Testing

Rear Attachment Mounts

Rear Attachment Weights

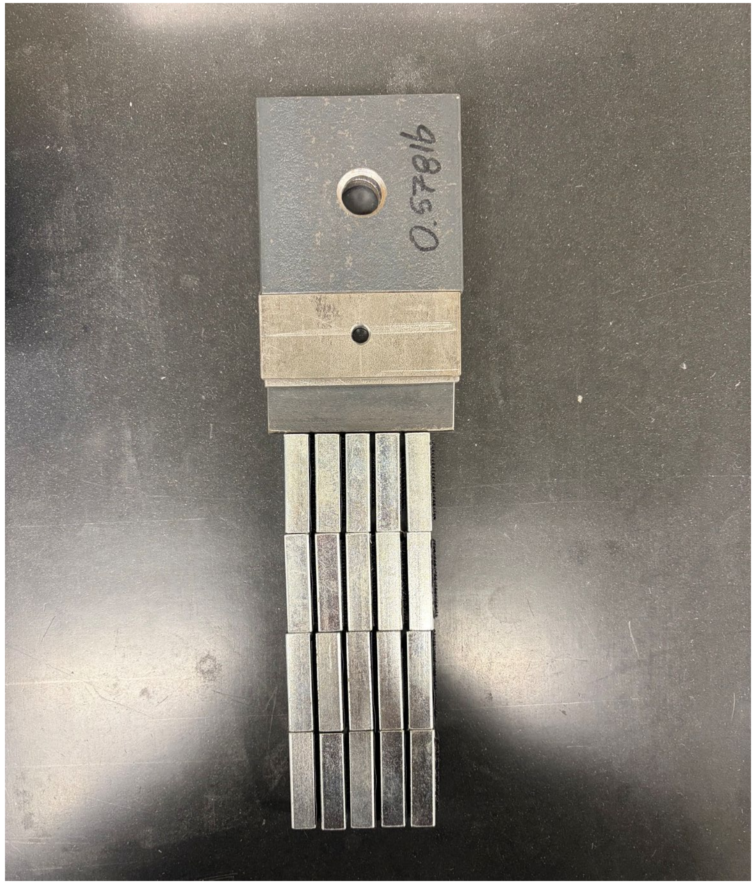

Data Analysis and Curve Fitting

1. Plot data for specific equipment configurations
2. Obtain curve fit data using LSCF
3. Determine ideal counterbalance weight for each configuration

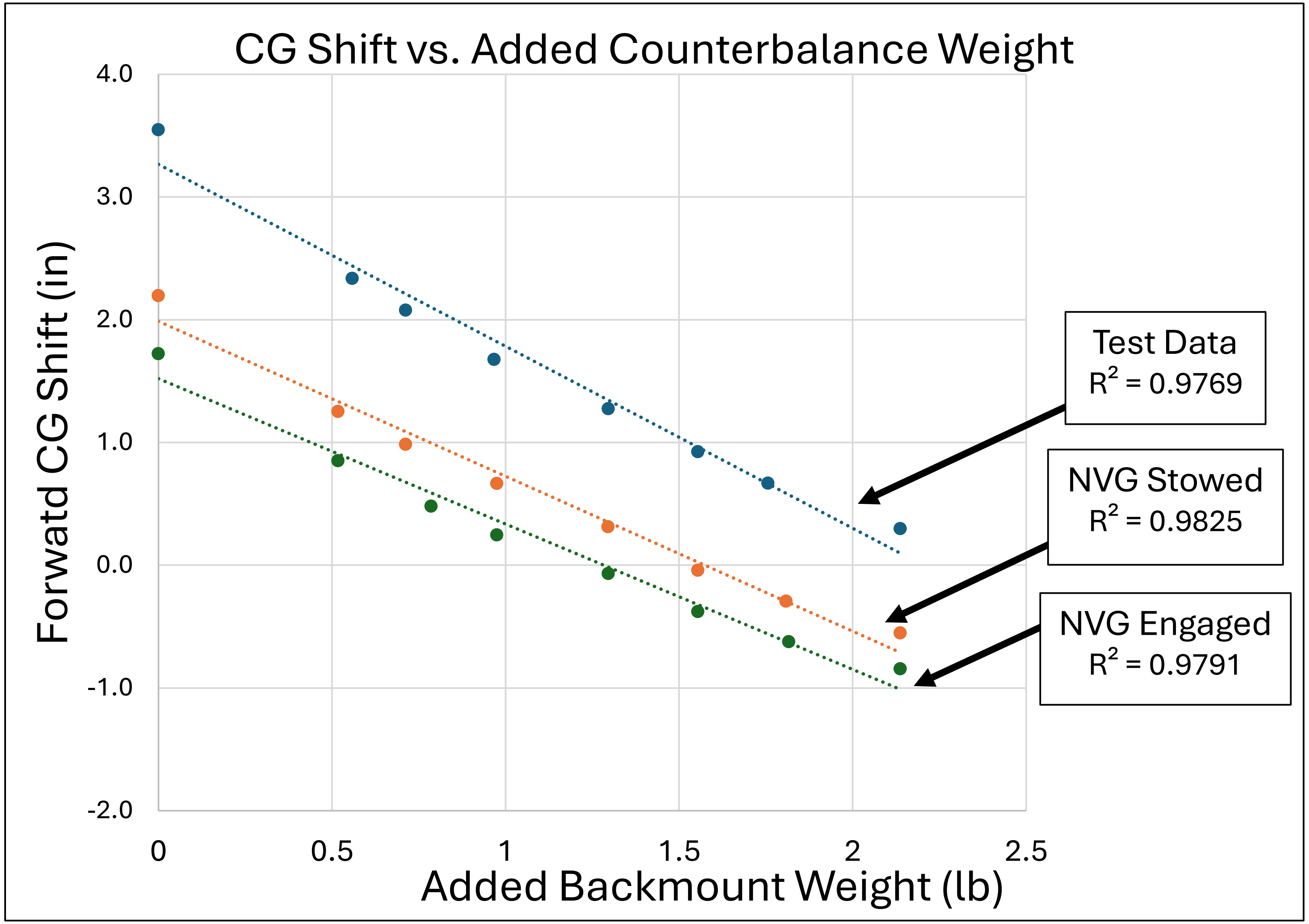

Main Objectives

Objective:

~~To determine the rear attachment mass necessary to offset anterior center of gravity shift~~ and quantify the equivalent reduction in cervical muscle forces due to rear attachment

Experimental Method:

1. ~~Physical Model Testing~~
2. ~~Data Analysis and Curve Fitting~~
3. Development of Numerical Model
4. Anatomical Data Research
5. Application of Numerical Model

Development of Numerical Model

Free Body Diagram of Helmet Model

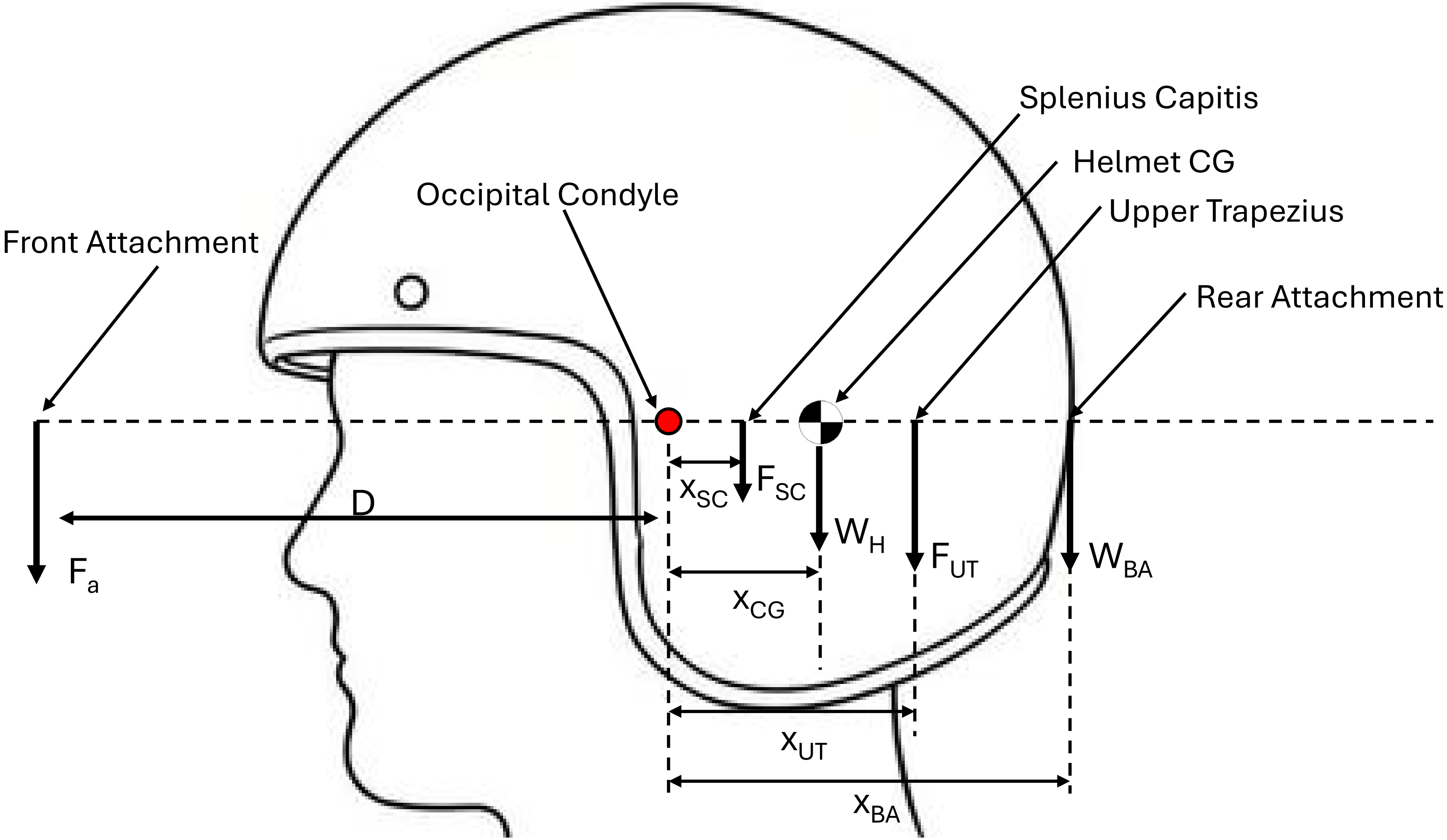

Development of Numerical Model

Key Assumptions

- Neglect Head CG
  - Assume Head is balanced prior to Helmet
- Neck muscle response is contained in SC and UT
- Balanced helmet generates zero muscle force
- Muscle Force can be modeled as purely vertical (conservative)

Development of Numerical Model

Considering **no back attachment**, sum moments about the OC:

$$\sum M_{OC} = -W_H * x_{HCG} - \boldsymbol{F}_{SC} * x_{SC} - \boldsymbol{F}_{UT} * x_{UT} + F_a * D = 0 \quad (1)$$

Solve for front-attachment moment F_a*D

$$F_a * D = \boldsymbol{W_H} * \boldsymbol{x_{HCG}} + \boldsymbol{F_{SC}} * \boldsymbol{x_{SC}} + \boldsymbol{F_{UT}} * \boldsymbol{x_{UT}} \quad (2)$$

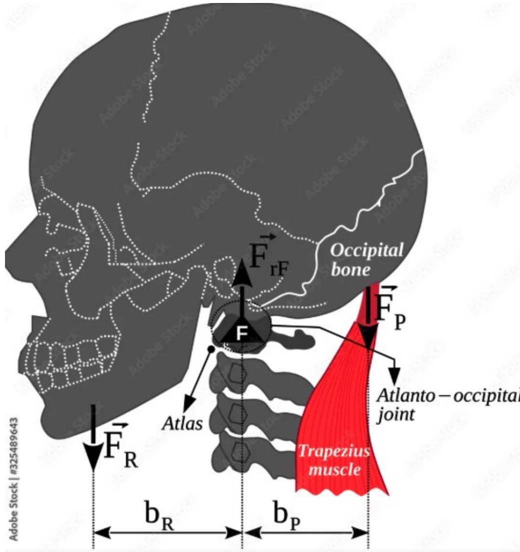

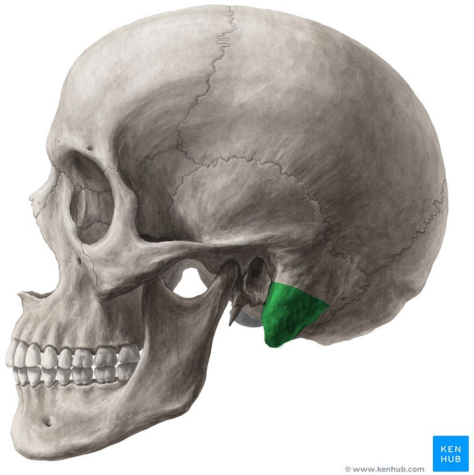

Development of Numerical Model

Considering **added back attachment with NO muscle forces**, sum moments about the OC:

$$\sum M_{OC} = -W_H * x_{HCG} - W_{\mathrm{BA}} * x_{\mathrm{BA}} + F_{\mathrm{a}} * D = 0 \qquad (3)$$

Solve for front-attachment moment F_a*D

$$F_{\mathrm{a}} * D = \boldsymbol{W_H} * \boldsymbol{x_{HCG}} + \boldsymbol{W}_{\mathrm{BA}} * \boldsymbol{x}_{\mathrm{BA}} \qquad (4)$$

Development of Numerical Model

Equate expressions for front attachment moment to obtain muscle/back attachment relationship

$$F_a * D = \boldsymbol{W_H} * \boldsymbol{x_{HCG}} + \boldsymbol{F_{SC}} * \boldsymbol{x_{SC}} + \boldsymbol{F_{UT}} * \boldsymbol{x_{UT}} \quad (2)$$

$$F_a * D = \boldsymbol{W_H} * \boldsymbol{x_{HCG}} + \boldsymbol{W}_{\mathrm{BA}} * \boldsymbol{x}_{\mathrm{BA}} \quad (4)$$

$$\boldsymbol{F_{SC}} * \boldsymbol{x_{SC}} + \boldsymbol{F_{UT}} * \boldsymbol{x_{UT}} = \boldsymbol{W}_{\mathrm{BA}} * \boldsymbol{x}_{\mathrm{BA}} \quad (5)$$

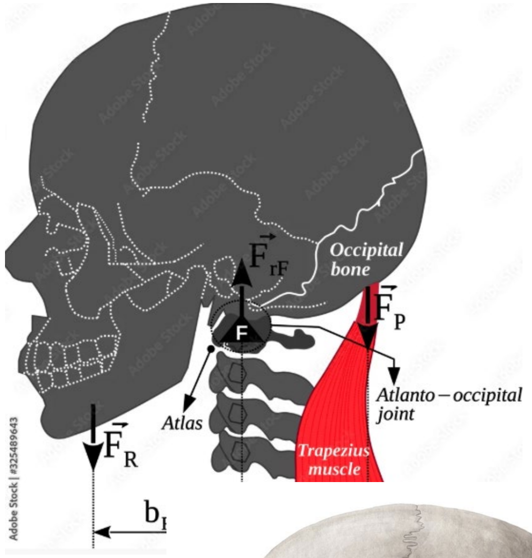

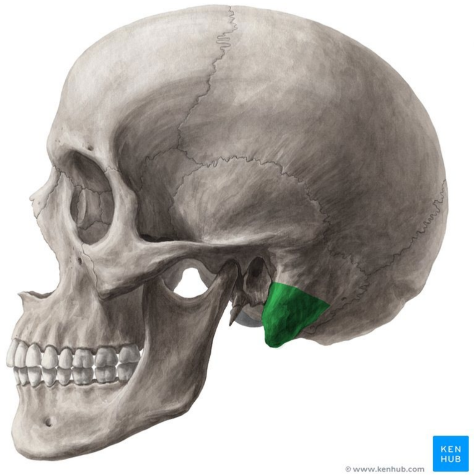

Development of Numerical Model

Assuming constant specific tension, relative muscle strength was estimated based on proportional physiological cross-sectional area *(Kawakami et al., 1994)*

$$\frac{F_{SC}}{A_{SC}} = \frac{F_{\mathrm{UT}}}{A_{\mathrm{UT}}} \qquad (6)$$

$$\boldsymbol{F_{SC} = \frac{F_{UT}}{A_{UT}} * A_{SC}} \qquad (7)$$

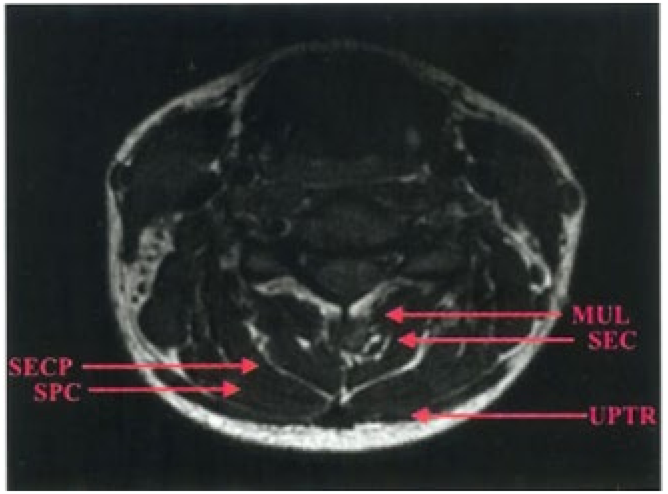

Development of Numerical Model

We combine expressions (5) and (7) to obtain the final expression used to quantify equivalent cervical neck forces removed by counterbalance weight

$$F_{UT} = W_{BA} * \frac{x_{BA}}{x_{SC} * \frac{A_{SC}}{A_{UT}} + x_{UT}} \qquad (8)$$

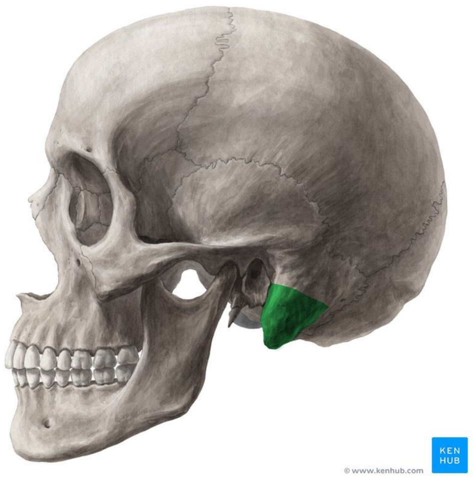

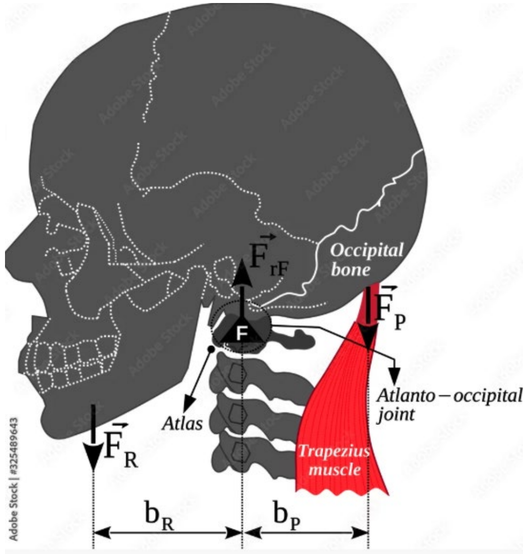

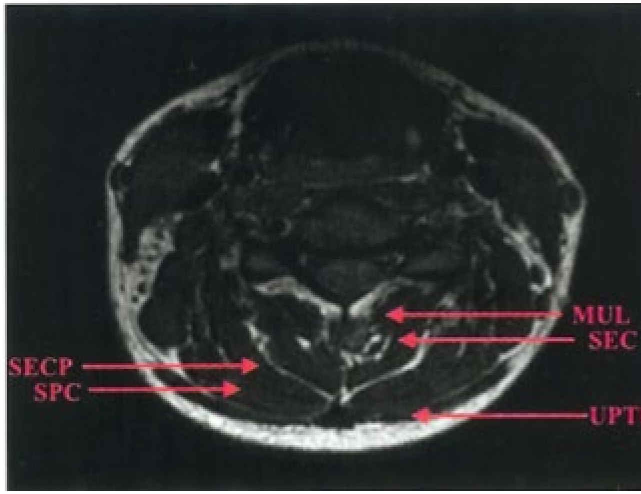

Anatomical Data Research

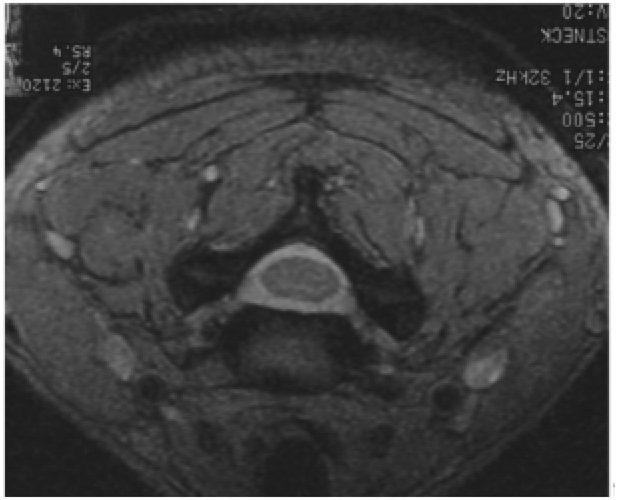

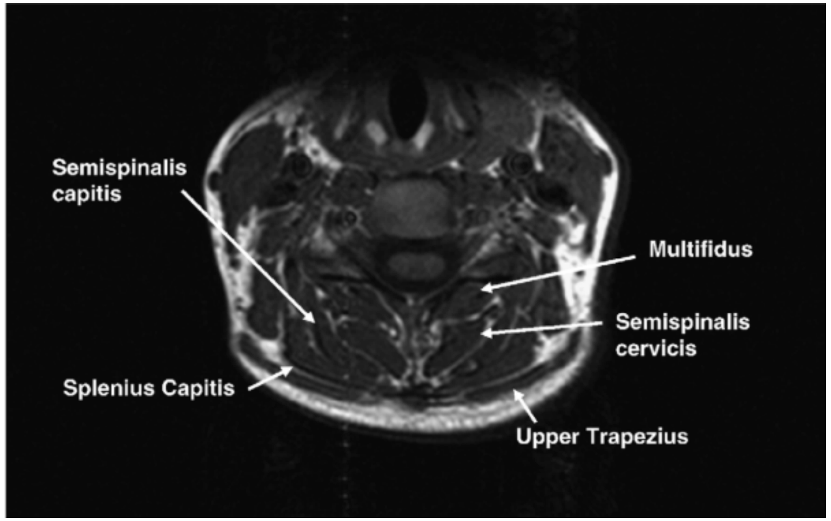

Averaged Relative Cross Sectional Area of Primary Muscles (rCSA)*	
Upper Trapezius	77.25 mm^2
Splenius Capitis	156.25 mm^2

*obtained from MRI study of the cross-sectional area for the cervical extensor musculature in patients with persistent whiplash associated disorders (WAD) (Elliott et al., 2008)

Anatomical Data Research

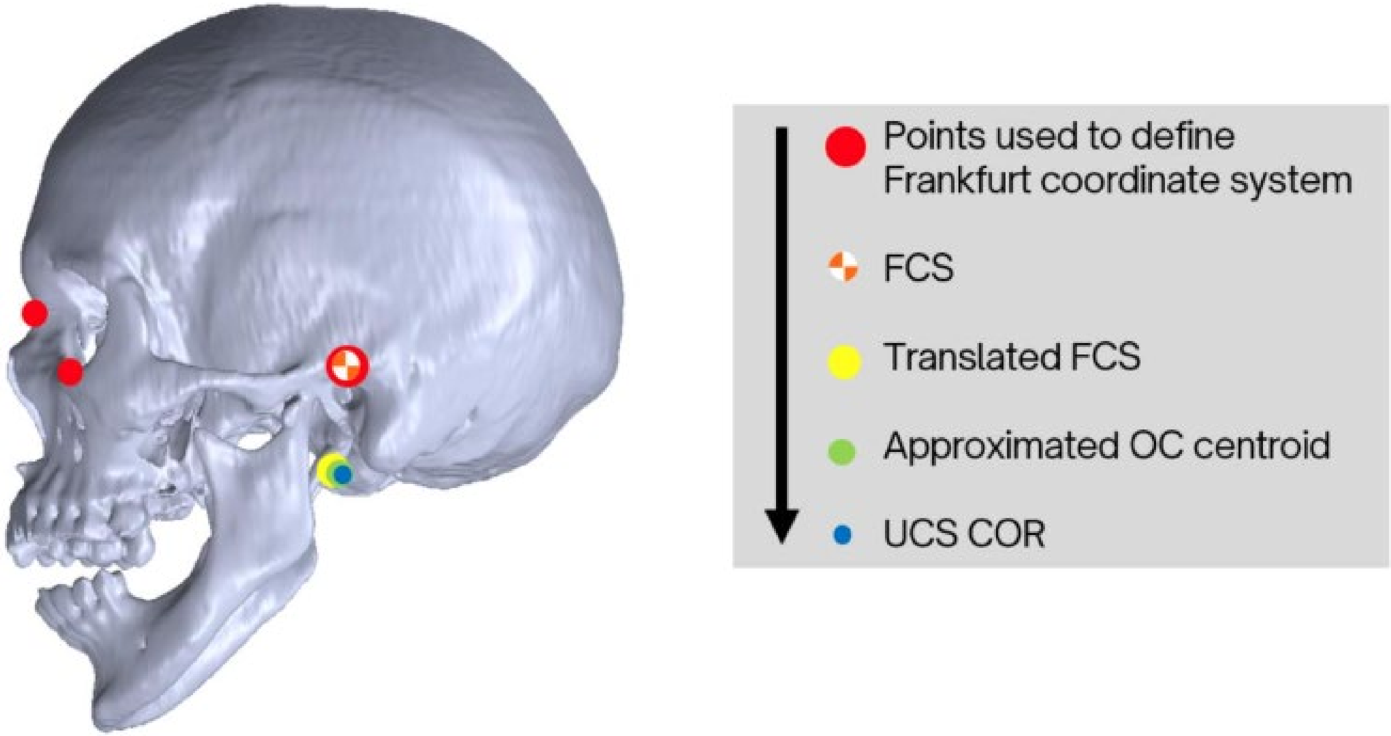

Muscle Type	OC-Muscle Distance as a Percentage of Max AP Skull Width*	OC Distance in the Model Case
Upper Trapezius	6.5%	0.463 in
Splenius Capitis	32.5%	2.316 in

*obtained from Pilot Helmet Customization (Krueger et al., 2024)

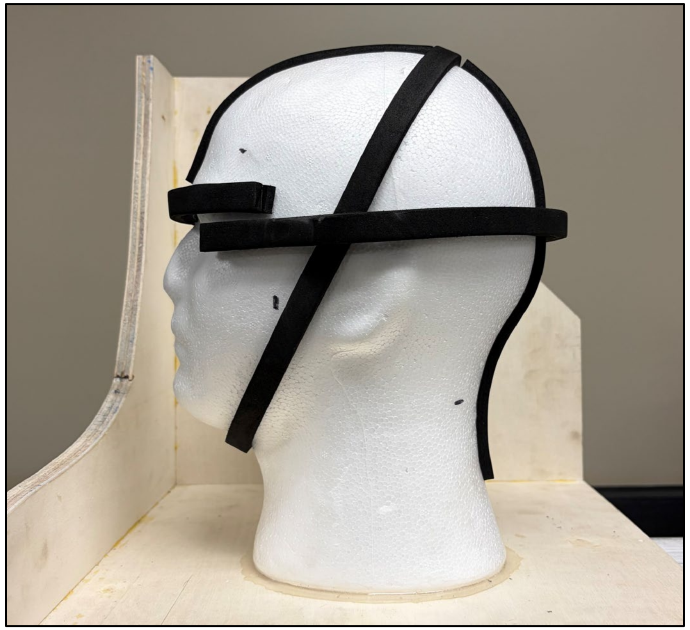

Model Max AP Width = 7.125 in

Application of Numerical Model

Completed Expressions relating Rear Weight and Cervical Muscle Load

$$F_{UT} = W_{BA} * \frac{x_{BA}}{x_{SC} * \frac{A_{SC}}{A_{UT}} + x_{UT}}$$

$$F_{SC} = \frac{F_{UT}}{A_{UT}} * A_{SC}$$

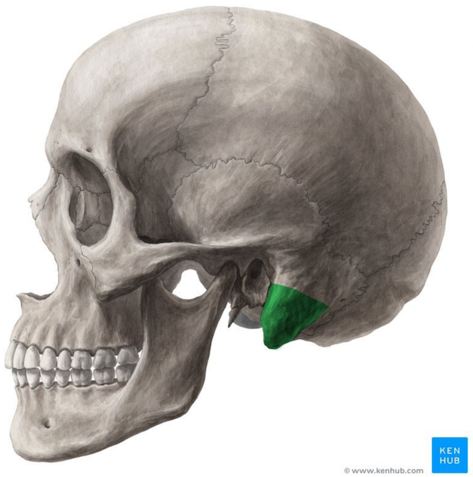

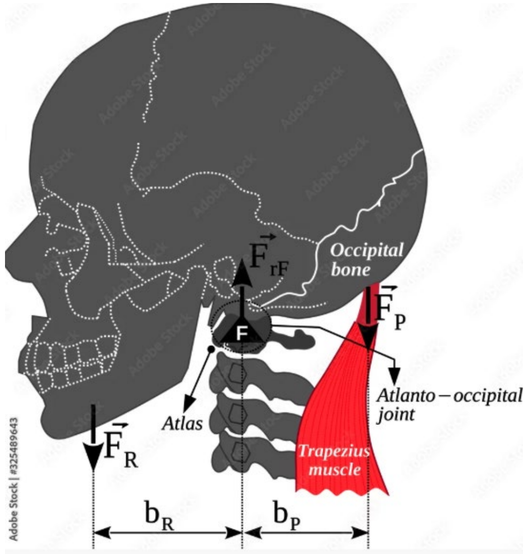

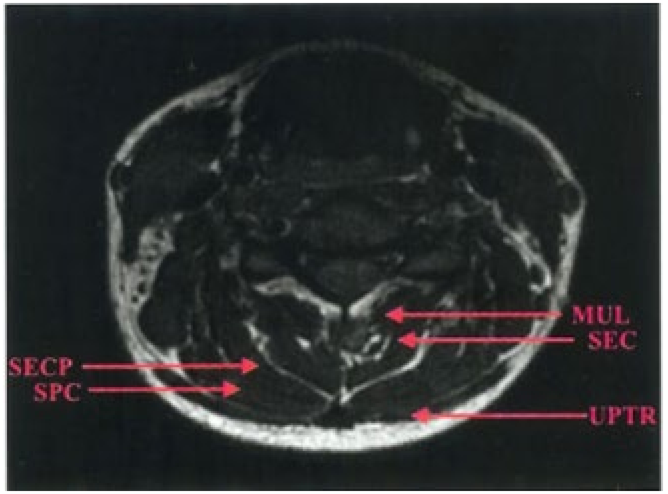

Results

Summary of Experimental Results

Configuration	Front Attachment Added Weight (lb)	Ideal Back Attachment Weight (lb)	Total Combined Weight (lb)
NVG Stowed	2.181	1.574	5.734
NVG Engaged	2.181	1.283	5.443

Configuration	Equivalent UT Force (lb)	Equivalent SC Force (lb)	Total Muscle Force (lb)	Net Correction Force Difference (lb)
NVG Stowed	2.547	5.152	7.699	6.125
NVG Engaged	2.076	4.199	6.276	4.993

Results

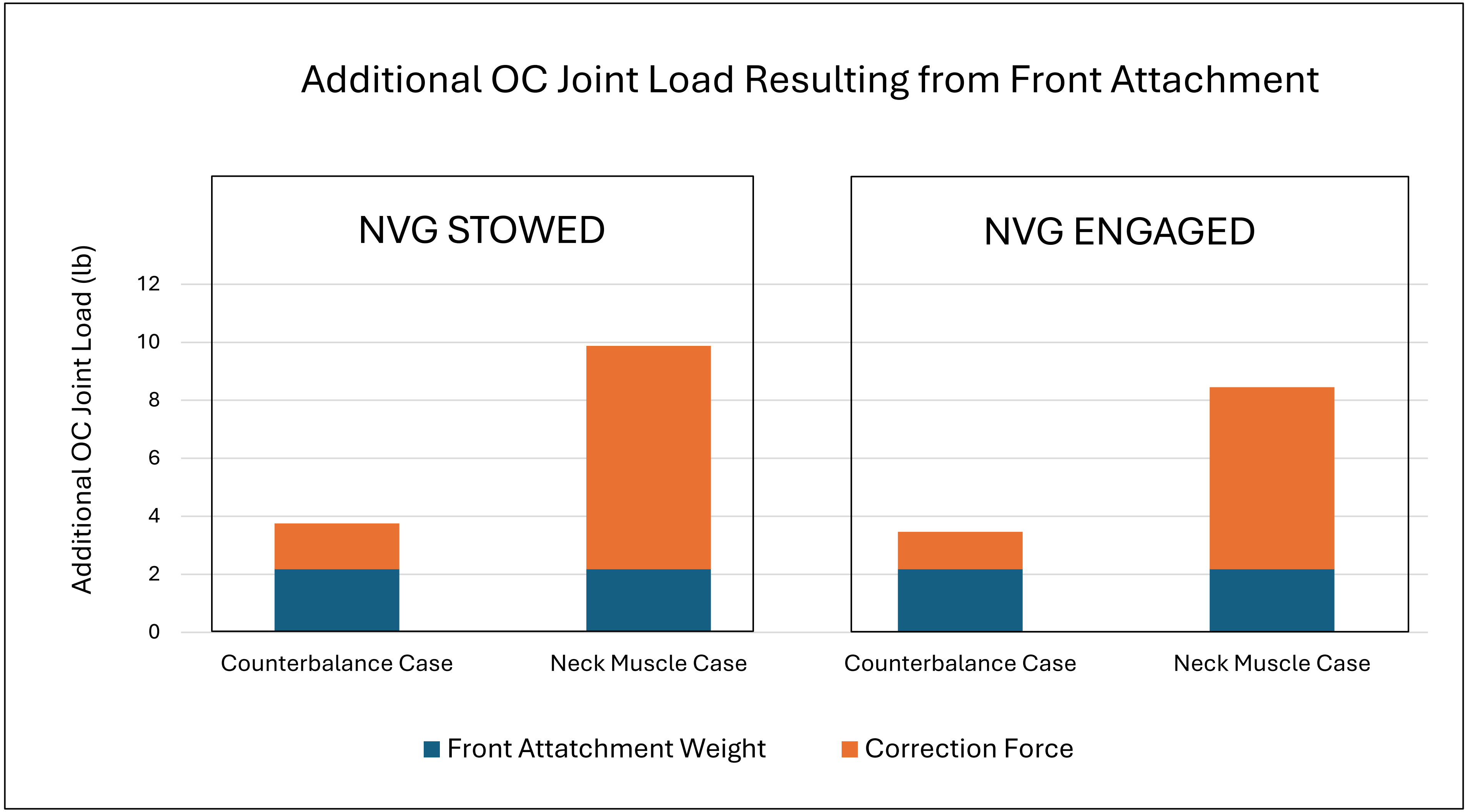

Additional OC Joint Load Resulting from Front Attachment
NVG STOWED
NVG ENGAGED
Additional OC Joint Load (lb)
12
10
8
6
4
2
0
Counterbalance Case
Neck Muscle Case
Counterbalance Case
Neck Muscle Case
Front Attatchment Weight
Correction Force

Results

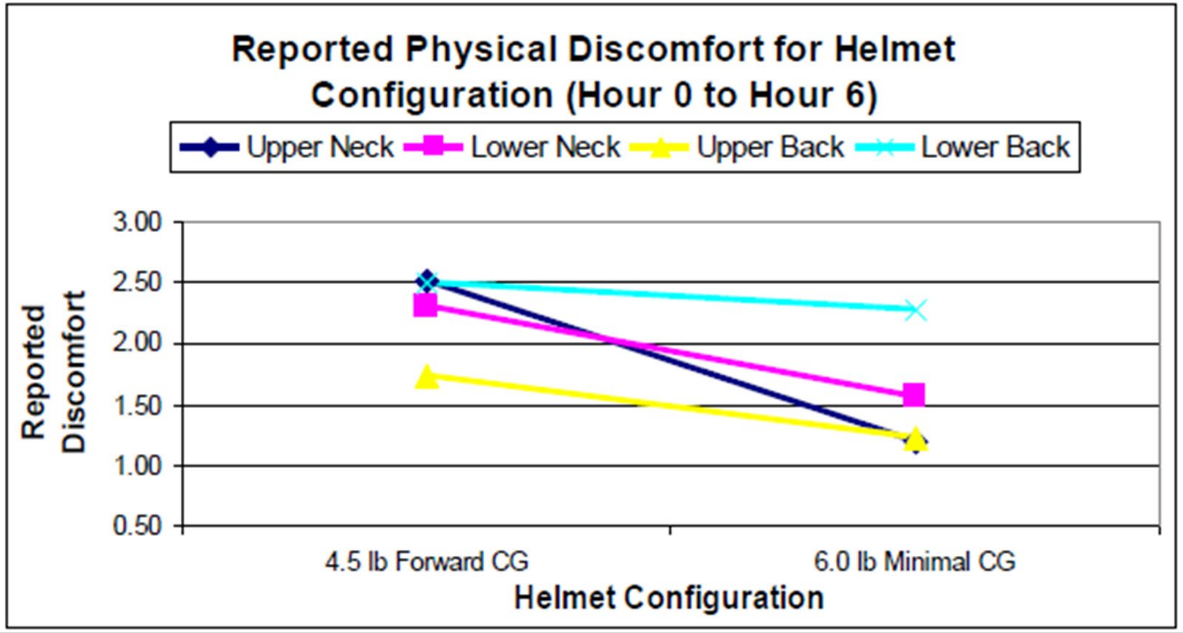

Forward CG Helmets vs Nominal CG Helmet

Figure 20 From Callagher, Caldwell and Albery, "Neck Muscle Fatigue Resulting from prolonged wear of weighted Helmets," 2008

Discussion of Results

Key Insights:

- The difference is highly magnified in the worse loading cases

Configuration	Anterior CG Shift (in)	Net Correction Force Difference (lb)
NVG Stowed	2.197	6.125
NVG Engaged	1.726	4.993

Discussion of Results

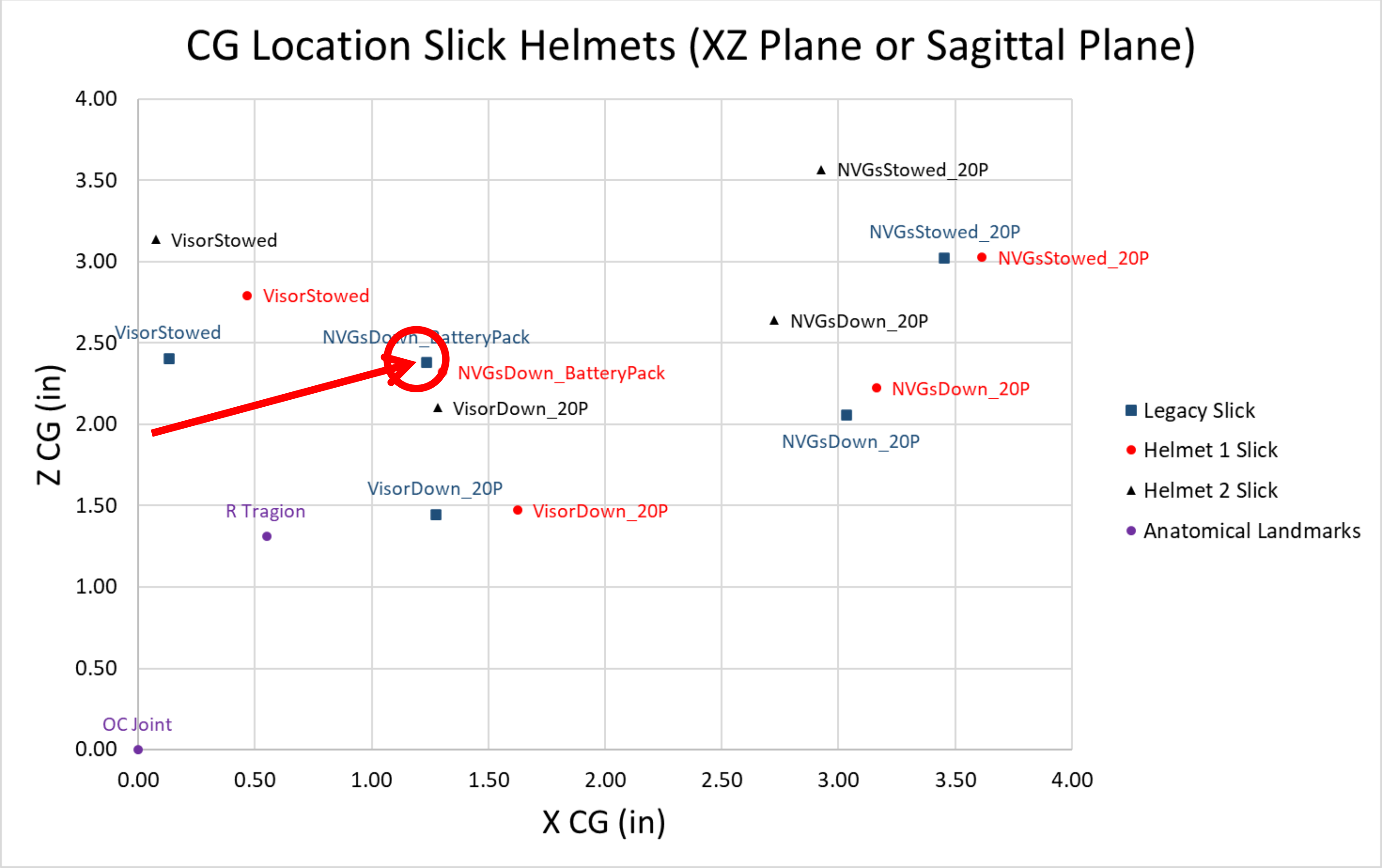

Forward CG Shifts due to Front Mounted Attachments

Figure 1 From Hicks et al., Customization of Airman's Helmet using Anthropometric Models

Discussion of Results

Key Insights:

- The difference is highly magnified in the worst loading case
- Rear counterbalances reduce load applied to the OC joint due to forward moment by more than 4.5x
    - In each case, the rear attachment is 20.4% of the equivalent cervical correction load

Discussion of Results

Key Insights:

- The difference is highly magnified in the worst loading case
- Rear counterbalances reduce load applied to the OC joint due to forward moment by more than 4.5x
- Sustained neck load removed by counterbalance is significant in magnitude, with exacerbated effects in high-g situations (ejection, maneuvers, etc.)

Discussion of Results

Future Efforts:

1. Modify rear counterbalance to account for frontal plane CG shift due to lateral redistribution (medial-lateral symmetry)
2. Expand anatomical-mechanical model to more clearly define effects of CG shift mitigation
3. Investigate negative moment of inertia for counterbalances and front attachments

Thank you

Segmentation Analysis of The Human Head: Influences of Tissue Property Assumptions, Coordinate System and Gender on Mass Properties

[1]Jennifer J Whitestone
[2]Timothy L Norman, [2]Thaddeus Krueger, [2]Kimiye Wenger, [2]Josiah Zurick,

[1] Solutions Through Innovation Technologies, Inc. (STI-Tec, Inc.)
[2]School of Engineering and Computer Science Cedarville University,

OCT 2024

"Leveraging Knowledge Assets and Emerging Technologies"

DEVELOPMENT AND VALIDATION OF MANIKIN HEADS FOR HELMET TESTING

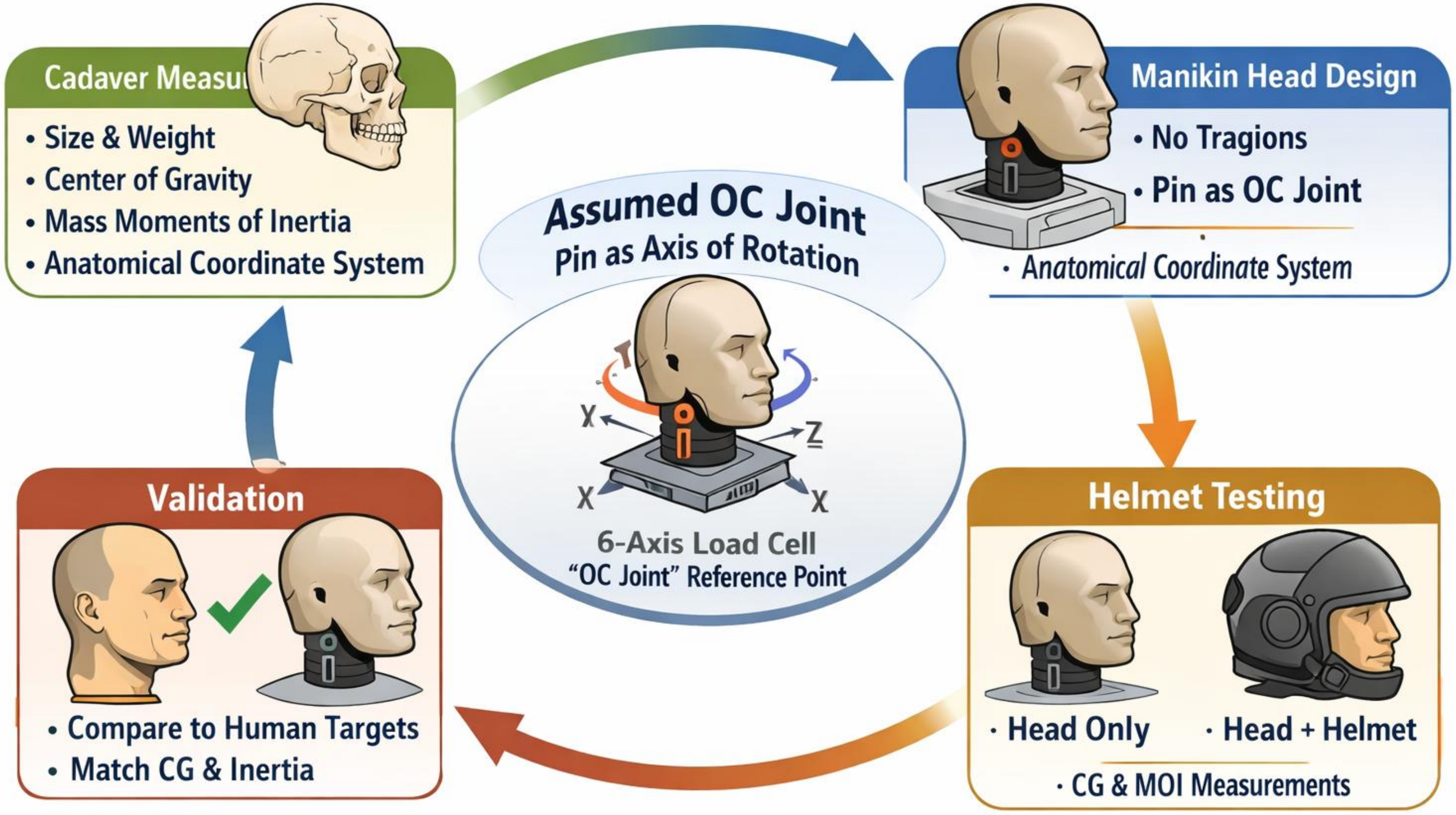

ADAM HEADFORM USED TO HELMET MASS PROPERTIES MEASUREMENTS

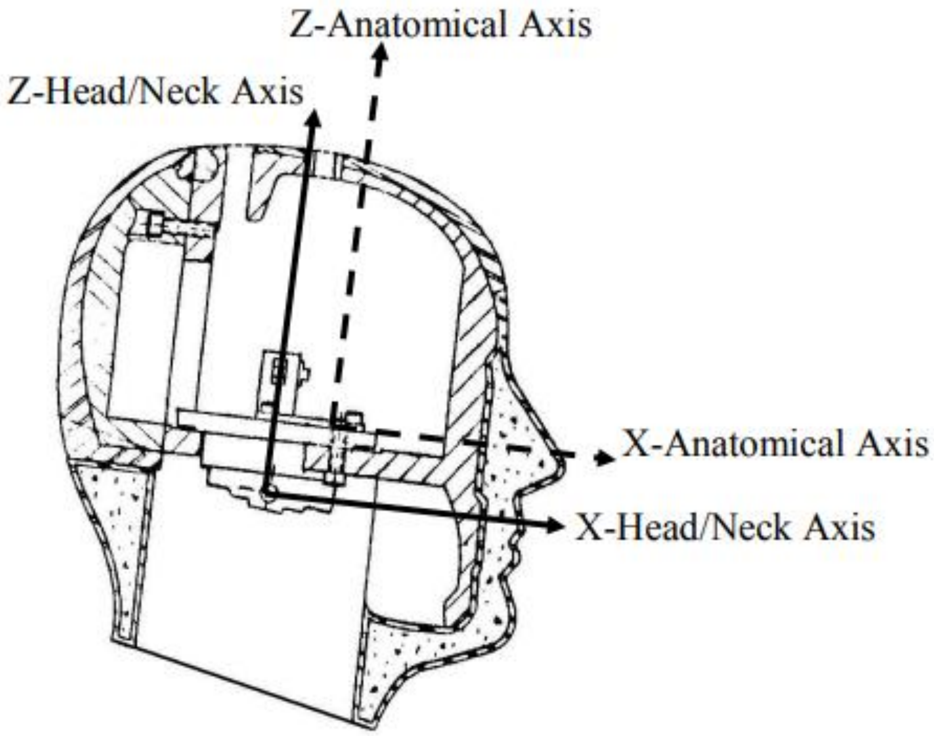

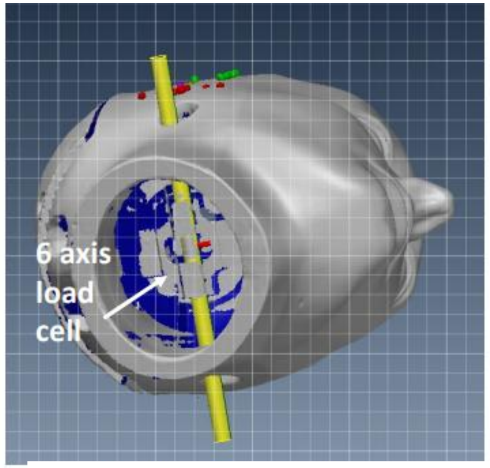

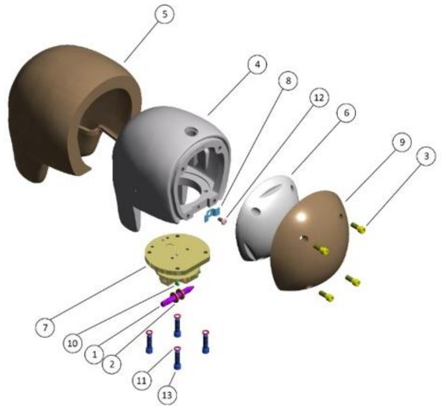

- Early assumptions – 80s
- Representation of human head on which to measure helmet systems
- No ears, so Tragion location was estimated from literature on landmarks
- OC joint was assumed to be coincident with the pin joint axis of the 6-axis load cell
- Tragion location measured from the OC joint and marked on headform
- Headform was ballasted to weigh male head weight from cadaver studies
- Headform was ballasted to represent cadaver CG location
- Skin does not slip wrt hardware

"Leveraging Knowledge Assets and Emerging Technologies"

Evolution of Helmet Mass & CG Criteria ("Knox Box")

1 Foundational Physics (Pre-1990s)
- Forward CG increases neck moment

2 Perry et al. (1993)
Tested helmets in catapult ejection
- ~2.27 kg (5 lb) acceptable
- +1.27 cm forward CG → 222 N neck load

3 Privitzer, King, Darrah (1990s)
- Confirmed forward CG increases neck moment
- Refined mass + CG design limits

4 Knox Box (2000s)
- Defined safe CG + mass 'box'
- ACES II ejection
- USAF standard

5 Modern Systems (2010s~)
- New HMDs, NVGs
- CG creep threatening Knox Box safety

1 Foundational Physics (Pre-1990s)
- Forward helmets in catapult ejection
- ~2.27 kg (5 lb) acceptable
- +1.27 cm forward CG → 222 N neck load
- Injury threshold ~1779 N

Knox Box Criteria

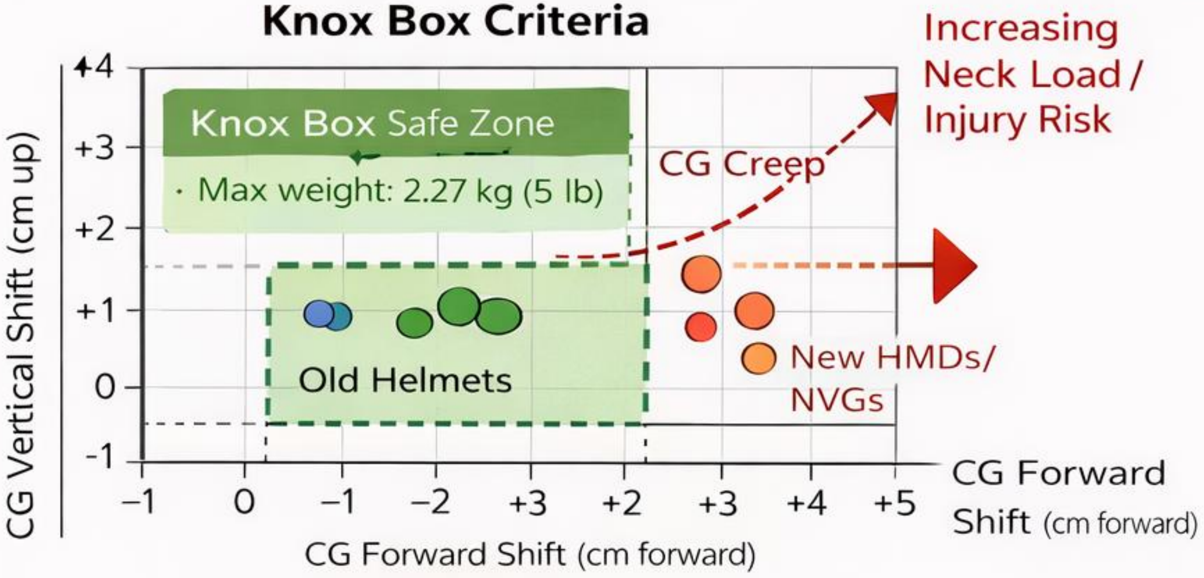

1 Physics (Pre-1990s) | **2 Perry et al. (1993)** Tested helmets in | **3 Privitzer, King Darrah (1990s)** | **4 Knox Box (2000s)** | **5 Modern Systems (2010s–)**

- Tested helmets in catapult jection
- Refined mass + CGdesign limits

STI-TEC

SENTIR RESEARCH LABS

KNOX BOX CRITERIA FOR HEAD/HELMET CGx, CGz

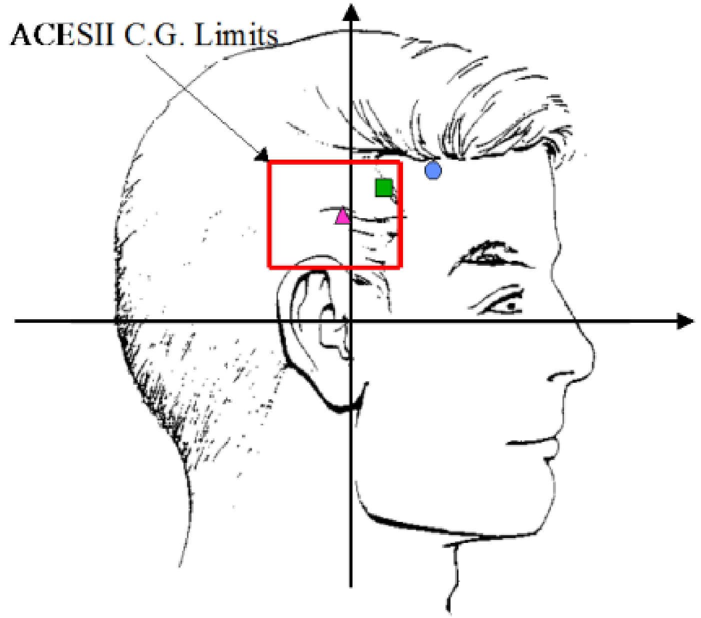

	X-Axis (inches)	Z-Axis (inches)
ACES II Limits	-0.8 – 0.5	0.5 – 1.5
Medium	0.69	1.44
Large	0.8	1.42
X-Large	0.76	1.34

- Large Helmet + 2 lb
- Large Helmet + 1 lb
- Large Helmet

- Developed by AFRL, the center of gravity (CG) shall fall within a volume around the ADAM head anatomical origin
- X range in the x-axis (fore-aft) from –0.8 to 0.5 in.
- Z range in the z-axis (vertical) from 0.5 to 1.5 in.
- Based on weights and CGs of the ADAM Head form, HGU-55/P Helmet, MBU-20/P Oxygen Mask (with 3 in. of hose), and the HMS.
- Limits are assumed to be valid for HMS weighing 5 lb or less and are applicable for ACES II ejection seat applications.

- ***NOTE: The origin of the axis system is Tragion, originally marked on a manikin headform with no ears (so estimated) and assumes headform is also the same CG and weight***

Sources of Uncertainty

1. Knox Box is based on a “mark” placed on the ADAM head meant to represent the Tragion landmark. The Tragion landmark is the origin for the head Anatomical Coordinate System. The Tragion landmark is the reference for all CG locations with respect to the Knox Box. The Tragion location has moved at some point in the last number of years. Therefore, the origin for the Knox Box is unreliable. (examples: different head, pen mark, and skin moves)

2. Right Infraorbitale is an anatomical mark placed on the manikin head to replicate what would be on a human head. (The hard bony ridge that forms the lower boundary of the eye socket). This is estimated on the manikin. The anatomical coordinate system is based on the location of the rt infra and tragions. This forms the X-Y plane.

3. The ADAM head was originally ballasted to locate the CG at a specific location within the head. The ballast has moved or been accidently adjusted resulting in a different CG location for ADAM. All helmet CG locations (wrt Knox Box) reported are combined with the ADAM head CG. Therefore, the combined CG helmet/ADAM head locations are unreliable.

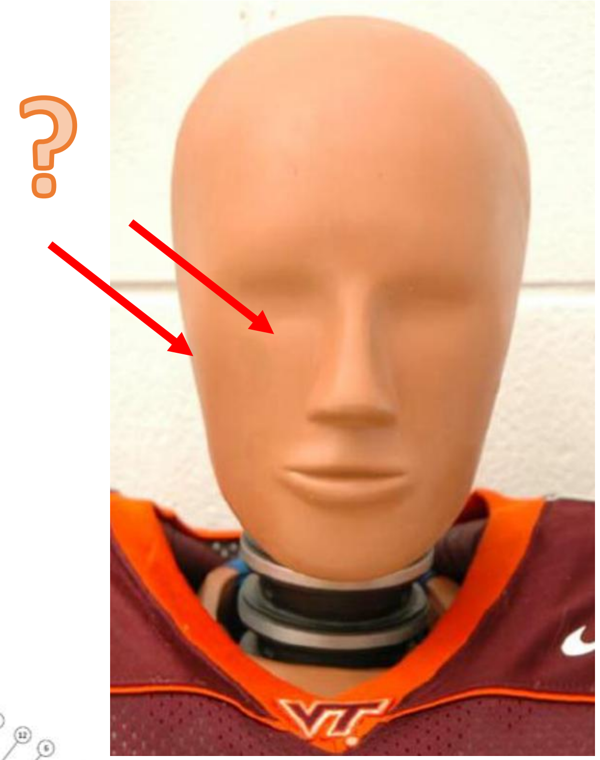

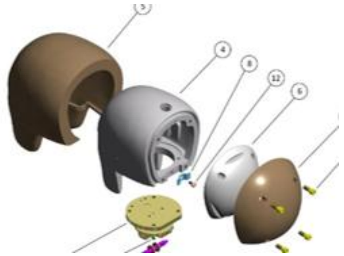

Sources of Uncertainty

4. The ADAM head is used to measure and report mass properties, including the CG location with respect to the head Anatomical Coordinate System. The dynamic testing of the helmets includes sled tests with manikins and centrifuge tests with human subjects. The manikins do NOT necessarily use the ADAM head, but potentially have other manikin heads with different shapes, weights, anatomical locations, CG locations and mass moments of inertia. The helmet/head spatial relationships for these tests are unique to these manikin heads or human heads. Therefore, the combined mass properties for each dynamic testing scenario are unknown.

5. Fit of helmet on manikin head. Fit determines the combined head/helmet mass properties including total weight, center of gravity location, and mass moments of inertia.

6. Use of manikin skin to reference coordinate system.

Examples of Manikin Headform CG and Weight

	CG WRT anatomical coord system and Weight of Adam Head							
Publication Date	**X(cm)**	**Y(cm)**	**Z(cm)**	**X(in)**	**Y(in)**	**Z(in)**	**Weight(kg)**	**Weight (lb)**
SPECIFICATIONS	-1.46	0.2	2.7	-0.57	0.08	1.06	4.35	9.6
1988	-1.24	-0.20	2.26	-0.49	-0.08	0.89	4.32	9.52
1988	-0.30	0.00	1.70	-0.12	0	0.67	4.50	9.92
1990	-0.79	0.00	3.25	-0.31	0	1.28	4.44	9.8
1994	-0.81	-0.08	2.57	-0.32	-0.03	1.01	4.05	8.93
1995	-0.75	-0.02	2.59	-0.3	-0.01	1.02		
1996	-1.24	-0.20	2.26	-0.49	-0.08	0.89	4.32	9.52
1997	-0.81	-0.08	2.57	-0.32	-0.03	1.01	4.05	8.93
2005	0.53	0.00	4.52	0.21	0	1.78	4.26	9.4
2013	0.28	-0.01	1.44	0.11	0.00	0.57	3.33	7.34
2017	-1.4	0.25	2.51	-0.55	0.1	0.99	4.24	9.34
average	-0.73	-0.01	2.58	-0.29	0.00	1.02	4.19	9.23
std dev	**0.66**	**0.14**	**0.81**	**0.26**	**0.06**	**0.32**	**0.33**	**0.74**
min	-1.46	-0.20	1.44	-0.57	-0.08	0.57	3.33	7.34
max	0.53	0.25	4.52	0.21	0.10	1.78	4.50	9.92

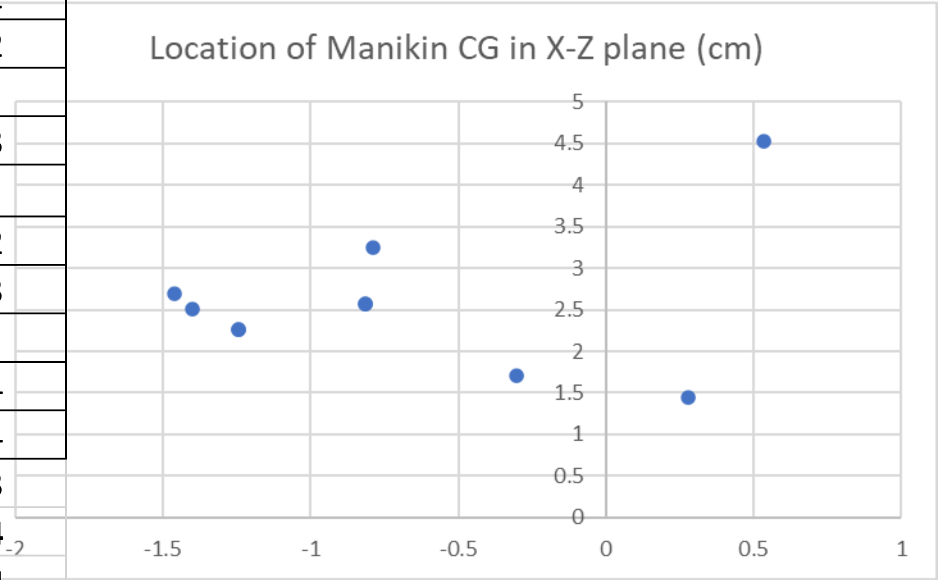

Helmet Evaluation Output Including Moments of Inertia

LANDMARKS IN SEGMENT ANATOMICAL AXIS SYSTEM

	CENTIMETERS			INCHES		
RT-TRAGION	0.00	-7.44	0.00	0.00	-2.93	0.00
LT-TRAGION	0.00	7.57	0.00	0.00	2.98	0.00
RT-INFRAORBITALE	6.94	-3.35	0.00	2.73	-1.32	0.00
SELLION	8.77	0.00	2.67	3.45	0.00	1.05
RT-END-HEAD-NECK	-3.09	-2.50	-2.22	-1.22	-0.98	-0.87
LT-END-HEAD-NECK	-3.02	2.24	-2.09	-1.19	0.88	-0.82
MIDPNT-HEAD-NECK	-3.26	-0.23	-2.78	-1.28	-0.09	-1.09
HEAD CG	**-0.75**	**-0.02**	**2.59**	**-0.30**	**-0.01**	**1.02**

TRANSFORMATION FROM THE ANATOMICAL AXIS SYSTEM TO THE UNASSIGNED PRINCIPAL AXES (APA)

COSINES	DEGREES		
0.85466 0.03468 0.51804	31.28	88.01	58.80
0.06481 -0.99705 -0.04016	86.28	175.60	92.30
0.51509 0.06788 -0.85439	59.00	86.11	148.69

TRANSFORMATION FROM THE ANATOMICAL AXIS SYSTEM TO THE ASSIGNED PRINCIPAL AXES (APAA)

COSINES	DEGREES		
0 85466 0.03468 0.51804	31.28	88.01	58.80
-0.06481 0.99705 0 04016	93.72	4.40	87.70
-0.51509 -0.06788 0.85439	121. 00	93 .89	31.31

with respect to anatomical coordinate system

YAW= 2.32 PITCH= -31.20 ROLL= 2.69

- origin of the coordinates is the center of mass.
- The main axis (z −axis) is principal axis with smallest moment of inertia
- The (x −axis) is the principal axis with the largest moment of inertia.

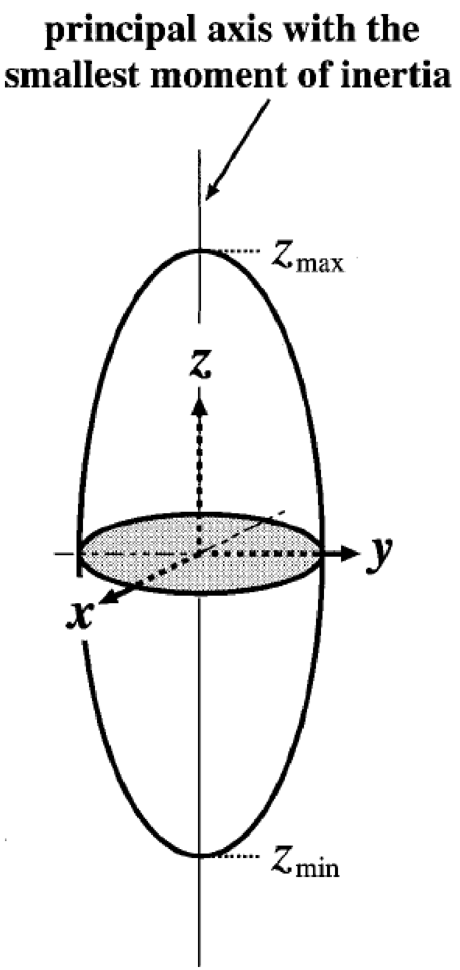

HUMAN HEAD MASS PROPERTIES

- Human head MOI varies
- Headforms disagree
- Coordinate systems differ

- No unified dataset
- No standard combination method
- No uncertainty bounds

- Helmet + HMD adds:
  - CG shift
  - MOI increase
- Dynamic response changes

We are designing to unknown inertia and calling it precise.

HUMAN HEAD MASS PROPERTIES

- **Medical imaging + segmentation is a valid method** for determining head mass properties, but results depend strongly on modeling assumptions.

- **Bone modeling matters:** treating the skull as all cortical bone is inaccurate—**including trabecular bone (via volumetric density) improves accuracy**.

- **Gender differences exist in head size and mass**, but **not in center of gravity (CG) location**, which is consistent across males and females.

- **OC (occipital condyle) location can be reliably estimated from external landmarks**, with no significant difference from internal joint-based references.

The average skull bone volumetric percentages were 46.5% for cortical bone and 53.5% for trabecular bone, which resulted in a calculated skull composite density of 1428 g/cm^3

MOMENTS OF INERTIA

Cannot just "add MOIs" unless:

- Same origin
- Same coordinate system
- Same axis orientation

Rigid body dynamics must be expressed in the principal axes to correctly model rotational response.

Measured with +/-33% error
Specified (often) +/- 10%

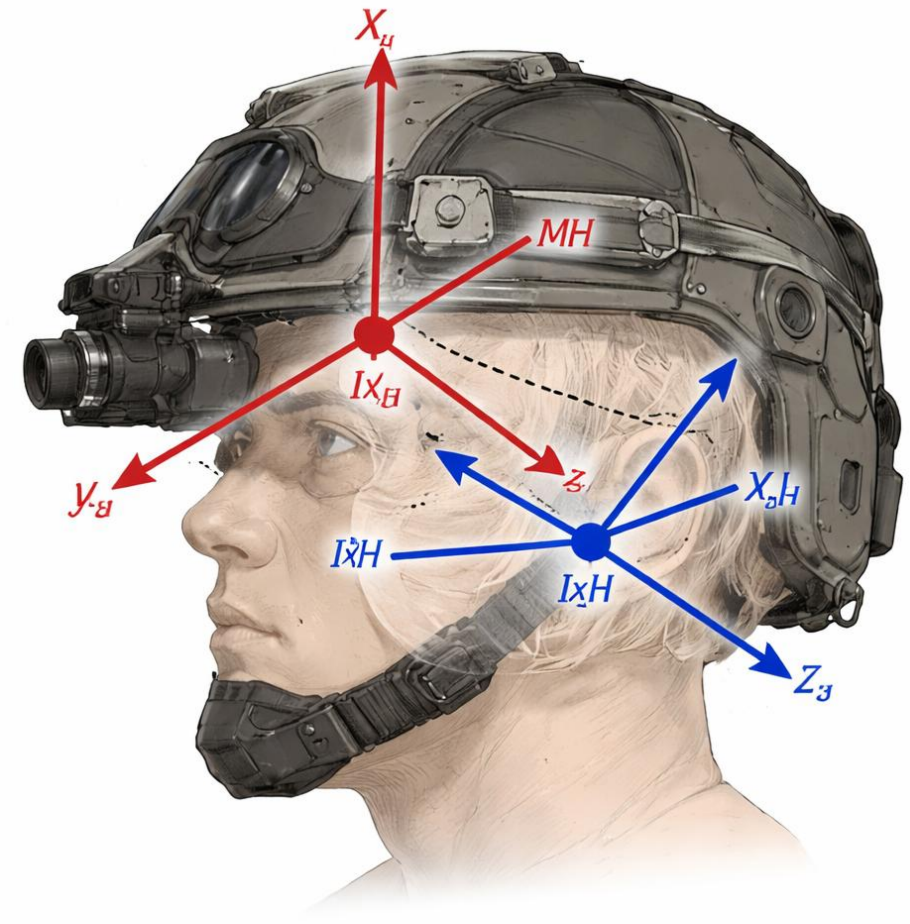

Measurements– Implications for Specifications

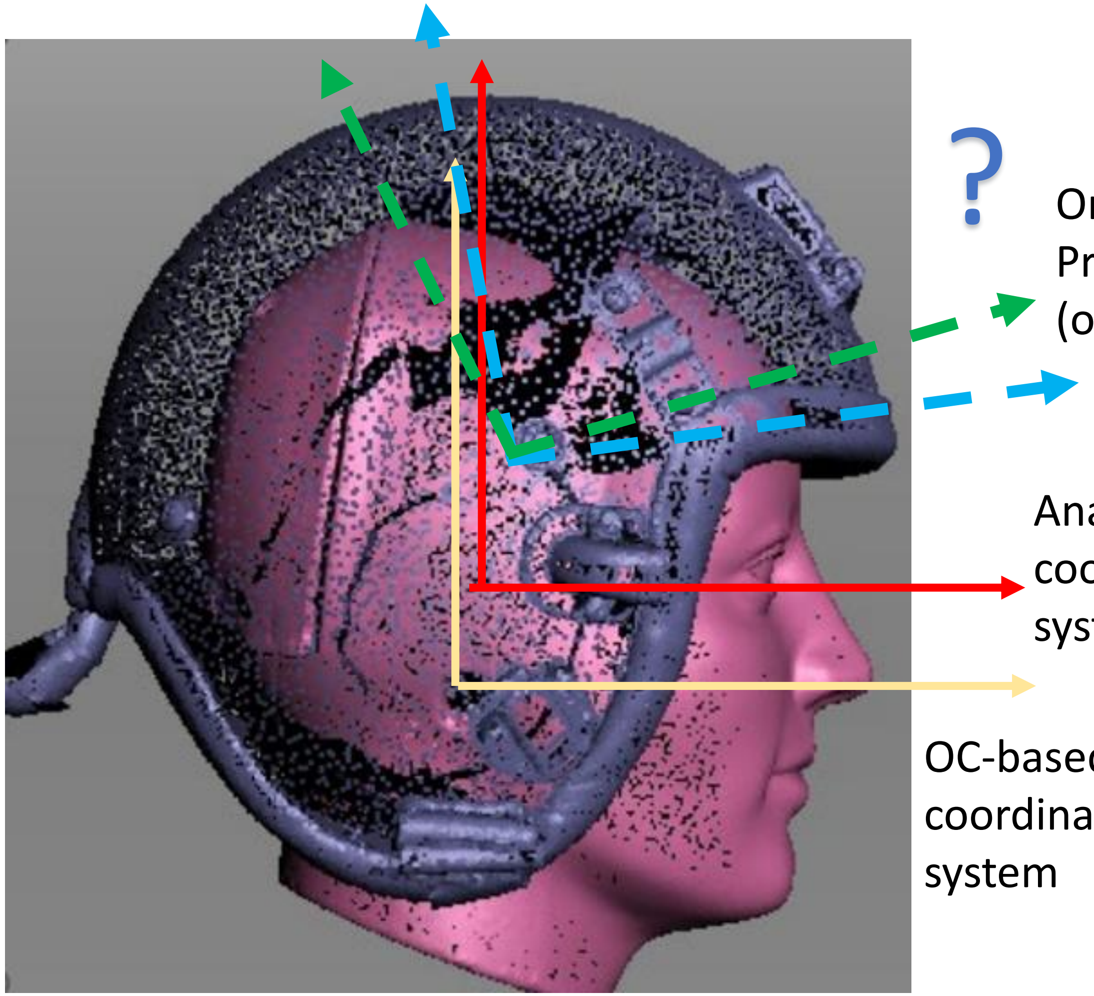

- Minimum required accuracy for center of gravity measurements is +/- 1.75 mm.
- Moments of inertia should be 0.6 to 1.0 % of true value as the object increases in size from small to large respectively.
- Overall variance should be less than 1.0% for all measurements.

KNOX BOX

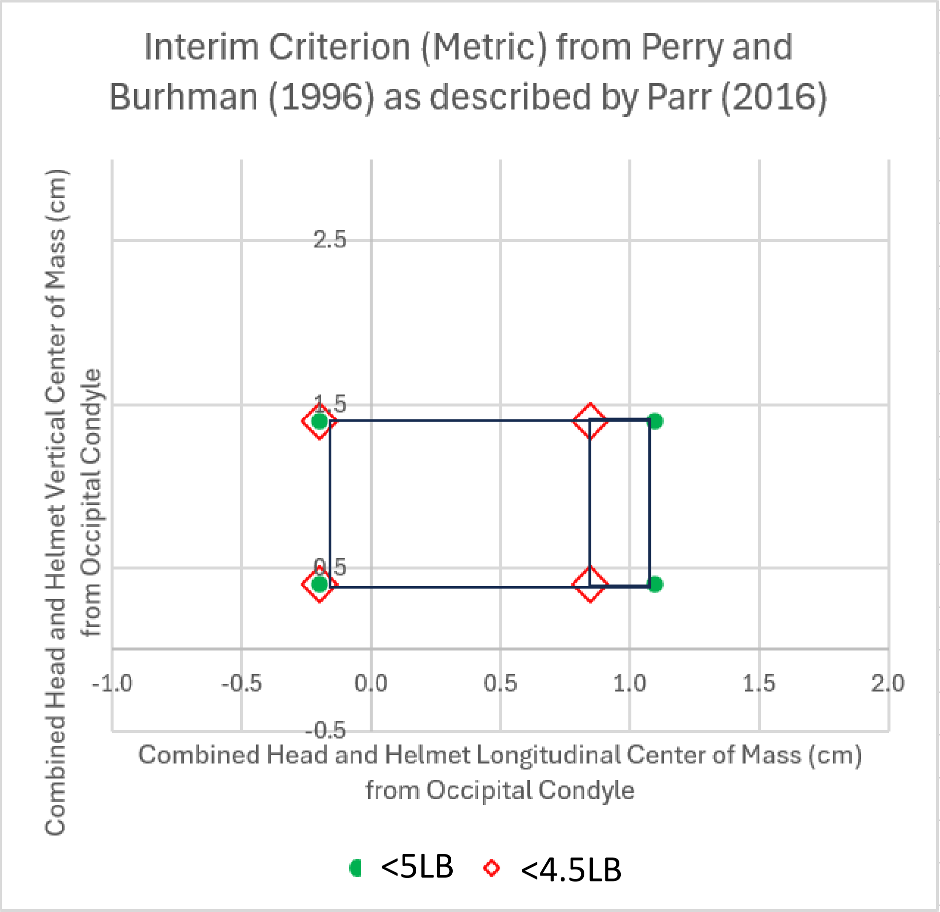

- Tragion is the origin of the coordinate system Frankfurt Plane
- center of gravity to be shifted 1.25” in horizontal
- 1.0” in vertical zone
- lack of injury risk data makes it difficult to use as a criteria when making system level trades

- (B-52) helmets weighting less than 4.5 pounds and having a combined head/HMD CG within limits defined by -0.2 to 0.85 inches on the x-axis and 0.4 to 1.4 inches on the z-axis (18G)

- (ACES II) helmets weighing less than 5 pounds and having CG limits of -0.2 to 1.1 inches on the x-axis and 0.4 to 1.4 inches on the z-axis (12G)

STI-TEC

“Leveraging Knowledge Assets and Emerging Technologies”

SENTIR RESEARCH LABS

MISREPRESENTATION OF KNOX BOX

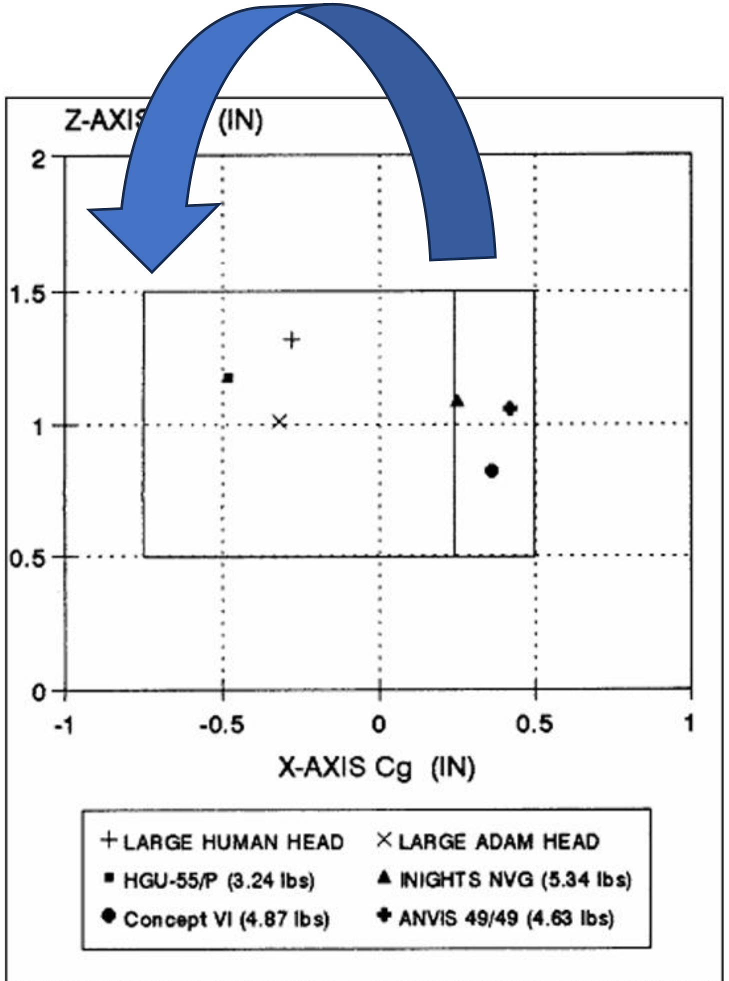

Outer Box Cg Limits: Weight Criteria... 4.0 lb for B-52 seat, 5.0 lb for ACES II
Inner Box Cg Limits: Weight Criteria... 4.5 lb for B-52 seat

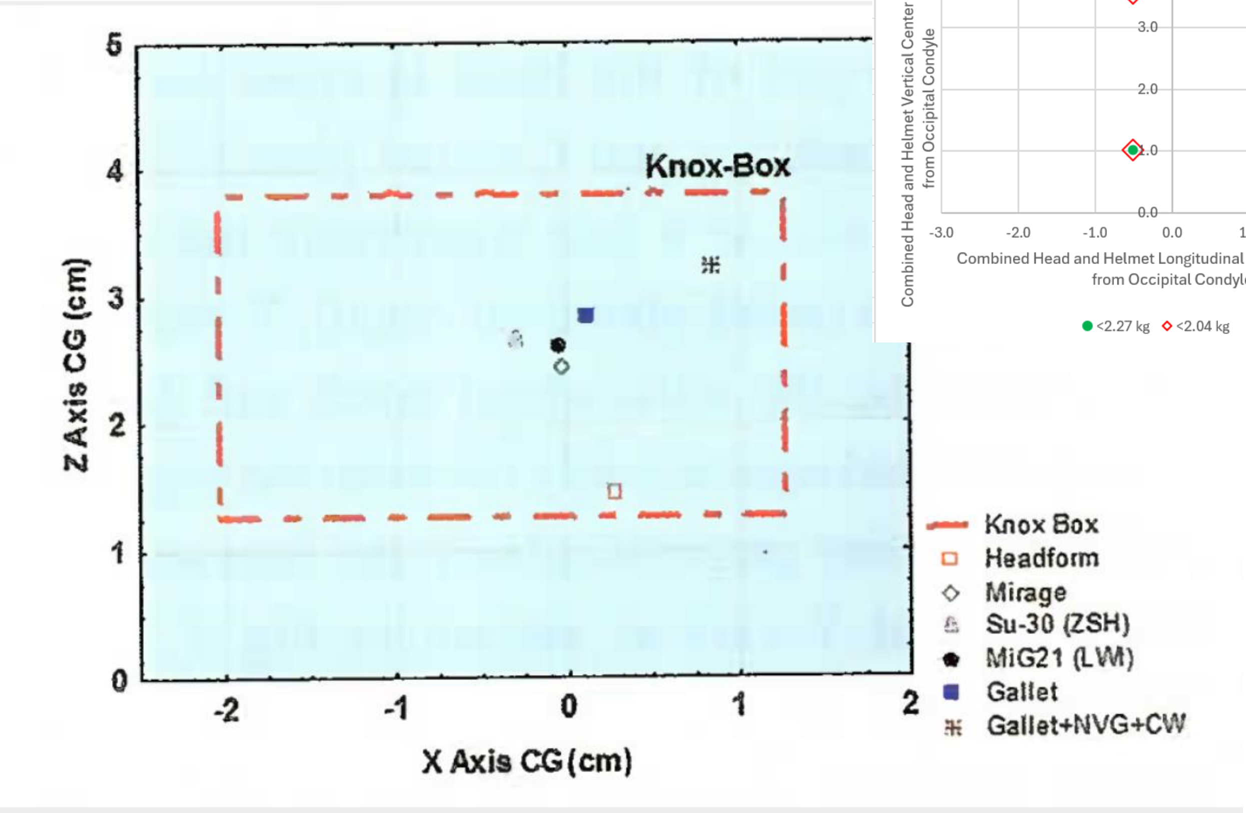

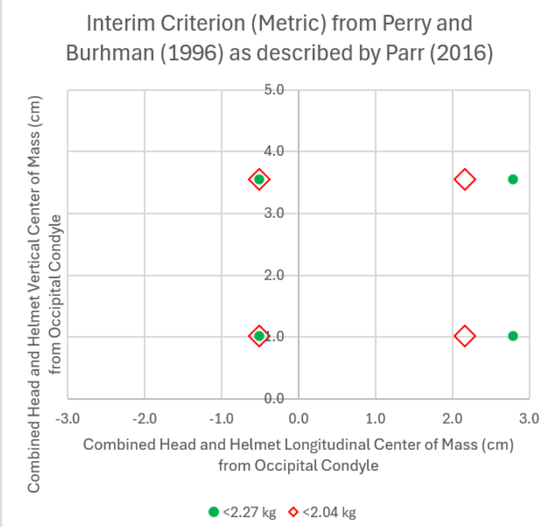

"Leveraging Knowledge Assets and Emerging Technologies"

FACTORS AFFECTING NECK INJURY AND FATIGUE

Neck injury is driven by:

- **Mass** (helmet + head)
- **Center of gravity offset**
- **Moment of inertia**
- **Acceleration direction + magnitude**
- **Anthropometry (huge factor)**

Example:

- Smaller pilots carry **~2× relative helmet mass burden** vs large pilots

Helmet-mounted displays (HMDs) increase **head-supported mass and shift the center of gravity**, which:

- Amplifies **neck loads during ejection**
- Increases risk of **cervical injury (strain → fracture)**
- Disproportionately affects **smaller pilots (e.g., females)** due to mass ratios

The key gap:

There is no adequate, aviation-specific, multi-axis neck injury criterion to guide design and testing.

Sensitivity of Factors on Neck Loading

$F \sim ma$ $M \sim rma + I\alpha$
and :
- **Mass sensitivity:** linear
- **CG sensitivity:** linear for moment, often high practical impact
- **MOI sensitivity:** linear for rotational loading, critical in dynamics
- **Acceleration sensitivity:** linear and usually dominant overall

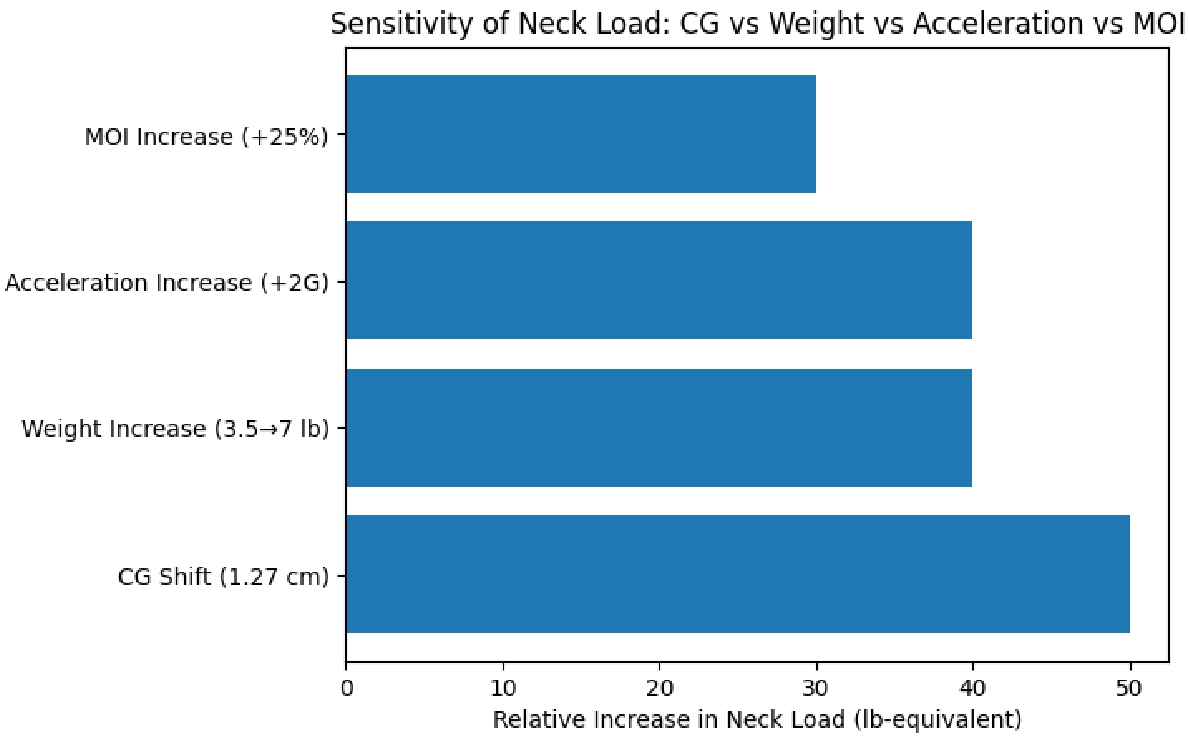

STI-TEC

"Leveraging Knowledge Assets and Emerging Technologies"

SENTIR RESEARCH LABS

Multi-Axial Neck Injury Criteria (MANIC)

Develop a **method to create neck injury criteria** that:
- Quantifies **probability of injury (risk-based)**
- Works across **all acceleration axes (Gx, Gy, Gz)**
- Translates into **testable design limits** for ejection systems
- Supports **Human Systems Integration (HSI) trade studies**

Multi-Axial Neck Injury Criterion (MANIC)
- Separate criteria for:
  - **Gx (forward/back)**
  - **Gy (lateral)**
  - **Gz (axial/tension/compression)**
- Each produces:
  - Risk curves (AIS-based)
  - Thresholds tied to probability (e.g., 5% injury risk)

Parr, J. C. (2014). *A method to develop neck injury criteria to aid design and test of escape systems incorporating helmet mounted displays* (Doctoral dissertation, Air Force Institute of Technology, Wright-Patterson AFB, OH).

MANIC: Multi-Axial Neck Injury Criteria

Structure:

MANIC = {MANIC(-Gx), MANIC(Gy), MANIC(-Gz)}

- Multi-axis framework
- Not a single equation
- Each axis → separate metric

Risk Model:

P(injury) = 1 / (1 + e^-(a + b·MANIC))

- Outputs probability
- AIS-based (2+, 3+)
- Replaces pass/fail logic

Axis Equations:

MANIC(-Gx) = f(Fx, My)
MANIC(Gy) = f(Fy, Mx)
MANIC(-Gz) = Fz

- Force + moment driven
- Axis-specific loading

MANIC transforms neck load → probability of injury across multiple axes

Hidden Risk: Neck Injury Models Assume Perfect Head Mass Properties

- Parr Risk Engine:
- Neck load -> injury probability (AIS-based)
- Multi-axial criteria (MANIC)
- Based on human + PMHS data
- Key Input Dependency:
- Neck Load = f(mass, CG, MOI, acceleration)
- Hidden Risk:
- Head CG varies (cm-level)
- MOI varies (±20–40%)
- Assumed constants → real variability
- Takeaway: If CG/MOI are wrong → load is wrong → risk is wrong

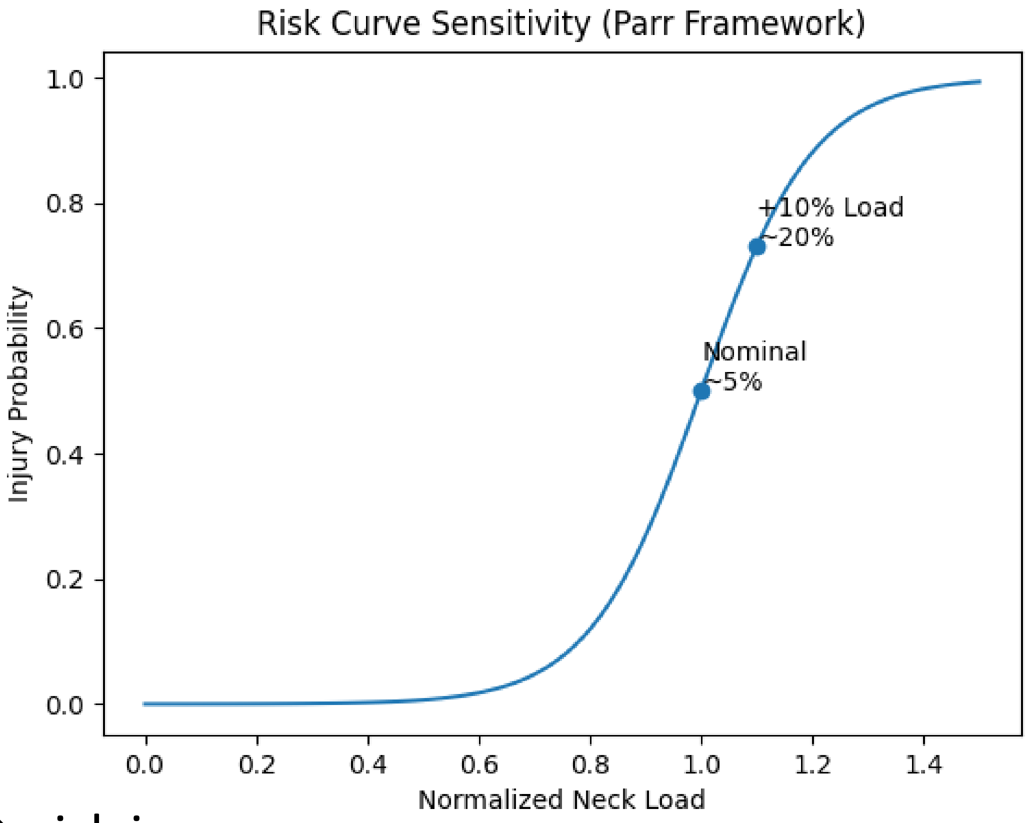

Parr risk curves are nonlinear — uncertainty in load becomes amplified risk

"Leveraging Knowledge Assets and Emerging Technologies"

STI-TEC

SENTIR RESEARCH LABS

Smaller occupants are hit harder by the same uncertainty

Parr repeatedly highlights anthropometry as a major driver and notes that smaller pilots can be at greater risk from the same helmet burden. So an error in assumed head CG or MOI is not just a generic modeling nuisance - it can bias risk unevenly across the population.

MANIC gives a risk framework from neck load to injury.
But if head CG/MOI are uncertain, then the neck load input to that framework is uncertain too.

Proposed Solutions

1. The weight and CG location for each helmet can be measured independently of any head form. The CG location can be identified and recorded with respect to a helmet-based coordinate system. Each helmet CG location can be measured reliably.

2. To determine KPP#3 "Mass Properties", "The resultant CG location for each of the NGFWH configurations 3.1.1.1-3.1.1.3 shall be no worse than legacy helmet configurations with respect to the human head CG. (T=O)", each helmet CG location should be measured with respect to the helmet based coordinate system. As the offered helmets are a size large, each helmet should be scanned on 3 selected large human heads to capture the position of the helmet/head spatial relationship. The legacy helmet will be scanned on the same subjects. The combined helmet/head spatial relationships will be geometrically captured and the combined CG locations for each of the candidate NGFW helmets can be compared to the legacy system.

3. The impact of moving the head's CG due to the weight distribution of the helmet system is that the loading on the neck increases. To determine if the NGFWH helmet CG is "no worse than" can be challenging to know if a decrease in the X coordinate relative to the head anatomical system is better than a decrease in the Z direction. An improved method of referencing the combined head/helmet CG is to use the occipital condyle (head/neck) joint as the origin for the head coordinate system. As the loading from the combined head/helmet CG acts as a moment arm around the OC joint, the "no worse than" can be measured as a resultant vector from the OC to the combined CG location

4. All of the dynamic tests employing manikins, including all of the different manikin heads, use a six-axis load cell. The axis around which the loads are measured is considered the head/neck joint axis as well. Each of the manikins used for the tests should be measured for weight and CG location relative to the load cell axis. Every manikin with the helmet to be tested should be scanned to capture the headform/helmet configuration. Each dynamic test using a manikin head will be accurately assigned the combined head/helmet CG location

5. The USAARL weight and CG tolerance curves can be compared to the results of the measured helmet systems using this method. The USAARL large head form was scanned and aligned (using a best fit method) to the ADAM head. The USAARL curves have been overlaid on the ADAM head such that any large helmet can be scanned with the ADAM head and compared to the accepted injury risk area. Particularly for rotary wing helmets, this method would provide additional data regarding safety of the proposed helmet system weight and CG, based on USAARL's injury data

6. The Airmen Accommodation Lab (AAL) within AFLCMC/WNU has the capability to measure weight and CG of the helmet systems and headforms. The AAL also provides the scanning capability as well as the image processing to capture the helmet and head configurations. An excel method has been set up to quickly combine weight and CG of any 2 systems (head and helmet) given known coordinate systems. The capability of measuring helmet systems' weight and CG with respect to either human or manikin headforms is now represented within WNU

Helmet Mass Properties Measurement Technique

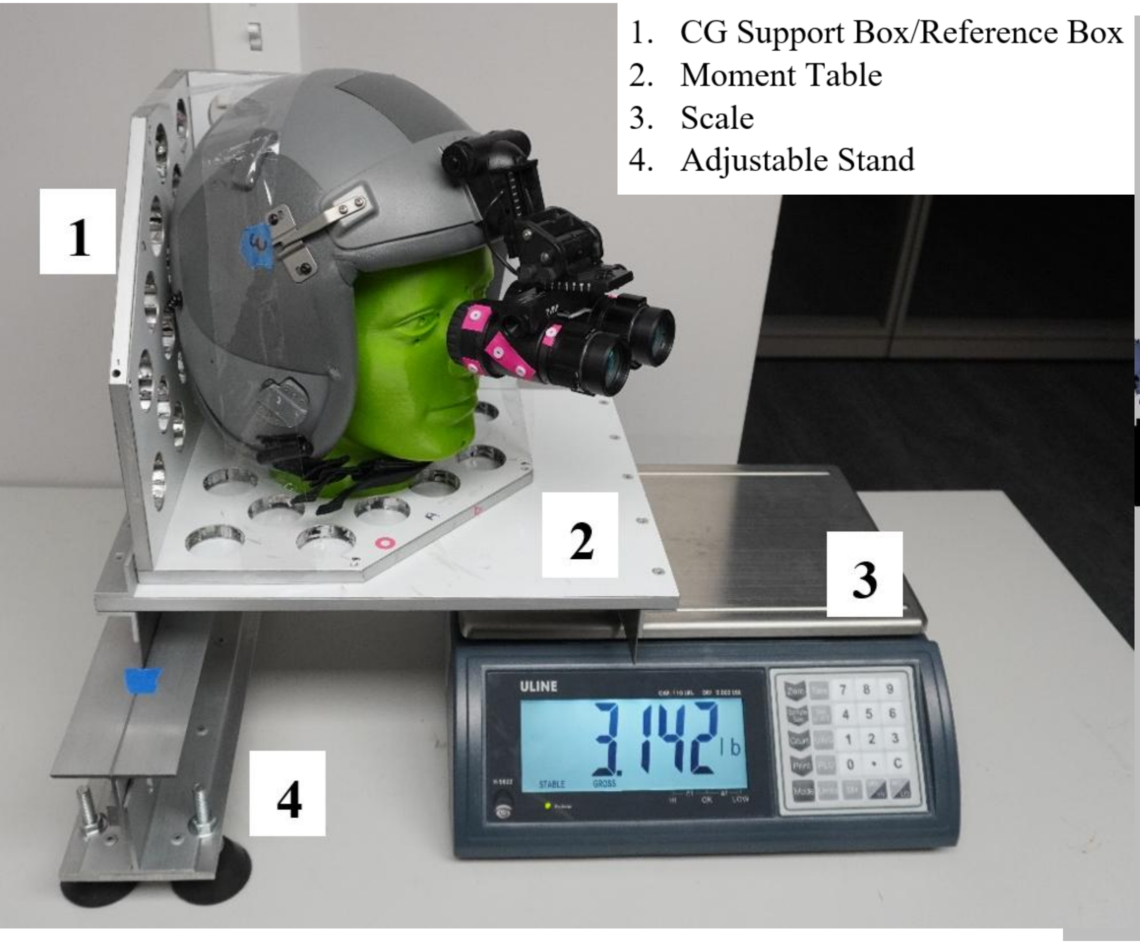

1. CG Support Box/Reference Box
2. Moment Table
3. Scale
4. Adjustable Stand

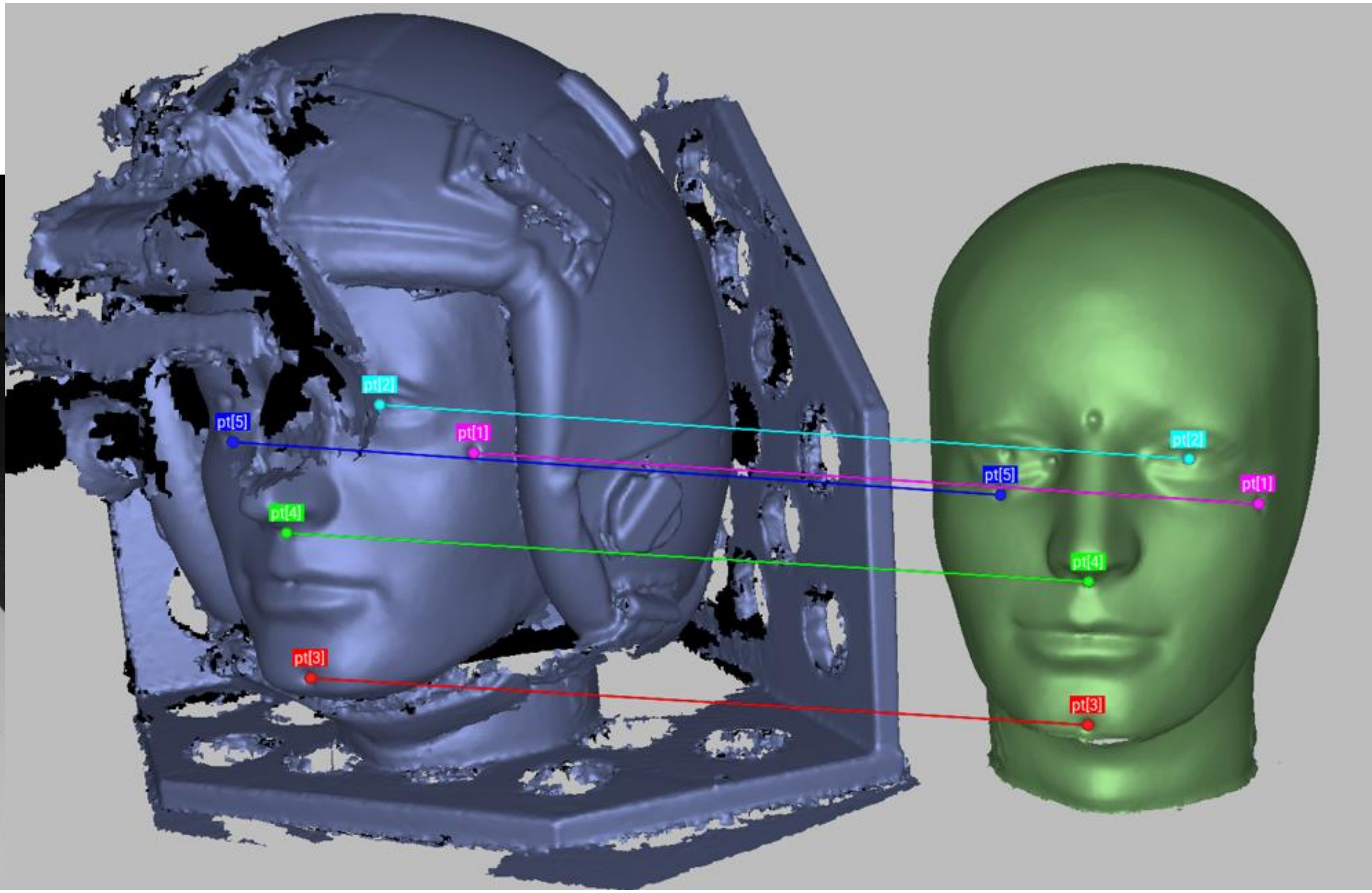

STI-TEC

"Leveraging Knowledge Assets and Emerging Technologies"

SENTIR RESEARCH LABS

Helmet Weight and CG Measurement Technique

Weigh all Objects of Interest (box, head, helmet system)

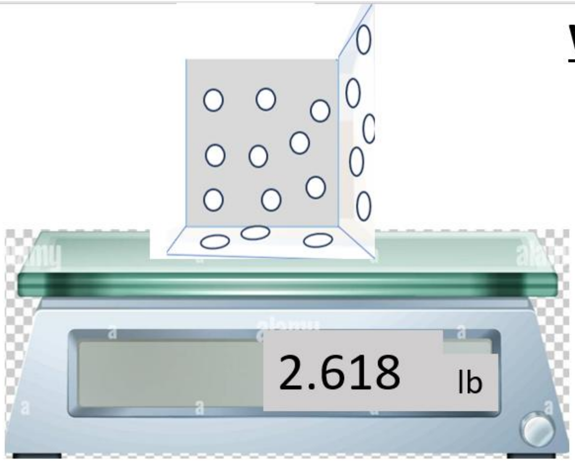

Weigh box

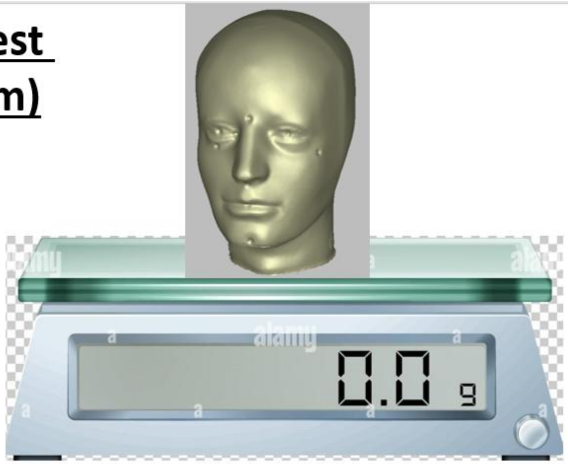

Weigh ABEL

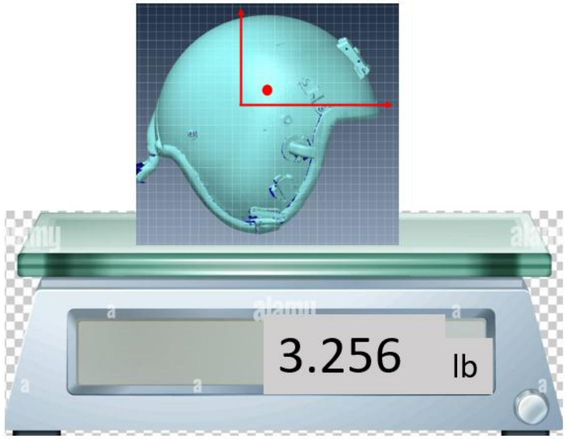

Weigh helmet system

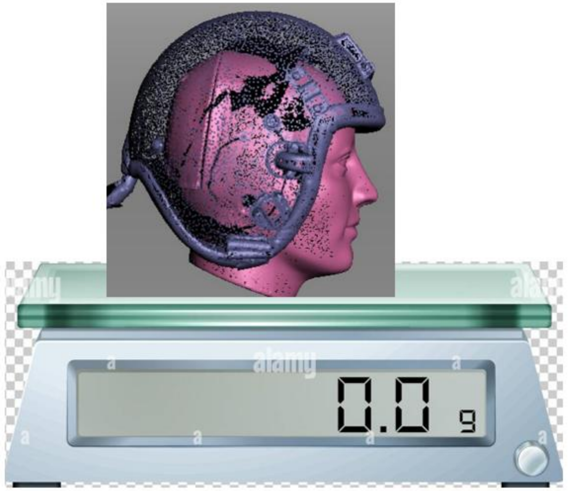

Weigh helmet system + ABEL

Combining Helmet Weight and CG wrt Human Head

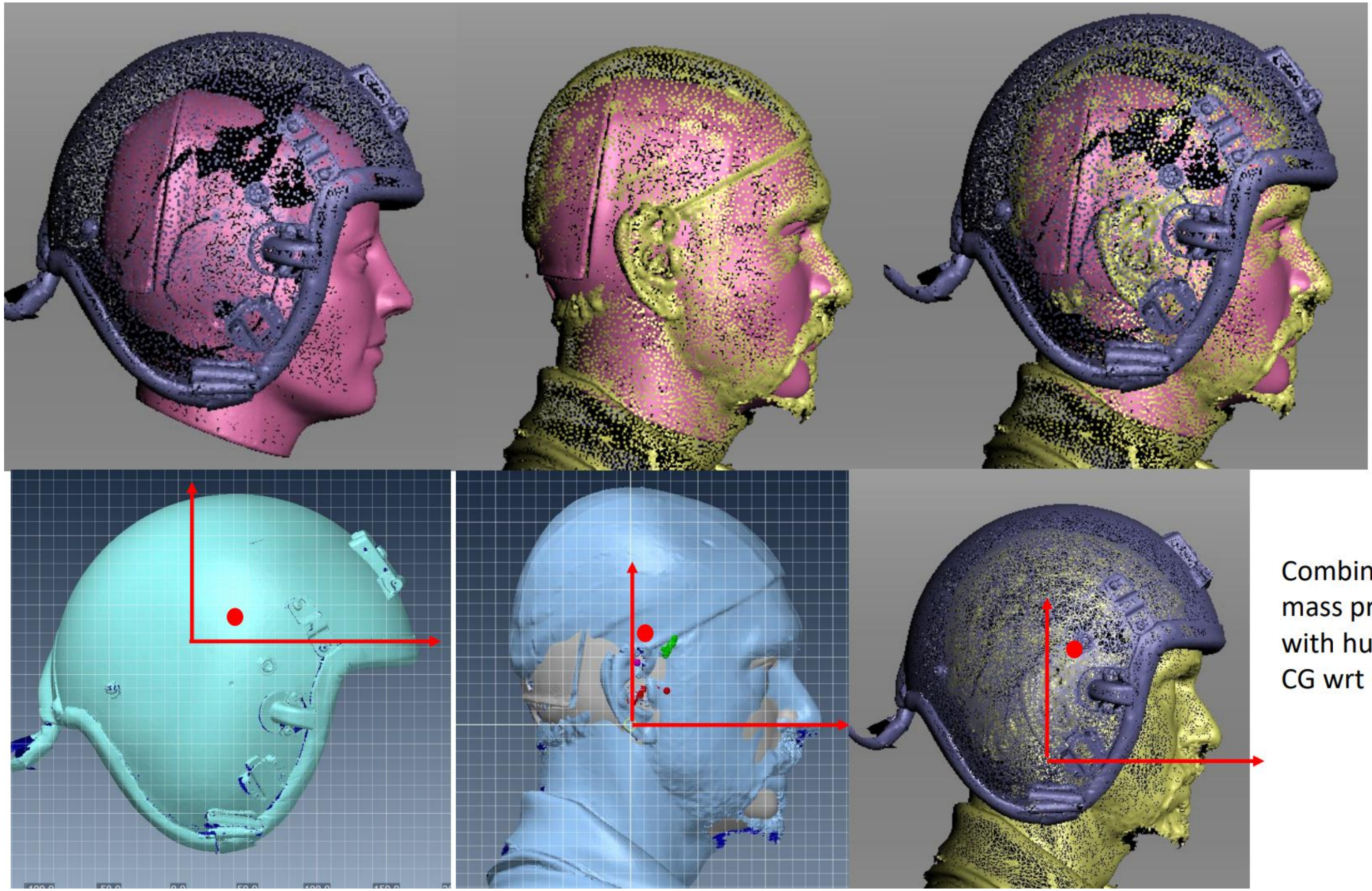

Combining helmet mass properties with human head CG wrt OC joint.

Potential Sources of Error

- **Instrumentation**: scale, FARO, calibration, resolution
- **Setup**: helmet fit, strap tension, alignment, fixture setup
- **Landmarks & coordinates**: reference frame, origin, digitized points
- **Configuration**: accessories, visor position, battery, cables
- **Analysis**: transformations, unit conversion, subtraction, uncertainty propagation

Mass Properties Sensitivity

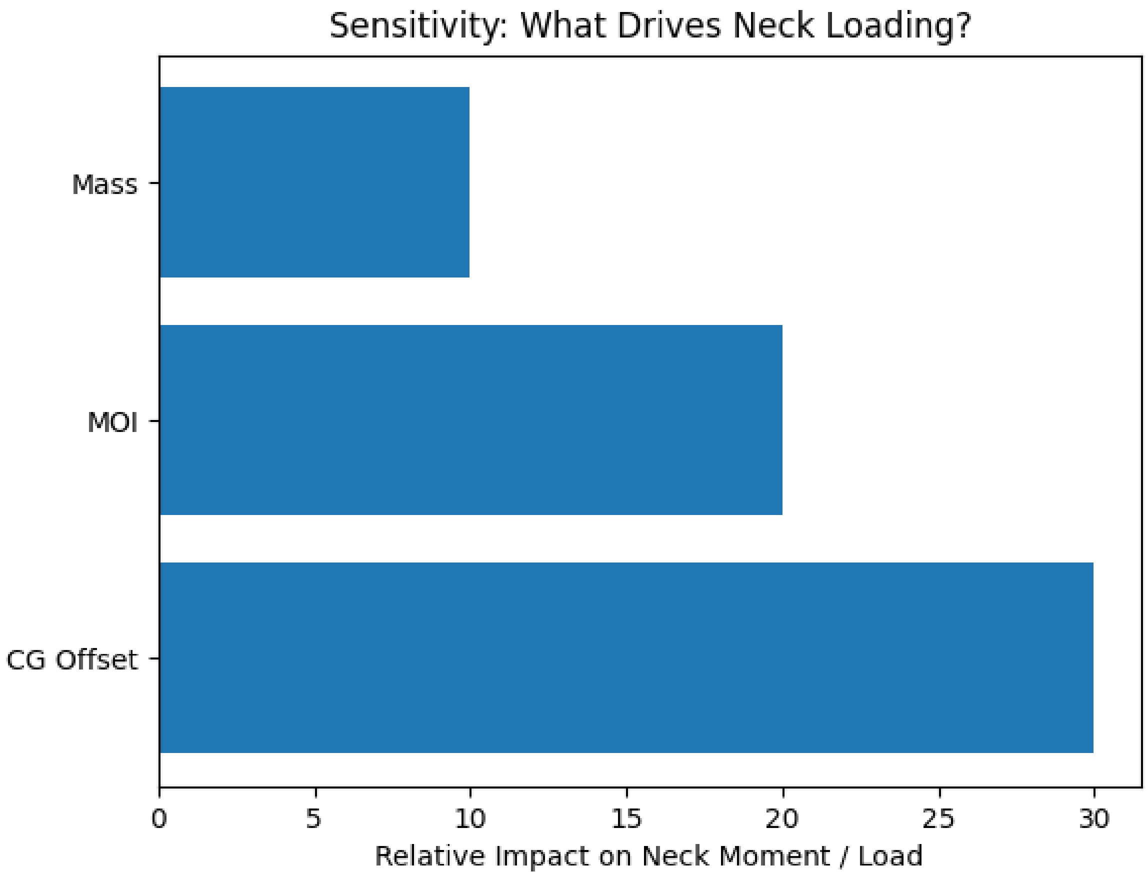

What about CGz vs CGx?

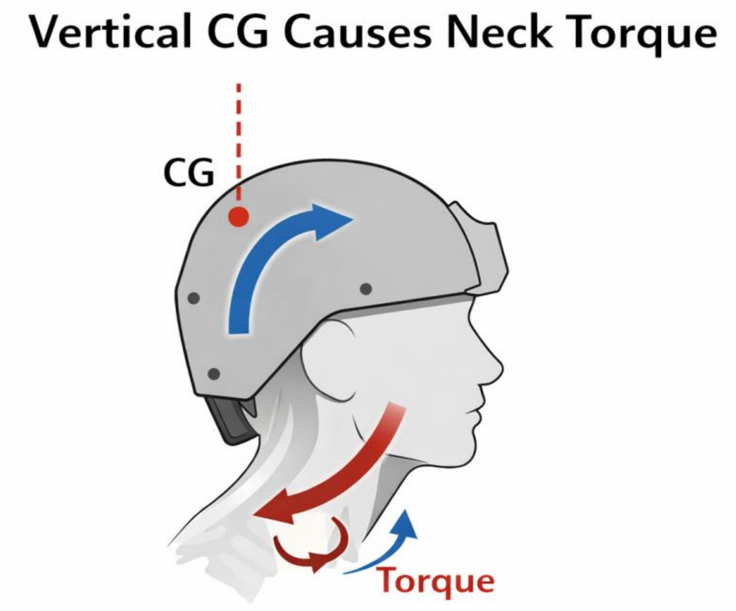

Approach moving forward:

(1) design a helmet system to allow the variation of inertial properties of the combined head and helmet for different test conditions;

(2) conduct experiments with volunteer human subjects exposed to a +Gz acceleration pulse while wearing the parametric helmet;

(3) measure the subject's biodynamic response including head and chest accelerations and head kinematics relative to the thorax;

(4) analyze the data to study the human biodynamic response relative to the test condition; and

(5) use analytical methods (computer model, etc.) to estimate the dynamic loading in the neck due to the parametric helmet

Armstrong Laboratory Vertical Decelerator Testing with Human Subjects/Manikins

- **Test Platform:**
  - Armstrong Laboratory vertical decelerator
  - Human subjects + 97th percentile manikin
- **Test Conditions:**
  - Seat impacts up to **+10 Gz (human)** and **+15 Gz (manikin)**
  - Helmet-mounted systems ranging from **3.2 to 6.6 lb**
- **Objective:**
  - Quantify effects of **helmet mass** and **seat acceleration** on **human dynamic response**
  - Compare results to **established injury tolerance limits**
- **Key Findings:**
  - ↑ Helmet mass → ↑ **neck compression, shear, and rotational loads**
  - ↑ Seat acceleration → further amplifies neck loading
- **Critical Threshold:**
  - **Helmet mass > 4.5 lb at +15 Gz**
    → Neck compression **exceeds cadaver injury limits**

TABLE I. EFFECTS ON HUMAN NECK LOADING OF VARIABLE HELMET WEIGHT.

Weight (lb)	Compress (lb)	Shear (lb)	Moment (in-lb)
3.23	205 ± 21	45 ± 23	324 ± 105
3.61	201 ± 21	47 ± 22	318 ± 88
5.34	264 ± 26	48 ± 28	484 ± 89
5.62	241 ± 31	53 ± 21	604 ± 188
5.96	264 ± 36	39 ± 15	442 ± 77
6.42	287 ± 37	56 ± 24	692 ± 192
6.51	297 ± 38	55 ± 23	561 ± 104
6.64	252 ± 23	67 ± 24	735 ± 309

IMPACT OF HELMET WEIGHT

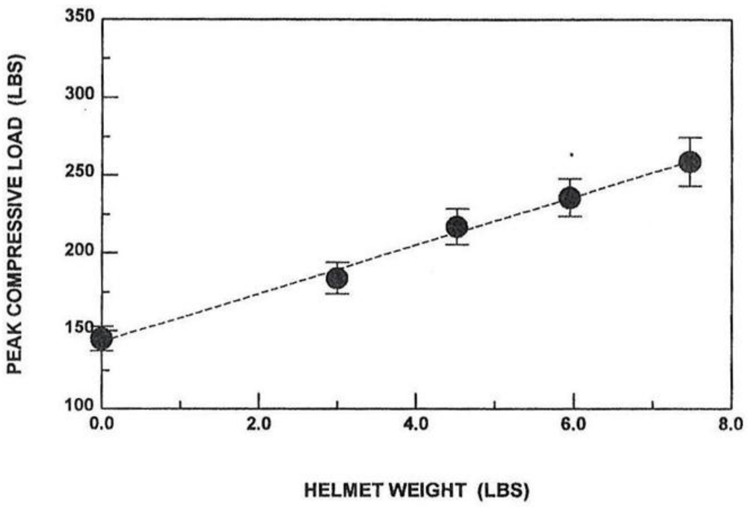

Figure 5. Calculated Cervical Compressive Load at the Occipital Condyle as a Function of Helmet Weight During a 10 G Impact

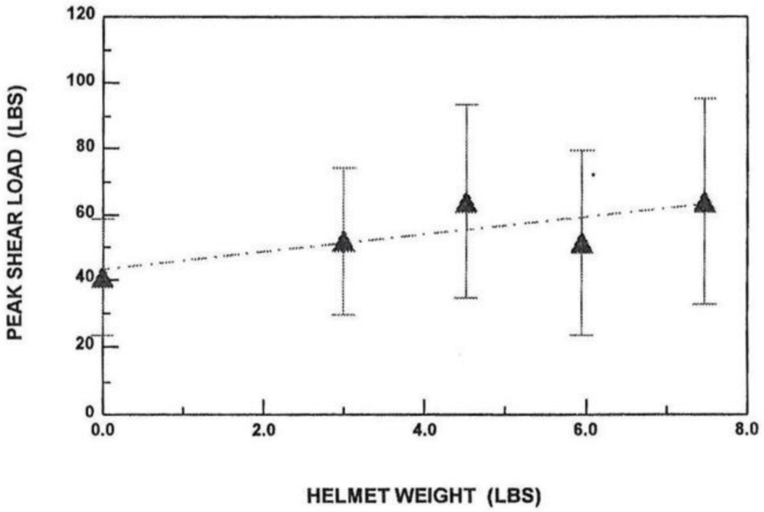

Figure 6. Calculated Cervical Shear Load at the Occipital Condyle as a Function of Helmet Weight During a 10 G Impact

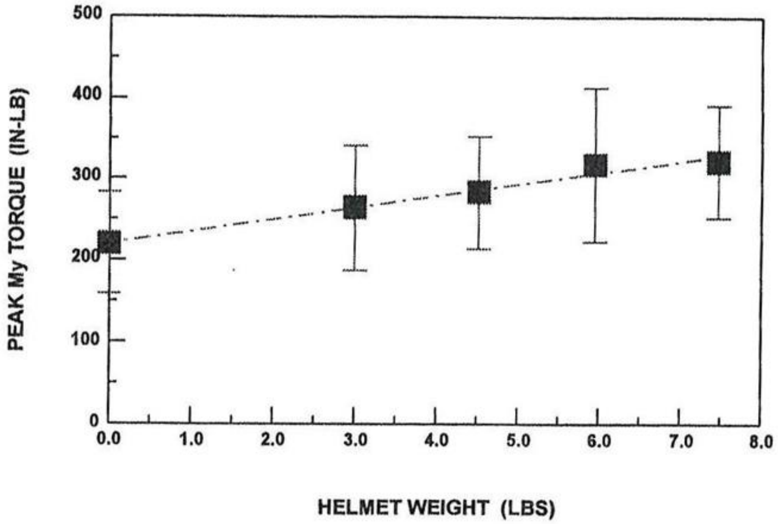

Figure 7. Calculated My Torque at the Occipital Condyle as a Function of Helmet Weight During a 10 G Impact.

USAARL Curves for Allowable Helmet Mass, CG

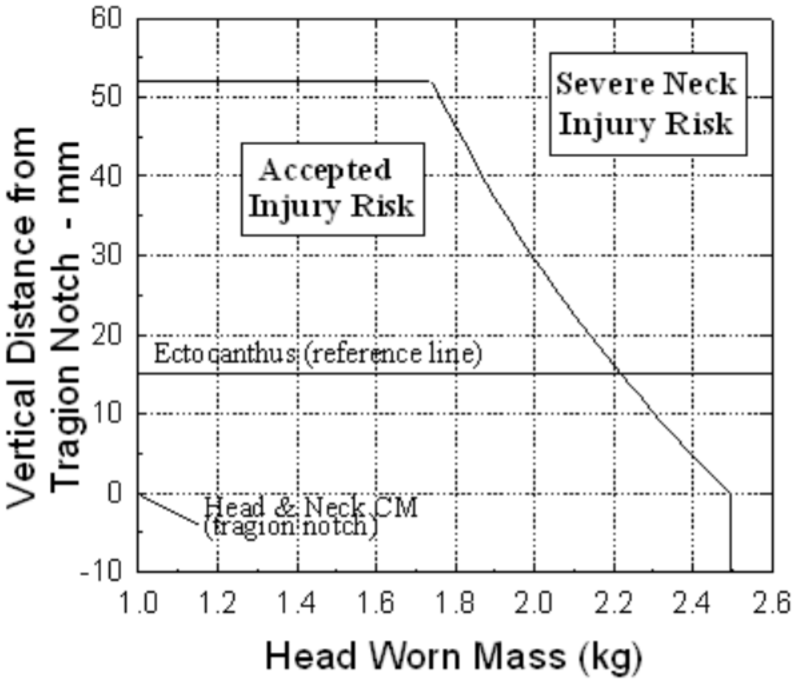

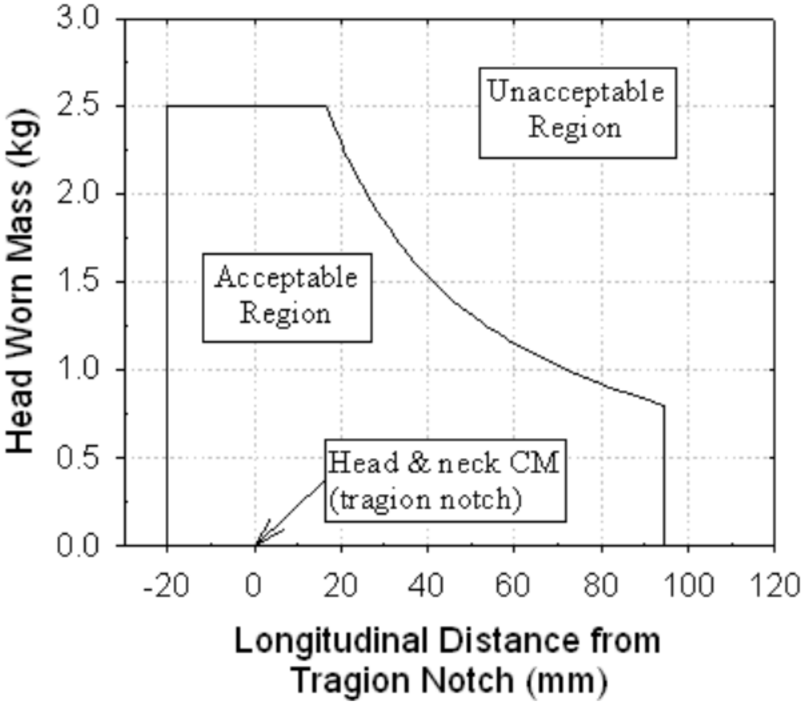

- Based on measured biodynamic responses of aviators wearing various helmet mass and CM combination
- The z-axis CM is based on maintaining a constant moment about the C7/T1 juncture resulting from the helmet mass and vertical CM position.
- Designed to evaluate and document the weight, center of gravity, and moments of inertia of the helmet system itself, excluding any additional mass properties that would come from a manikin or wearer

Cedarville Senior Capstone Project

- Prove that Segmentation analysis on CT scans using Solidworks and 3D Slicer provides accurate results for mass properties of the human head.
- Compare methods of Segmentation Analysis that considers trabecular and cortical bone density differences.
- Identify location of OC joint with respect to anatomical coordinate system

Cedarville Senior Capstone Project

PROCEDURE

CT SCANS → 3D SLICER → SOLIDWORKS

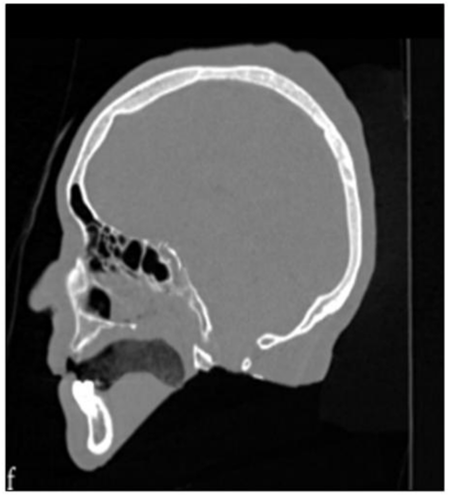

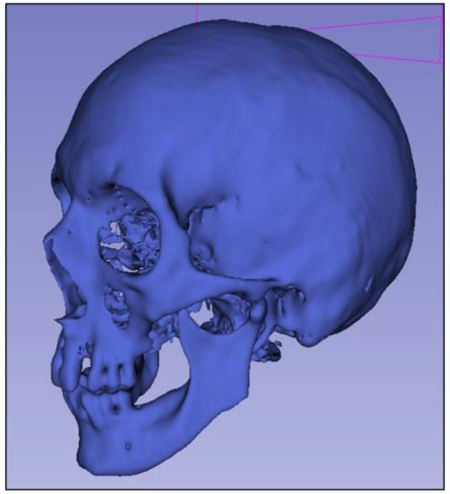

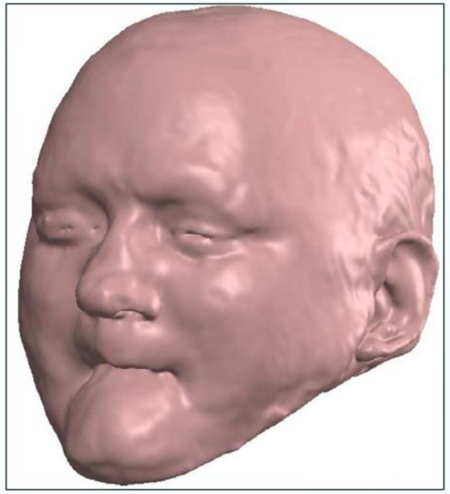

Denser Tissues outside Skull

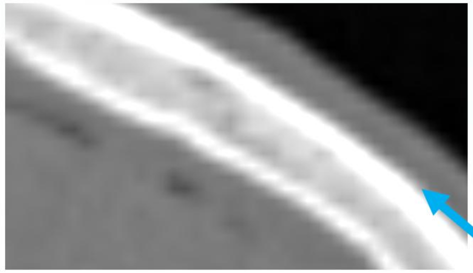

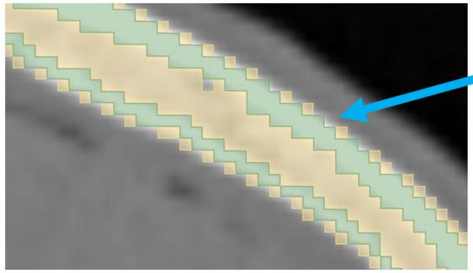

"Trabecular tissue" is identified in CT scan both between cortical layers and in a thin layer outside skull.

Trabecular only appears within Cortical layers only, not outside

This "Trabecular tissue" appears to be denser tissue outside the skull.

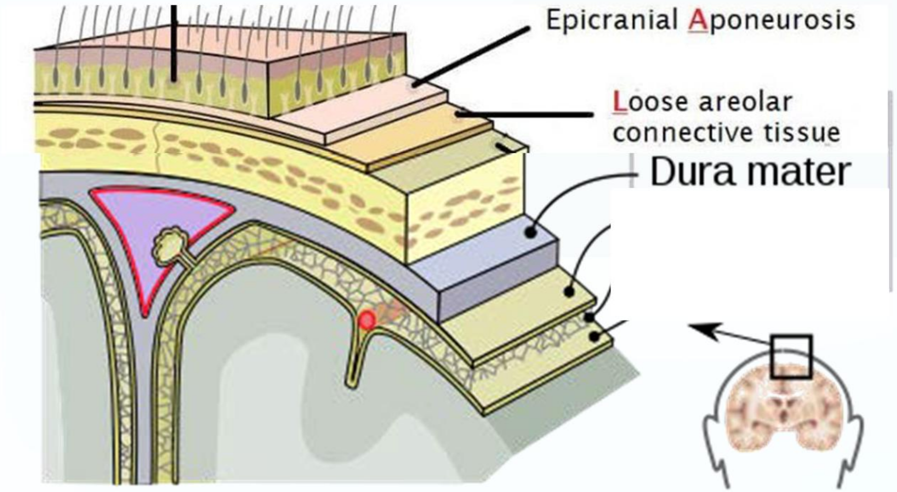

- Dura matter on the skull's interior (1174 kg/m^3)
- Connective Tissue on the skull's exterior (1027 kg/m^3)
- Trabecular Bone (1105 kg/m^3)

The densities of these tissues are similar and can, therefore be considered as one segmentation

STI-TEC

"Leveraging Knowledge Assets and Emerging Technologies"

SENTIR RESEARCH LABS

Different Segmentation Techniques

METHOD # 1 (CONTROL/ 2 PARTS)

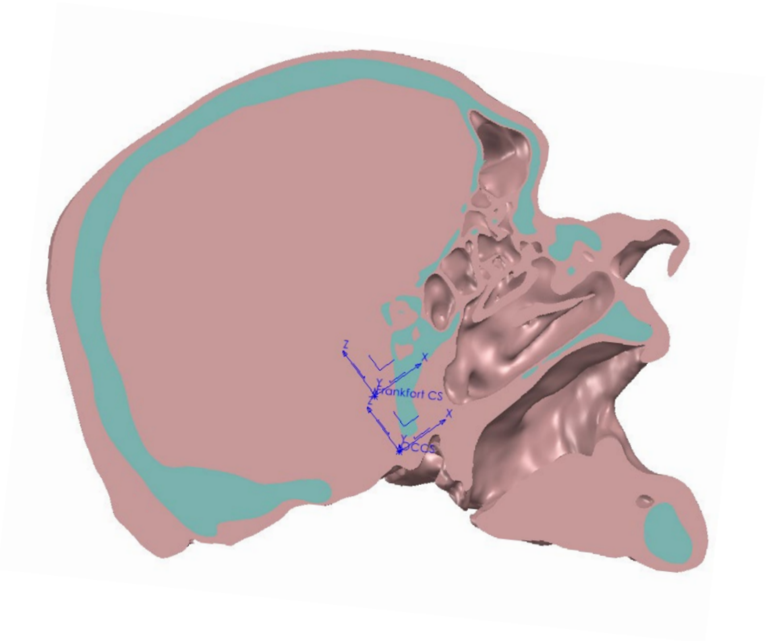

Skull Density Assigned:
Cortical Bone Density
$(1800\ \frac{kg}{m^3})$

Method used in:
Roush, 2010*
C. Albery and J. Whitestone**

# of Heads:
16

*Finding Cadaveric Human Head Masses and Center of Gravity: A Comparison of Direct Measurement to 3D ing
**Comparison of Cadaveric Human Head Mass Properties: Mechanical Measurement vs. Calculation from Medical Imaging

Approach: Methods 2 and 3

METHOD # 2 (R.O.M. INDIVID.)

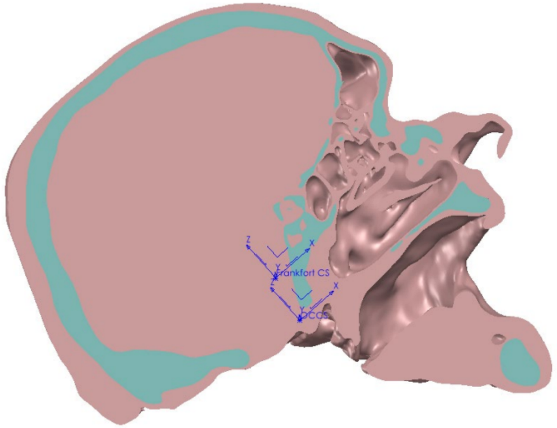

For Head M2:
$V_{cort\%}$=60.8%
$V_{trab\%}$=39.2%

→

ρ_{skull}:
(Head M2 only)
1378 kg/m^3

Rule of Mixtures

$$\rho_{skull} = \rho_{cort}V_{cort\%} + \rho_{trab}V_{trab\%}$$

Where: ρ_{cort}= 1800 kg/m^3 & ρ_{trab}= 1105 kg/m^3

# of Heads: 16

METHOD # 3 (R.O.M. TOTAL)

Groups	Average	ANOVA
Trabecular	53.49	P-value
Cortical	46.51	0.0301

$V_{cort\%}$=53.5%
$V_{trab\%}$=46.5%

→

ρ_{skull}:
(All heads)
1428 kg/m^3

STI-TEC

SENTIR RESEARCH LABS

Approach: Method 4

METHOD # 4 (3 PARTS)

CORTICAL	TRABECULAR	SOFT TISSUE
1800 kg/m^3	1105 kg/m^3	1040 kg/m^3

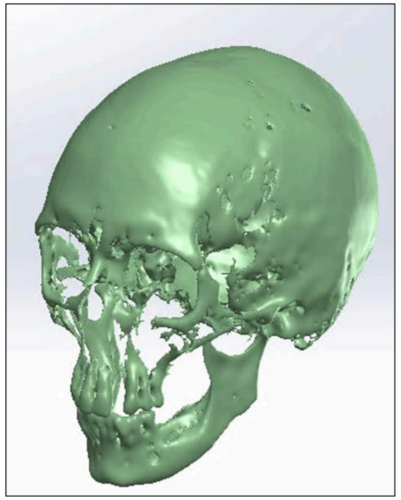

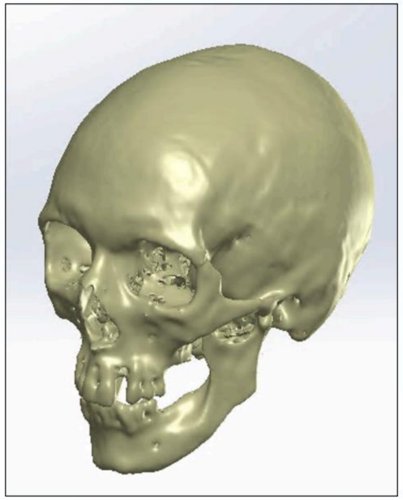

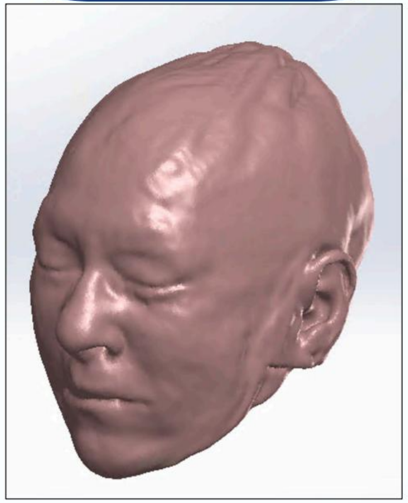

# of Heads: 8

Approach: Method 4 (3 parts)

METHOD # 4 (3 PARTS)

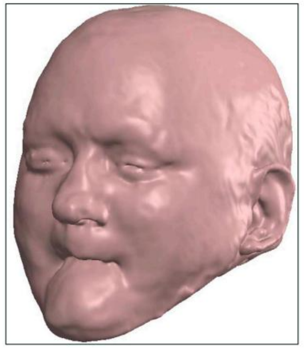

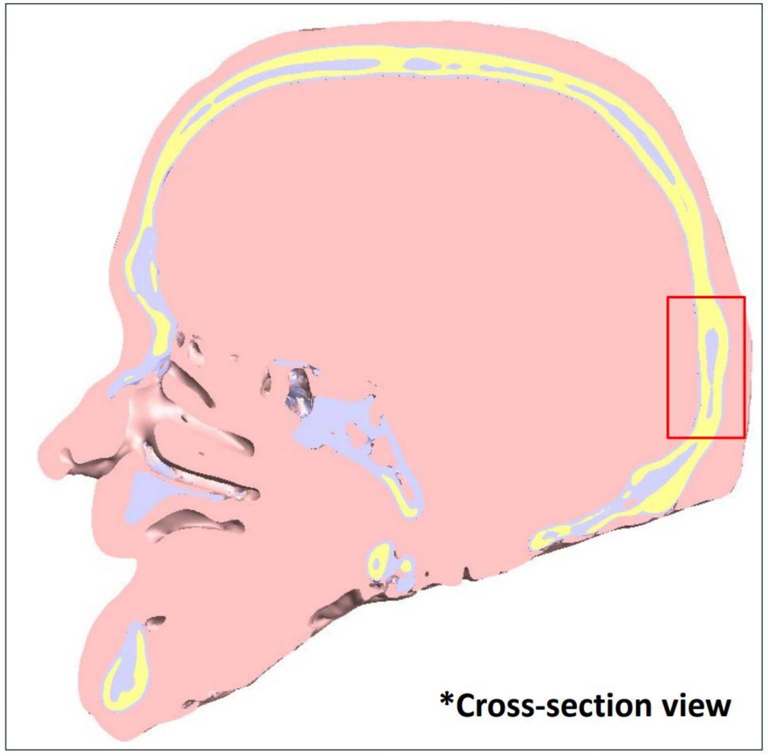

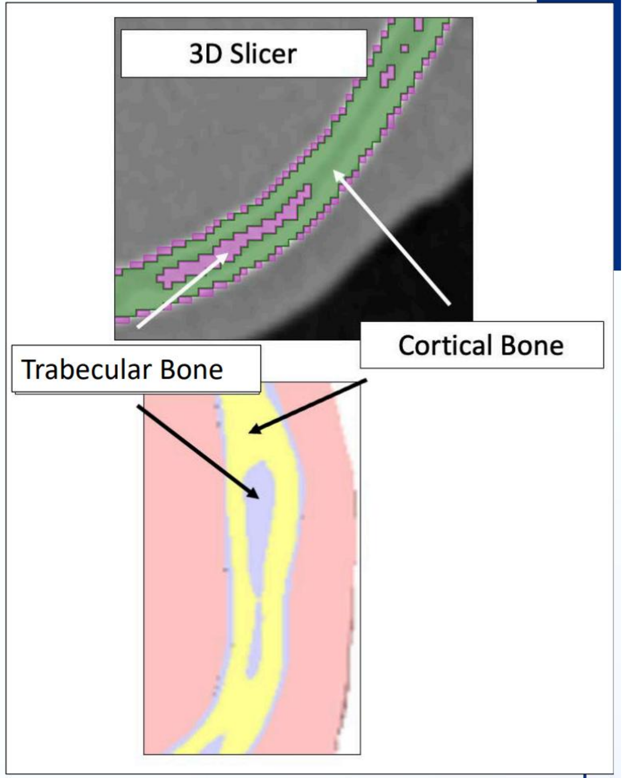

Statistical Analyses using jmp

METHODS

jmp

Tukey-Kramer HSD

Groups
- Experimental
- Method #1
- Method #2
- Method #3
- Method #4

Mass Properties
- Weight
- Volume
- CG Location (X, Y, Z-Directions)

$p < \sim 0.05$
(significantly different)

SUMMARY OF RESULTS

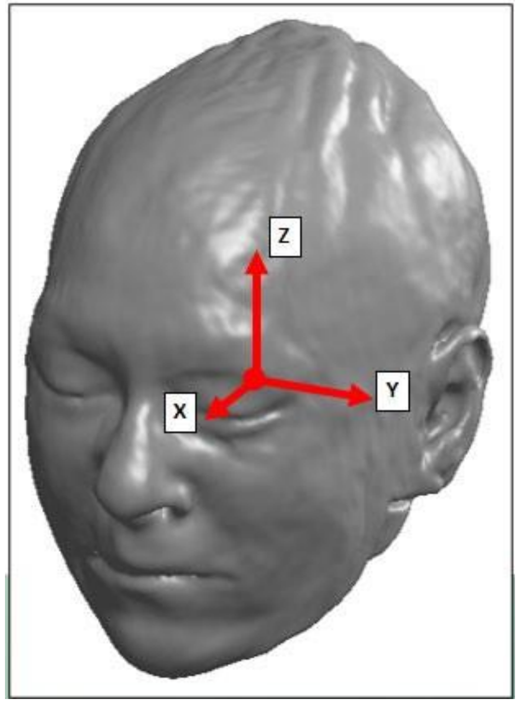

Xcg Location

Method	Compared Method	p-Values	Rank
Experimental	Control	0.3405	2
Experimental	ROM Indi.	0.2901	4
Experimental	ROM Full	0.2913	3
Experimental	3 Parts	0.9881	1

Zcg Location

Method	Compared Method	p-Values	Rank
Experimental	Control	0.0578	4
Experimental	ROM Indi.	0.1316	3
Experimental	ROM Full	0.1329	2
Experimental	3 Parts	0.2453	1

Method	Compared Method	p-Value
Control	Experimental	0.0578

DISCUSSION

- Previous work conducting segmentation analysis has been reported by Rousch (2010). In this study segmentation analysis was used to calculate weight and CG Location. Rousch found NSD when comparing experimental to calculated mass properties, but the study was limited to only four heads.
- In an additional study by Albery and Whitestone, segmentation analysis was used to calculate weight, CG location and moments of Inertia using 15 heads. Statistical analysis revealed that there was significant differences for weight and the moments of inertia of the X and Y axes and between calculated and measured properties.

DISCUSSION

Rankings				
	Method #1 (Control)	Method #2 (ROM Indl)	Method #3 (ROM Full)	Method #4 (3 Parts)
Weight [lb]	4	1	2	3
Volume [mm^3]	2	2	2	1
Xcg [mm]	2	4	3	1
Ycg [mm]	4	3	2	1
Zcg [mm]	4	3	2	1
Overall Rank	16	13	11	7

← Least Accurate   Most Accurate →

The Trabecular Bone should be taken into consideration when mass properties are calculated; specifically, Method #4 proved to be the most accurate.

CONCLUSIONS

- We found that methods of segmentation analysis that consider trabecular bone resulted in mass properties predictions that were not significantly different than measured values.
- Of the methods we employed, the method (Method 4) that considered the human head as three distinct tissues was the most accurate in determining mass properties.
- ***When cortical and trabecular bone were not considered distinct tissue, there were significant differences between the CG location when compared to experimental measurements.***

For 50th %tile head/ neck joint C7/T1 is located approximately at 2.2 cm backward and 11.95 cm below of the anatomical origin.

	X(cm)	Y(cm)	Z(cm)
OC	-2.56	0.02	-10.60

Investigation of OC Joint Location from CT Data

Upper Cervical Spine (UCS) Center of Rotation (COR)

- The UCS is an important anatomical region in injury/fatigue studies
- Identifying an anatomical location for this COR can be difficult

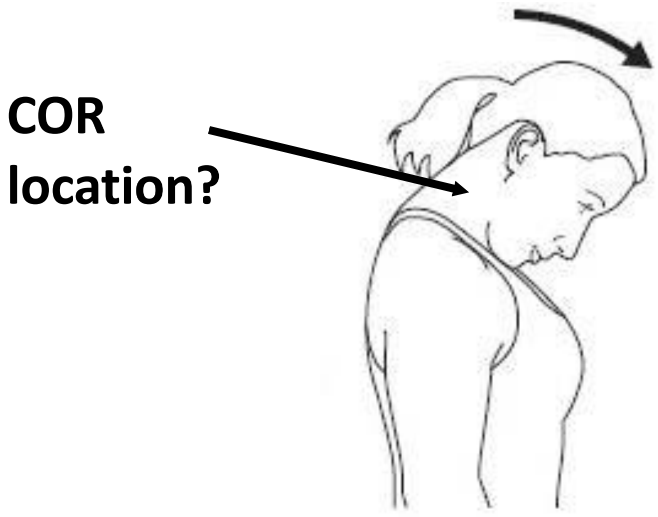

Flexion

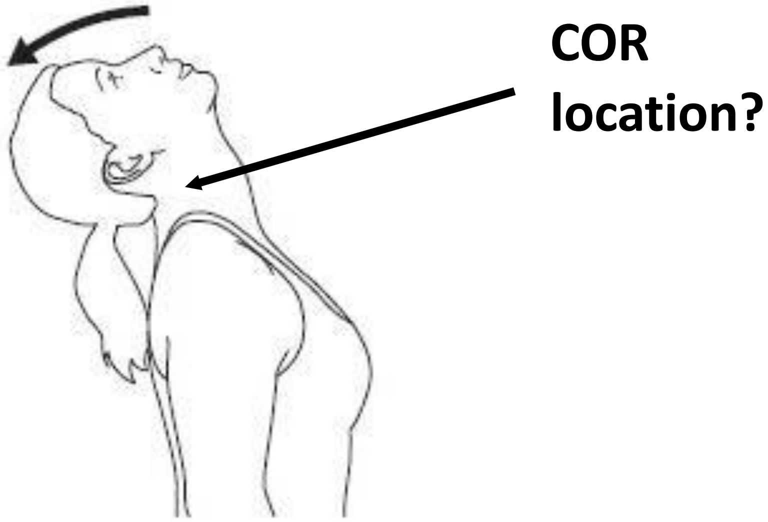

Extension

OCCIPITAL CONDYLES (OCs)

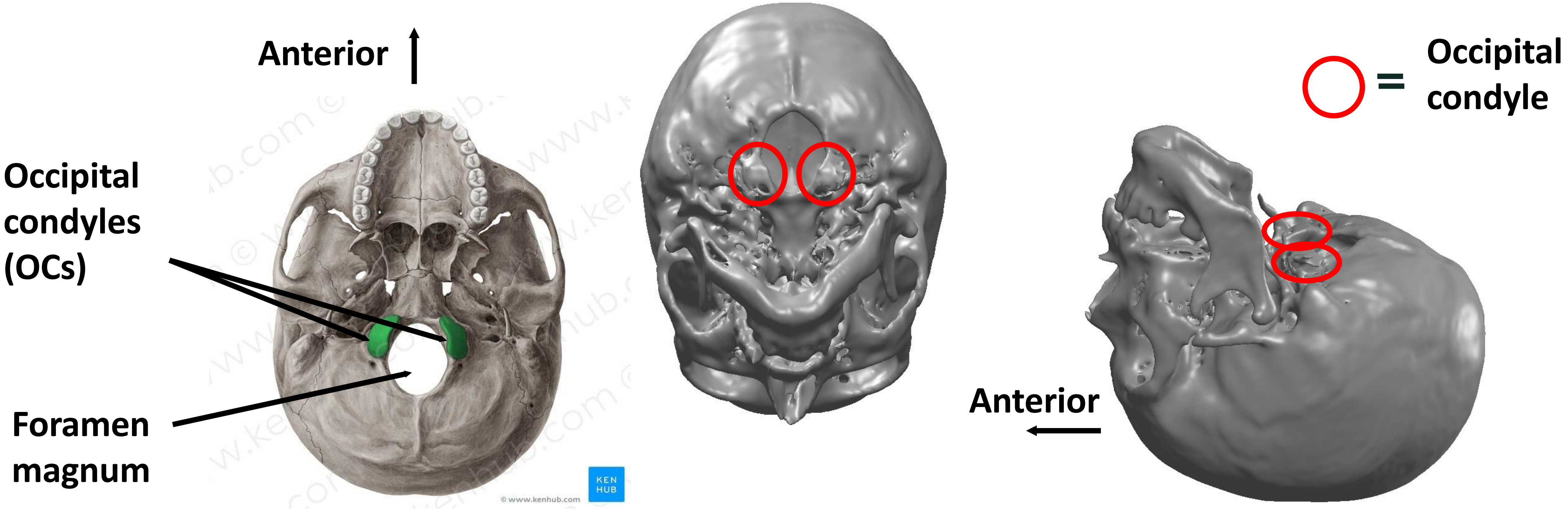

OBJECTIVES

- Prior work correlates UCS COR with OC centroid
  - "There was no significant difference between the OC -C2 COR and the occipital condylar centroid" – (Chancey et al. 2007)

- Identify an approximate UCS COR location using only the external anatomical landmarks that define the Frankfurt coordinate system (FCS)
  - Compare geometrically approximated OC centroid location to a location offset by a constant from the FCS
  - Compare approximated OC centroid location to UCS COR
  - Also compare approximated OC centroid location to precise OC centroid location

METHODS OC APPROX.

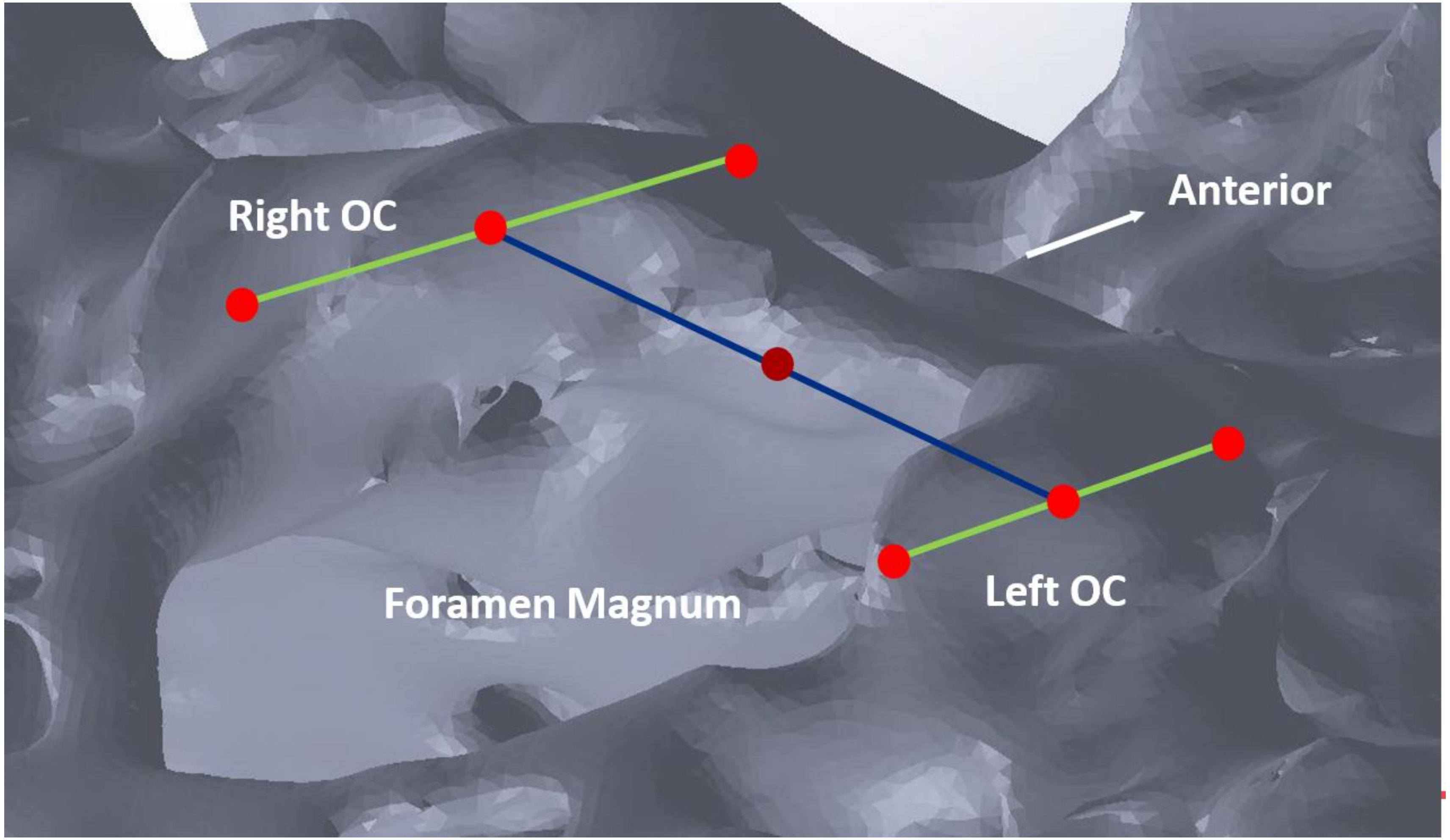

METHODS (1)

- For each specimen, visually identified locations for OC centroid approximation method in SolidWorks (Dassault Systèmes Concord, Massachusetts)
    - Performed approximation method to determine OC centroid location
- For each specimen, used "measure" feature to determine the offset between the approximated OC centroid location and the FCS origin (for X -, Y-, and Z-coordinates)
- Took the average of the offsets across the 17 specimens
- Subtracted this average difference from the location of the FCS for each specimen to create a "Translated" FCS location for each specimen
- Compared the Translated FCS location to the approximated OC centroid location using a Tukey-Kramer analysis in JMP

DISCUSSION

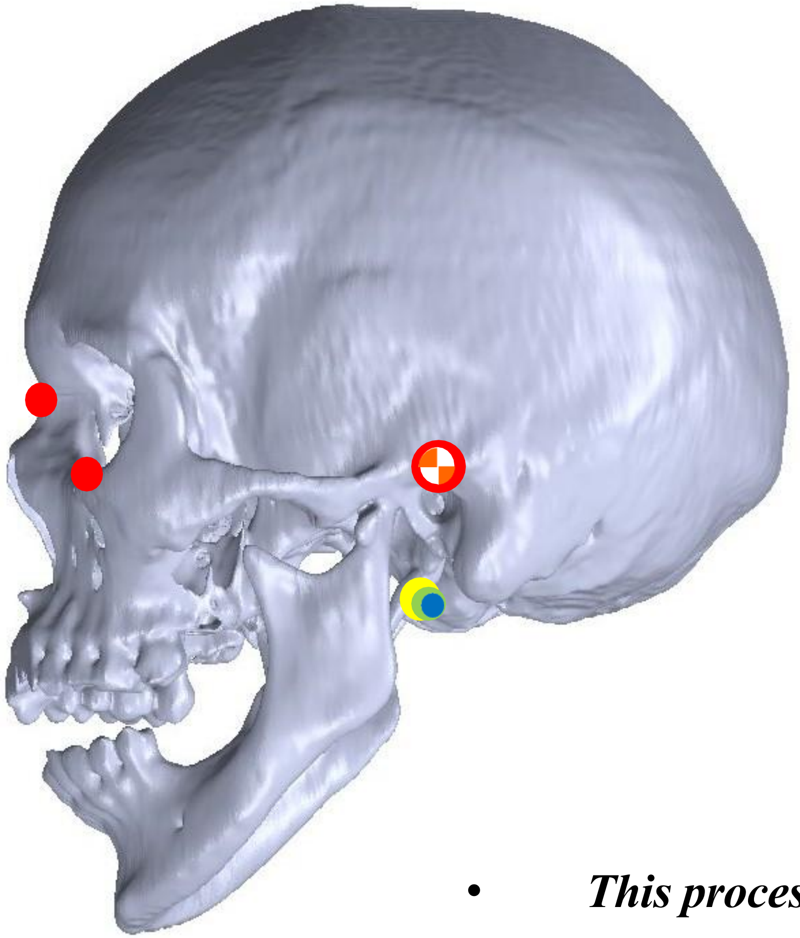

- Points used to define Frankfurt coordinate system
- FCS
- Translated FCS
- Approximated OC centroid
- UCS COR

- *This process may simplify future biodynamics head/neck simulations*

CONCLUSION

- No statistical difference found for these comparisons
  - Geometrically approximated OC centroid location vs. translated FCS
  - Approximated OC centroid location vs. UCS COR
  - Approximated OC centroid location vs. precise OC centroid location
- In the X- and Z- directions, it is possible to identify an approximate UCS COR location using only the external anatomical landmarks that define the FCS.

How do we move forward?

DIGITAL INNOVATION GROUP

- Model what we know to be true
- Establish standard headforms
  - Geometry
  - Landmarks (divets)
  - Multiple Sizes
- Conduct Round Robin Testing among Services
- Investigate Human Head Data Properties (Cedarville approach)
- Investigate combined human head with helmet system to determine potential differences in head/helmet properties (particularly for females)
- Further develop Modeling

REFERENCES

Albery, CB, Whitestone, JJ, (2003). A Comparison of Cadaveric Human Head Masses, Centers of Gravity and Moments of Inertia: Direct Measurement vs. Computed Tomographic Calculation. Proceedings of the Aerospace Medical Association 74th Annual Scientific Meeting.
Backaitis, S.H., Mertz, H.J. (Eds.), 1994. Hybrid III: The First Human-Like Crash Test Dummy. Society of Automotive Engineers, Warrendale, PA. Becker, E., 1972. Measurement of mass distribution parameters of anatomical segments. In: Proceedings of the Stapp Car Crash Conference, pp. 525–538.
Been, B., Philippens, M., de Lange, R., van Ratingen, M., 2004. WorldSID dummy head-neck biofidelity response. Stapp Car Crash J. 48, 431–454.
Beier, G., Schuller, E., Schuck, M., Ewing, C.L., Becker, E.D., Thomas, D.J., 1980. Center of gravity and moments of inertia of human heads. In: Proceedings of the IRCOBI, pp. 218–228.
Chandler, RF, Clauser, CE, McConville, JT, Reynolds, HM, and Young, JW, (1974). Investigation of inertial properties of the human body. AMRL-TR-74-137. Aerospace Medical Research Laboratory, Wright-Patterson AFB, Ohio.
Clauser, CE, McConville, JT, and Young, JW, (1969). Weight, volume, and center of mass of segments of the human body. AMRLTR-69-70. Aerospace Medical Research Laboratory, Wright-Patterson AFB, Ohio.
Braune, W., Fischer, O., 1889. Uber der schwerpunkt des menschlichen korpers mit rucksucht auf die ausrustung des desuschen infabteristen. Abhandl. D. Kl. Sachs. Ges. Wiss. Math. Phys. Kl 15 (7), 561–572.
Cavanaugh, J., Walilko, T., Malhotra, A., Zhu, Y., King, A., 1990. Biomechanical response and injury tolerance of the thorax in twelve sled side impacts. In: Proceedings of the Stapp Car Crash Conference, Orlando, FL, pp. 23–38.
Chancey, V.C., Ottaviano, D., Myers, B.S., Nightingale, R.W., 2007. A kinematic and anthropometric study of the upper cervical spine and the occipital condyles. J. Biomech. 40 (9), 1953–1959.
Chandler, R.M., Clauser, C.E., McConville, J.T., Reynolds, H.M., Young, J.W., 1975. Investigation of the inertial properties of the human body-AMRL-TR-74-102 (AD A016 485).
Cheng, R., Yang, K., Levine, R., King, A., Morgan, R., 1982. Injuries to the cervical spine caused by a distributed frontal load to the chest. In: Proceedings of the Stapp Car Crash Conference, pp. 1–40.
Clauser, C.E., McConville, J., Young, J.W., 1969. Weight, volume, and center of mass of segments of the human body. Wright Patterson Air Force Base, OH. Dempster, W., 1955. Space requirements of the seated operator-Wright-Patterson Air Development Center-WPAFB-TR-55-159. Wright-Patterson Air Force Base (AS 87 892), OH.
Dempster, W.T., Gaughran, G.R., 1967. Properties of body segments based on size and weight. J. Anat. 120, 33–54.
Eppinger, R., Sun, E., Bandak, F., Haffner, M., Khaewpong, N., Maltese, M., Kuppa, S., Nguyen, T., Takhounts, E., Tannous, R., Zhang, A., Saul, R., 2000. Development of Improved Injury Criteria for the Assessment of Advanced Automotive Restraint Systems-II. US DOT/National Highway Traffic Safe[illegible] Administration, Washington, DC.
Fischer, O. (Ed.), 1906. Theoretical Fundamentals for a Mechanics of Living Bodies, vol. 15. B. Teubner, Leipzig, and Berlin. FMVSS-202a, 2007. PART 571-Federal Motor Vehicle Safety Standards. pp. 531–545.
FMVSS-208, 2007. PART 571-Federal Motor Vehicle Safety Standards. pp. 580–667.
FMVSS-214, 1990. Federal Register, Docket No. 88-06. 49 CFR; Parts 571, et al. Side Impact Protection. Vol. 55. US Government Printing Office, Washington, DC, pp. 43722–45780).
Hall, M.C., 1965. Luschka's Joint. CC Thomas, Springfield, IL, p. 141. Harless, E., 1857. Lehrbuch der plastichen anatomie. Ebner u. Seubert, Stuttgart, Germany 2, 170–180.
Hodgson, V.R., Brinn, J., Thomas, L.M., Grenberg, S.W., 1970. Fracture behavior of the skull frontal bone against cylindrical surfaces. In: Proceedings of the Stapp Car Crash Conference, pp. 341–355.
Hodgson, V.R., Mason, M.W., Thomas, L.M., 1972. Head model for impact. In: Proceedings of the Stapp Car Crash Conference, pp. 1–13.
Hodgson, V.R., Thomas, L.M., 1971. Breaking strength of the human skull vs. impact surface curvature. US Department of Transportation, Springfield, VA. Hrdlicka, A.T.R.J., 1940. On measuring and photographing the cadaver. Am. J. Phys. Anthropol. 2[illegible] 433-[illegible]
Hubbard, R.P., McLeod, D.G., 1974. Definition and development of a crash dummy head. In: Proceedings of the Stapp Car Crash Conference, pp. 599–628.
ISO, 1999. WorldSID anthropometry requirements and performance. ISO TC22/ SC12/WG5, pp. 1–23.
Kumaresan, S., Yoganandan, N., Pintar, F.A., Maiman, D.J., Kuppa, S., 2000. Biomechanical study of pediatric human cervical spine: a finite element approach. J. Biomech. Eng. 122 (1), 60–71.
Kuppa, S., Eppinger, R.H., McKoy, F., Nguyen, T., Pintar, F.A., Yoganandan, N., 2003. Development of side impact thoracic injury criteria and their application to the modified ES-2 dummy with rib extensions (ES-2re). Stapp [illegible]rash[illegible] 47, [illegible]
Liu, Y.K., Laborde, J.M., Van Buskirk, W.C., 1971. Inertial properties of a segmented cadaver trunk: their implications in acceleration injuries. Aerosp. Med. 42 (6), 650–657.
Margulies, S.S., Thibault, K.L., 2000. Infant skull and suture properties: measurements and implications for mechanisms of pediatric brain injury. J. Biomech. Eng. 122 (4), 364–371.
McConville, J.T., Churchill, T.D., Kalpes, I., Clauser, C.E., Cuzzi, J., 1980. Anthropometric relationship of body and body segment moments of inertia. In: A.M.R. Laboratory, ed. McIntosh, A., Kallieris, D.,
Mattern, R., Miltner, E., 1993. Head and neck injury resulting from low velocity direct impacts. In: Proceedings of the Stapp Car Crash Conference, San Antonio, TX, pp. 43–57.
Melvin, J.W., Weber, K., 1985. Review of Biomechanical Imapct Response and Injury in the Automotive Environment. UMTRI, Ann Arbor, MI. Mertz, H., 1967. The kinematics and kinetics of whiplash. Ph.D. Thesis, Wayne State University, Detroit, MI, p. 370.
Mertz, H., 1985. Bifidelity of the Hybrid III head. In: Proceedings of the Stapp Car Crash Conference, pp. 111–119.
Nelson, L., Lowne, R., Tarriere, C., Bendjellal, F., Gillet, D., Maltha, J., Cesari, D., Bouquet, R., 1985. The Eurosid side impact dummy, In: Proceedings of the Enhanced Safety of Vehicles, Oxford, England, pp. 153–165.
Njus, G.O., Liu, Y.K., Nye, T.A., 1984. The inertial and geometrical properties of helmets. Med. Sci. Sports Exerc. 16 (5), 498–505. Padgaonkar, A.J., Krieger, K.W., King, A.I., 1975. Measurement of angular acceleration of a rigid body using linear accelerometers. J. Appl. Mech. 42, 552–556.
Philippens, M., Wismans, J., Yoganandan, N., Pintar, F., 2000. Whole body kinematics using post mortem human subjects in experimental rear impact. In: Proceedings of the IRCOBI, Montpellier, France, pp. 363–378.
Pintar, F.A., Yoganandan, N., Baisden, J., 2005. Characterizing occipital condyle loads under high-speed head rotation. Stapp Car Crash J. 49, 33–47.
Pintar, F.A., Yoganandan, N., Stemper, B.D., Bostrom, O., Rouhana, S.W., Digges, K.H., Fildes, B.N., 2007. Comparison of PMHS, WorldSID, and THOR-NT responses in simulated far side impact. Stapp Car Crash J. 51, 313–360.
Pintar, F.A., Yoganandan, N., Stemper, B.D., Bostrom, O., Rouhana, S.W., Smith, S., Sparke, L., Fildes, B.N., Digges, K.H., 2006. WorldSID assessment of far side impact countermeasures. Annu. Proc. Assoc. Adv. Automot. Med. 50, 199–219.
Plaga, J.A., Albery, C., Boehmer, M., Goodyear, C., Thomas, G., 2005. Design and development of anthropometrcially correct head forms for Joint Strike Fighter ejection seat testing, Wright-Pattersons AFB, OH, p. 56.
Reynolds, H.M., Clauser, C.E., McConville, J., Chandler, R., Young, J.W., 1975. Mass distribution properties of the male cadaver. SAE Trans., 1148–1150.
Rhule, H.H., Maltese, M.R., Donnelly, B.R., Eppinger, R.H., Brunner, J.K., Bolte, J.H.t., 2002. Development of a new biofidelity ranking system for anthropomorphic test devices. Stapp Car Crash J. 46, 477–512.
Robbins, D., 1983. Anthropometric Specifications for the Mid-Sized Male Dummy. Department of Transportation, NHTSA, Washington, DC, 1–123. Robbins, D., Schneider, L., Snyder, R., Pflug, M., Haffner, M., 1983. Seated posture of vehicle occupants. In: Proceedings of the Stapp Car Crash Conference, pp. 199–224.
Saczalski, K., Sances Jr., A., Kumaresan, S., Pozzi, M., Saczalski, T., Burton, J.L., Lewis Jr., P., 2004. Multivariate head injury threshold measures for various sized children seated behind vehicle seats in rear impacts. Biomed. Sci. Instrum. 40, 381–386.
Thomas, D.J., Ewing, C.L., 1971. Theoretical mechanics for expressing impact acceleration response of human beings. In: Proceedings of the AGARD, Porto, Portugal. Todd, T.W., Lindala, A., 1928. Thickness of the subcutaneous tissue in the living and the dead. Am. J. Anat. 41 (2), 153–169.
Walker, L.B., Harris, E.H., Pontius, U., 1971. Center of gravity of the human head and neck. Anat. Rec. 169, 448.
Walker, L.B., Harris, E.H., Pontius, U., 1973. Mass, volume, center of mass, and mass moment of inertia of head and head and neck of human body. In: Proceedings of the Stapp Car Crash Conference, 525–538.
Wismans, J., Van Oorschot, H., Woltring, H.J., 1986. Omni-directional human headneck response. In: Proceedings of the 30th Stapp Car Crash Conference San Diego, CA, 313–332.
Yoganandan, N., Pintar, F.A., Larson, S.J., Sances, Jr., A. (Eds.), 1998. Frontiers in Head and Neck Trauma: Clinical and Biomechanical. IOS Press, The Netherlands.
Yoganandan, N., [illegible]tar, F.A., Stemper, B.D., Wolfla, C.E., Shender, B.S., Paskoff, G., 2007. Level-dependent coronal and axial moment-rotation corridors of degeneration-free cervical spines in lateral flexion. J. Bone Joint Surg. Am. 89 (5), 1066–1074.
Yoganandan, N., Pintar, F.A., Zhang, J., Stemper, B.D., Philippens, M., 2008. Upper neck forces and moments and cranial angular accelerations in lateral impact. Ann. Biomed. Eng. 36 (3), 406–414.
Yoganandan, [illegible]., Zhang, J., Pintar, F.A., King Liu, Y., 2006. Lightweight low-profile nine-accelerometer package to obtain head angular accelerations in short

Thank you!